

NASA Contractor Report 4020

Computation of Multi-Dimensional Viscous Supersonic Jet Flow

Y. N. Kim, R. C. Buggeln,
and H. McDonald
Scientific Research Associates, Inc.
Glastonbury, Connecticut

Prepared for
Lewis Research Center
under Contract NAS3-22759

NASA
National Aeronautics
and Space Administration
**Scientific and Technical
Information Branch**

1986

TABLE OF CONTENTS

	Page
SUMMARY	1
INTRODUCTION	2
LIST OF SYMBOLS	10
ANALYSIS	13
SOLUTION OF THE GOVERNING EQUATIONS	21
TEST CASES	24
DISCUSSION AND CONCLUSIONS	30
USER'S MANUAL	31
Flow Diagram	31
PEPSIN Subroutines	36
Logical File Units Utilized by PEPSIN Computer Code	40
PEPSIN Input	42
Namelist Input Description	45
Error Conditions in the PEPSIN Computer Code	59
PEPSIN FORTRAN Variables	63
Sample Input and Sample Output	85
REFERENCES	87
FIGURES	90

PRECEDING PAGE BLANK NOT FILMED

SUMMARY

A new method has been developed for two and three-dimensional computations of viscous supersonic flows with embedded subsonic regions adjacent to solid boundaries. The approach employs a reduced form of the Navier-Stokes equations which allows solution as an initial-boundary value problem in space, using an efficient noniterative forward marching algorithm. Numerical instability associated with forward marching algorithms for flows with embedded subsonic regions is avoided by approximation of the reduced form of the Navier-Stokes equations in the subsonic regions of the boundary layers. Supersonic and subsonic portions of the flow field are simultaneously calculated by a consistently split linearized block implicit computational algorithm. The results of computations for a series of test cases relevant to internal supersonic flow is presented and compared with data. Comparison between data and computation are in general excellent thus indicating that the computational technique has great promise as a tool for calculating supersonic flow with embedded subsonic regions. Finally, a User's Manual is presented for the computer code used to perform the calculations.

INTRODUCTION

The interaction of a supersonic jet with an external stream has received considerable attention due to its critical role in determining both the thermodynamic and acoustic signatures from a vehicle producing a supersonic jet. The physics of supersonic jet flow is characterized by the formation of shock and expansion waves, the development of viscous mixing layers and the interaction of these phenomena (Figs. 1 and 2). As a consequence, a complicated multiple shock cell flow structure comes into existence in the jet. The detailed flow structure of a given jet including a shape of jet interface is determined primarily by the conditions of an ambient flow. At the jet interface, these two different flows form a turbulent mixing layer which strongly interacts with both shock and expansion waves. In the presence of interactions with waves, the turbulence structure in the mixing layer may be strongly affected. Both compressibility effects and pressure gradients in the jet can also influence the turbulence structure in the mixing layer. Under certain operational conditions, Mach disc(s) may occur and complicate the turbulent jet flow structure (Fig. 2). The mixing process that is present downstream of the disc has wake-like characteristics, and the entrainment process induces large streamline displacement which can appreciably alter pressure levels from those occurring in the inviscid limit. Because of the strong viscous/inviscid interactions as discussed above, inviscid theoretical methods have been found to be inadequate for predicting jet/external flow interactions. Therefore, very costly experimental testing has been the primary means of determining the complex flow patterns associated with these flows. However, in recent years, advances in computational fluid dynamics have demonstrated that the dependence on the experimental analysis of such a complex flow can be reduced by utilizing computational analysis. Unlike the experimental testing, computational analysis is not necessarily restricted by Reynolds number and other flow or testing conditions. Furthermore, experimental costs are steadily increasing, whereas the computational costs have been and are expected to decrease. Thus, the goal of the current work was to develop an efficient and reliable numerical approach for the prediction of the detailed flow structure of a supersonic jet exhausted into the external flow.

Early computational viscous solutions of the nozzle flow field region consisted of viscous-inviscid interaction techniques called patching methods (for example, Refs. 1-3). The techniques consist of dividing the various viscous and inviscid regions of the flow according to the physical nature and mathematical behavior of the equations applicable to each region. Each of these regions was then analyzed independently and was iteratively coupled using appropriate matching conditions consistent with weak-interaction theory. Although these solutions gave reasonable results for specific data sets, the required matching limited the usefulness of this method as a predictive technique. It is quite natural to consider solving the full time-dependent, compressible Navier-Stokes equations as an alternative approach for such a complex flow (for example, Refs. 4-5). However, the widely disparate length scales and flow characteristics in the various regions involved could lead to perhaps unacceptable computer time and storage requirements in achieving the results of adequate resolution, especially in three dimensions. In this study, it was decided that such a procedure should be used only if no suitable alternative exists. A compromise approach would possess the general three-dimensional, viscous nature of the Navier-Stokes equations, but would take advantage of realistic physical approximations to limit the computer running time and storage requirements associated with the solution of the complete three-dimensional Navier-Stokes equations.

During the past two decades much effort has been expended in developing such numerical procedures which can be used as an alternative to solving the full Navier-Stokes equations for certain classes of problems. These procedures treat a reduced form of the steady state Navier-Stokes equations, often referred to as the parabolized Navier-Stokes equations, as an initial boundary value problem that can be solved by spatial forward marching. The ability to forward march the governing equations from an initial streamwise location to some desired downstream location rather than perform a simultaneous solution of the governing equations at all streamwise locations, as is required for the solution of the full Navier-Stokes equations, results in a considerable reduction of computational time. Although the amount of reduction will depend on the problem considered, the efficiency of the solution procedures and numerous other variables, this reduction has been the primary motivation for the development of marching procedures.

To devise a set of governing equations suitable for the spatial forward marching of supersonic flows, three steps must be taken. First, a nominally primary flow direction must be identified. Second, a coordinate system must be constructed with one of its coordinate directions aligned with the primary flow direction. Third, all diffusion in the primary flow direction must be neglected. These steps when applied to the steady state Navier-Stokes equations produce a set of governing equations which is well posed for the spatial forward marching of supersonic flows (e.g. Ref. 6). The introduction of no-slip surfaces into a supersonic flow usually results in the formation of embedded subsonic regions adjacent to these surfaces. Also, under certain operating conditions of the vehicle supersonic flow coexists with the subsonic flow as can be found in the case of supersonic jet exhaust into the subsonic ambient flow. When the set of reduced equations is forward marched with embedded or coflowing subsonic regions, the governing equations are not well posed and hence the solution procedure may become unstable. This instability, which is often referred to as the branching phenomenon, has been the subject of much research (e.g. Refs. 7-8) and the techniques used to suppress this instability are a convenient way to differentiate between procedures for solving the reduced form of the Navier-Stokes equations for supersonic flow with subsonic regions. In one of the earliest works in this area Garvine (Ref. 7) demonstrated (for a model problem) the existence of exponentially growing (divergent) terms in the solution of the reduced form of the Navier-Stokes equations when applied to a viscous (inviscid supersonic flow interacting with a viscous boundary layer) interaction problem. The author concluded that for this problem the reduced form of the Navier-Stokes equations was improperly set as an initial value problem, because the interaction dynamics contained upstream "elliptic" influence. In the model problem if the upstream conditions are not precisely set to cause the divergent terms to be multiplied by zero, the exponentially growing terms will cause the streamwise pressure gradient terms to grow exponentially large resulting in unrestrained acceleration or deceleration of the flow. In general it is not possible to pick the upstream conditions to negate the exponentially growing modes, hence several investigators have attempted to suppress the unstable (or branching) behavior by further modification of the reduced form of the Navier-Stokes equations for supersonic flows with embedded subsonic regions.

Much of the early work on the solution of the reduced form of the Navier-Stokes equations is based on the work of Rudman and Rubin (Ref. 8). Rudman and Rubin solved the equations for the hypersonic flow over slender bodies with sharp leading edges. Based on an order of magnitude analysis they demonstrated that for this class of problems the streamwise pressure gradient term was negligible when compared with the inertia and viscous terms of the streamwise momentum equation. Neglecting the streamwise pressure gradient term in this equation prevented the branching behavior in their calculation. Although this approach does yield a set of equations that is well posed for spatial forward marching, its assumption of negligible streamwise pressure gradient limits the cases which can be considered. In a later work Lubard and Helliwell (Ref. 9) proposed a method for preventing branching that involved explicit spatially lagged evaluation of the streamwise pressure gradient term. The above authors found that in addition to the frequently encountered problem of instability associated with exceeding some marching direction step size, a further instability was encountered when the step size was reduced below some limit. By examining the eigenvalues of a model set of equations (Ref. 12) they were able to develop a criterion for this minimum step size. Numerical experimentation with their computer code demonstrated reasonable correlation with their criterion. Several test cases using this method have been successfully run (mainly for cone flow cases) by the authors of Ref. 9 and others (Refs. 13-14) and in these cases evidently the restriction on the minimum marching step size was not a problem in allowing sufficiently accurate results to be obtained. However, the restriction on minimum marching step size is in principle not a desirable feature. Since it does prevent arbitrary mesh refinement, and thereby the assurance that an accurate unique solution has been obtained. In at least one case (Ref. 9) this minimum step size restriction prevented the successful running of a case. In a later technique developed by Vigneron, Rakich and Tannehill (Ref. 10) a variant of the technique of Lubard and Helliwell was used to prevent branching. In this particular variant the streamwise pressure gradient term was evaluated by an implicit backward difference in the supersonic portion of the flow. However, in the subsonic region only that portion of the streamwise pressure gradient term that could be included without causing branching was evaluated implicitly. The stability analysis through the investigation of the

eigenvalues of a model set of equations also produces a restriction on the minimum allowable step size. When that portion of the subsonic pressure gradient excluded from the implicit evaluation is evaluated explicitly by a lagged technique similar to Lubard and Helliwell, the investigators noted that the scheme became unstable. Thus, in order to achieve stability this technique neglected the explicit portion of the streamwise pressure gradient term in the subsonic region. Schiff and Steger (Ref. 11) treat the subsonic streamwise pressure gradient term by either a first- or second-order streamwise extrapolation technique in the subsonic regions. The first order technique is equivalent to setting the streamwise pressure gradient term equal to zero in the subsonic region while the second order technique is equivalent to the explicit evaluation of the streamwise pressure term (as was done by Lubard and Helliwell). As with the two previously discussed techniques, these authors also report a restriction on the minimum marching step size that they may take and still retain a stable calculation. On the other hand, Rubin and Lin (Ref. 15) have developed a global relaxation procedure for solving the reduced form of the Navier-Stokes equations. This technique was primarily developed for application to cases where upstream influence is strong. To obtain the upstream influence with the reduced form of the Navier-Stokes equations requires a global iteration or relaxation procedure. The above authors do this by approximating the streamwise pressure gradient term by a forward difference. When marching the solution from the i^{th} to the $i+1^{\text{st}}$ station the pressure gradient term is evaluated in terms of the pressure at the $i+1^{\text{st}}$ (current) and $i+2^{\text{nd}}$ (unknown) station ($i+1^{\text{st}}$ station is the implicit station; all other streamwise derivatives are backward differenced between $i+1$ and i). Initially the pressure at the unknown $i+2^{\text{nd}}$ station is guessed; during subsequent global iterations the previously calculated value is used. Global iteration of the governing equations is continued until the solution converges. Rubin and Lin report that convergence is typically obtained in five to ten iterations for cases with small streamwise pressure gradients (cases run to date have been limited to flow over cones). The authors also report that there is no minimum marching step size requirement with their approach.

The supersonic jet exhausted from a nozzle is essentially turbulent and has associated with it large streamwise pressure gradients, e.g., turbulent mixing layer interacting with multiple shock wave-cells. It is expected that one would desire to take a small streamwise marching step to accurately

resolve the phenomenon, for example, the near-field plume-mixing interactions.

As reviewed above, the methods of Refs. 8-11 all make an attempt to consider the effects of streamwise pressure gradient in the embedded subsonic regions. However, they give only an approximate treatment to this possibly dominant term, and all of those methods have a minimum marching step size limitation which, in the cases of interest in this study, may not either allow for an accurate or in some cases even a minimally acceptable solution. Although there is no minimum marching step size requirement with the global relaxation procedure developed by Rubin and Lin (Ref. 15), the computation time would increase considerably in more complex flow situations. If the number of iterations were to increase much beyond the five to ten iterations it took to converge a small streamwise pressure gradient case, the computation time would then become comparable to that required for a solution of the full Navier-Stokes equations.

Hence, a noniterative approach is sought with a consequent reduction in computer cost relative to either the global iteration approach to solving the reduced Navier-Stokes equations or solution of the full Navier-Stokes equation. Further as a prerequisite it is required that there exist no numerical limitation on the minimum marching step and it is desired to keep to a minimum any approximation to the streamwise pressure gradient term.

Such an approach which meets these requirements has been developed by the present authors as reported elsewhere (Ref. 16). A detailed explanation of the techniques will be presented in the next analysis section. Unlike other noniterative methods, the streamwise pressure gradient term is maintained and evaluated by an implicit backward difference in the supersonic as well as the subsonic region. However, approximations were made on both the normal (to the wall usually) momentum and continuity equation in the subsonic region(s) to suppress the branching behavior of solution. In the (thin) subsonic flow region, the normal momentum equation is approximated by the conventional boundary layer form of that equation, and the continuity equation is approximated by integrating the continuity equation from the wall to an arbitrary point in the subsonic portion of the boundary layer. This approximation of continuity equation is a major difference between the

present technique and other noniterative methods. As discussed in Ref. 16, numerical experimentation with various cases indicates no restriction on the minimum step size. Thus, an accurate resolution of the flow fields has been successfully obtained without being limited by the requirement of minimum step size. Since no approximations were made on the streamwise pressure gradient term, the predictions for the flow field under the condition of non-negligible streamwise pressure gradient agreed very well with the data as discussed in Ref. 16.

Thus, application of this approach to the analysis of steady three-dimensional supersonic jet interacting with an ambient flow was a major concern in this study. The flow field calculation by the existing computer program, called PEPSIS, was limited to a computational domain without any embedded solid objects except for the wall boundary. Thus, the first task of this study was to extend a capability of PEPSIS so that the flow field could be analyzed in a computational domain with one or more embedded solid bodies such as nozzle walls. The extended PEPSIS computer program, which is called PEPSIN, is the same as PEPSIS as far as its basic assumptions and approximations are concerned. One of the basic assumptions for PEPSIS approach was the thinness of subsonic layer within a boundary layer. As a result of this assumption, approximations were made on the governing equations within this thin, subsonic layer based on the fundamental properties of a boundary layer. However, analysis of supersonic jet interactions under certain low conditions is expected to encounter subsonic regions of a different nature. One of such subsonic regions may be present when a Mach disc appears in the jet. Another type of subsonic region may be encountered when a supersonic jet exhausts into an ambient subsonic stream. First of all, these two kinds of subsonic regions may not be necessarily thin. Furthermore, since these subsonic regions are not located in the vicinity of a wall boundary, approximations based on boundary layer properties become questionable. Therefore, it was decided to exclude such subsonic regions from consideration in the present study. Those subsonic regions require further separate investigations before they can be incorporated in the PEPSIN approach. Thus, as will be discussed later, test cases considered in the present case were limited to the analysis of a supersonic jet interacting with supersonic external stream.

Two other investigators have utilized forward marching techniques to solve the jet/external flow interactions. First, Dash and co-workers (Refs. 17 and 18) developed an explicit spatial marching method to predict both the inviscid plume structure and the viscous mixing layer. Their approach employs a multiple-domain solution algorithm to solve a reduced form of the Navier-Stokes equations. Their approach has been primarily applied to the two-dimensional axisymmetric cases, although they presented some results for nonaxisymmetric three-dimensional cases (rectangular cross sections of various aspect ratios) in a recent paper (Ref. 19). However, the marching step size in their procedure is limited by numerical stability conditions of explicit schemes. On the other hand, Vatsa and his co-workers (Ref. 18) developed a method to solve the problem of a slightly underexpanded supersonic jet in a subsonic co-flowing mainstream. First, they solved the inviscid problem which was formulated in terms of linearized perturbation potentials to estimate the streamline curvature. Then they obtained governing equations of parabolic type through the use of an approximate inviscid flow intrinsic coordinate system. Their solution based on a marching technique produces the class of weak interactions wherein the viscous interaction has a formally second-order effect. In this approach, prediction of streamline curvature, in general, may become as difficult as the viscous problem if the difference between jet and external flow conditions become large or if the problem is three-dimensional. A difficulty may arise also if the viscous effects become significant and have a strong influence on the secondary flow.

The present study is concerned with the application of an implicit forward marching procedure for the reduced form of the Navier-Stokes equations (Ref. 16) to the three-dimensional analysis of supersonic jet flow interacting with a co-flowing stream. The approach is noniterative and is not limited by a minimum step size criterion. Furthermore, being implicit the maximum allowable step size is expected to exceed that of explicit methods by a significant amount. The remainder of this report will consist of (1) a discussion of the analysis used in the study, (2) a discussion of the solution of the governing equations, (3) the results of a series of test cases run to demonstrate the applicability of the analysis and to exercise and to validate the resulting computer code and (4) a User's Manual for the computer code, termed PEPSIN.

LIST OF SYMBOLS

A	Square Matrix of coefficients
C_H	Nondimensional heat transfer coefficient
C_p	Specific heat
D	Column vector whose elements are spatial differential operators
D:D	Second invariant of the mean flow rate of deformation tensor
H	Column vector associated with marching direction terms
L	Linear differential operator
M	Mach number
P	Static pressure
Pr	Prandtl number
Re	Reynolds number
S	Source term
T	Static temperature
U	Streamwise velocity component
V	Transverse velocity component
W	Spanwise velocity component
X	Distance from leading edge
\vec{V}	Velocity
\mathcal{D}	Damping coefficient
h	Metric coefficient, enthalpy
l_m	Mixing length
\vec{n}	Unit vector normal

LIST OF SYMBOLS

q	Heat transfer
r	Radius
w	Velocity component
x	Coordinate direction
y	Distance from a surface
γ^+	Nondimensional distance from a surface

Greek Symbols

γ	Ratio of specific heats
δ_b	Boundary layer thickness
κ	von Karman constant
μ	Viscosity
ρ	Density
τ	Viscous stress tensor
∇	Nabla operator
ΔX	Marching direction step size

Subscripts

i	i th d direction
j	j th direction, jet flow condition
l	Laminar
n	Normal direction
w	Wall
E	External stream condition
J	Jet flow condition
R	Reduced
S	Sonic line
T	Turbulent, tangential direction
0	Stagnation condition
1	Streamwise direction
2	Cross plane direction
3	Cross plane direction
∞	Free stream condition

Superscripts

i	i th streamwise station
T	Transpose

II. ANALYSIS

Governing Equations

The steady state fluid dynamic conservation laws of mass, momentum and energy respectively can be written in nondimensional vector form as

$$\nabla \cdot \rho \vec{V} = 0 \quad (1)$$

$$\nabla \cdot (\rho \vec{V} \vec{V}) + \nabla P - \frac{\nabla \cdot \tau}{Re} = 0 \quad (2)$$

and

$$\nabla \cdot (\rho h_0 \vec{V}) - \nabla \cdot \left[\frac{C_p}{Re} \left(\frac{\mu_l}{Pr_l} + \frac{\mu_T}{Pr_T} \right) \nabla T \right] - \nabla \cdot \frac{(\tau \cdot \vec{V})}{Re} = 0 \quad (3)$$

This form of the governing equations, often referred to as the full Navier-Stokes equations, requires several auxiliary relations and models before these equations can be solved. In this study the stagnation enthalpy, h_0 , is related to the static temperature, T , and the velocity \vec{V} , through the relationship (assuming a calorically perfect gas)

$$h_0 = C_p T + \frac{\vec{V} \cdot \vec{V}}{2} \quad (4)$$

while the temperature, T , pressure P , and density, ρ , are related by means of the calorically perfect gas equation of state

$$P = \frac{\gamma - 1}{\gamma} C_p \rho T \quad (5)$$

The stress tensor, τ , is represented by the relationship

$$\tau = \mu (\nabla \vec{V} + \nabla \vec{V}^T) - \frac{2}{3} \mu \nabla \cdot \vec{V} \quad (6)$$

where the superscript T refers to the transpose of the tensor. The components of the velocity vector, \vec{V} , are interpreted as the mass weighted mean velocity components and ρ , P and T are the ensemble-averaged

density, pressure and temperature (Ref. 21). Hence, these equations can be applied to both laminar and turbulent flows if the effective viscosity, μ , is interpreted as the sum of the laminar, μ_l , and turbulent, μ_T , viscosities, i.e.,

$$\mu = \mu_l + \mu_T \quad (7)$$

It is assumed that the laminar viscosity can be computed from Sutherland's law and that the laminar and turbulent Prandtl numbers, Pr_l and Pr_T are constant. For this study an algebraic mixing length turbulence model of the form

$$\mu_T = Re \rho l_m \sqrt{D:D} \quad (8)$$

was used where l_m is the algebraic mixing length and $D:D$ is the second invariant of the mean flow rate of deformation tensor (Ref. 22). In this study the mixing length of McDonald and Camarata (Ref. 23) was used.

$$l_m = 0.09 \delta_b \tanh \left[\kappa \tilde{y} / (0.09 \delta_b) \right] \mathcal{D} \quad (9)$$

where δ_b is the local boundary layer thickness, κ is the von Karman constant, \tilde{y} is the distance to the nearest wall, and \mathcal{D} is the sublayer damping term of van Driest (Ref. 24).

To obtain what is often referred to as the reduced form or the 'parabolized' form of the Navier-Stokes equations involves approximation of the diffusion terms (both stress and Fourier heat conduction) of Eqs. (2), (3) and (6). This approximation neglects all derivatives of the stress tensor and the Fourier heat conduction terms in a selected 'marching' or 'streamwise' direction. In addition all streamwise derivatives of the velocity components of the stress tensor are neglected.

Hence, the general reduced form of Eqs. (2) and (3) can be recast as

$$\nabla \cdot (\rho \vec{V} \vec{V}) + \nabla P - \frac{(\nabla \cdot \tau)_R}{Re} = 0 \quad (10)$$

and

$$\nabla \cdot (\rho h_0 \bar{V}) - \left\{ \nabla \cdot \left[\frac{C_P}{Re} \left(\frac{\mu_l}{Pr_l} + \frac{\mu_T}{Pr_T} \right) \nabla T \right] \right\}_R - \left[\nabla \cdot \frac{(\tau \cdot \bar{V})}{Re} \right]_R = 0 \quad (11)$$

where the subscript R refers to the approximated or reduced form of the noted term.

The reduced form of the Navier-Stokes equations, Eqs. (1), (10) and (11) is the starting point for the discussion of the governing equations to be used for this study. As discussed in detail in Ref. (16), this set of equations is not well posed for solution by spatial forward marching when applied to the class of problems considered in this study, i.e., supersonic flow with embedded subsonic layers. In this investigation, the same strategy as in Ref. (16) was adopted. The flow is divided into supersonic and subsonic flow regions and different sets of governing equations are utilized in each region. The reduced form of the Navier-Stokes equations in the supersonic region(s) of the flow and what can be considered to be a model set of equations in the subsonic region(s) are utilized. The model set of equations used in the subsonic region(s) is obtained by starting with the reduced form of the Navier-Stokes equation and making appropriate physical approximations in this region such that the coupled system of equations in both supersonic and subsonic flow are stable when solved as an initial value problem in space. There are several important features of the subsonic model set of governing equations. First, no approximation is made to either the streamwise or the tangential momenta equations, and second, the terms tangential and normal refer to some adjacent solid surface. Hence, the full effect of the pressure gradient terms will be felt in both the streamwise and tangential direction of the subsonic portion of the flow. The assumption needed to modify the normal momentum and continuity equations in the subsonic regions is the relatively unrestrictive condition that the subsonic layer is thin relative to the characteristic transverse dimension of the flow device. For the case of an impermeable wall this leads to the condition that within the viscous subsonic layer the normal velocity component is negligible. The importance of the specification of the normal velocity is that a mechanism can now be established to prevent the growing

mode caused by the interaction between the subsonic and supersonic layers, i.e., the branching phenomenon. This approximation can be obtained by integrating the continuity equation from the wall to an arbitrary point in the subsonic portion of the boundary layer X_s . Thus,

$$h_1 h_T \rho w_n \Big|_s = - \int_0^{X_s} \left[\frac{\partial}{\partial x_1} (h_2 h_3 \rho w_1) + \frac{\partial}{\partial x_T} (h_1 h_n \rho w_T) \right] dx_n + h_1 h_T \rho w \Big|_w \quad (12)$$

where the subscripts n and T refer to the crossflow direction normal and tangential to the walls, s refers to the evaluation at the arbitrary point in the subsonic region, and the subscript W refers to the evaluation at the wall. Restricting our attention to flows where the subsonic region is sufficiently thin allows the integral in Eq. (12) to be neglected and hence this equation can be approximated by

$$h_1 h_T \rho w_n \Big|_s = h_1 h_T \rho w_n \Big|_w \quad (13)$$

As mentioned above, for the case of an impermeable wall Eq. (13) further reduces to

$$w_n \Big|_s = 0 \quad (14)$$

As a consequence of the thin subsonic layer assumption, the normal (to the wall) momentum equation then can be expressed as a balance only between the normal pressure gradient and the centrifugal (curvature) forces in the subsonic layer. For example, in general orthogonal coordinates, X_1 , X_2 , and X_3 with corresponding metric coefficients h_1 , h_2 and h_3 and velocity components w_1 , w_2 and w_3 this equation is expressed as

$$\frac{\partial P}{\partial x_n} = (-1)^T \frac{w_T}{h_T} \left(w_3 \frac{\partial h_3}{\partial x_2} - w_n \frac{\partial h_n}{\partial x_3} \right) + (-1)^n \frac{w_1}{h_1} \left(w_1 \frac{\partial h_1}{\partial x_n} - w_n \frac{\partial h_n}{\partial x_1} \right) \quad (15)$$

where X_n and X_T respectively refers to the appropriate cross-sectional direction normal and tangential to the wall (n and T have values of 2 or 3; direction 1 is the nominally streamwise direction). In summary, the new set

of governing equations consisting of the reduced form of the Navier-Stokes equations in the supersonic portion of the flow and the model set of equations in the subsonic regions of the flow (Eq. 13 instead of continuity equation and Eq. 15 for the normal momentum equation) has, on the bases of numerical experimentation (Ref. 16), been found to be well posed for solution by spatial forward marching for a wide range of practical problems.

Initial and Boundary Conditions

To uniquely define the problem of interest it is necessary to specify both initial and boundary conditions. For a spatial forward marching procedure, the initial conditions refer to the set of conditions that must be specified at the initial marching station. Boundary conditions must be set on the boundaries of the cross-sectional marching plane. For the calculation of the supersonic jet flow interacting with the coflowing stream, information must exist at an initial plane such that a reasonable approximation to a complete set of initial data can be constructed. In its most pure form this would be an initial plane where experimental or computational data was available such that all the initial conditions were known and consistent with the constitutive relations. In general, automatic generation of initial profiles is not straightforward for the present type of flow. However, if the flow is two-dimensional, a limited automation is possible. Usually a limited amount of information is available, where, for instance, freestream conditions with a boundary layer thickness and a skin friction coefficient on the nozzle surface might be known. In this case, a theoretical boundary layer profile of the pertinent variables (velocity components, temperature, pressure, etc.) can often be derived and matched with the flow outside the boundary layer. Analysis of the characteristics of the supersonic three-dimensional Euler equation shows that there are five characteristics entering the upstream boundary of the computational domain. It is argued that the reduced form of the Navier-Stokes equations used here would not require more boundary conditions than the Euler equations and this certainly appears reasonable at very high Reynolds numbers far from the solid walls. Thus, it is argued that five conditions must be set on the inflow boundary. In this study those conditions are chosen as the three velocity components, the pressure and the temperature. It is to be emphasized that the initial

conditions must in some sense be consistent with the governing equations in a hyperbolic system. In supersonic flow computations inconsistencies, perturbations, etc. can persist far downstream.

As used in this investigation the boundary conditions utilized on the boundaries of the cross-sectional plane can be divided into three categories: (1) wall conditions, (2) symmetry conditions and (3) external flow conditions. Analysis of the characteristics of the boundary layer equations shows that four conditions must be specified on walls. Arguing that in the limit as the present system approaches the wall it should approximate the boundary layer equations, the same four conditions are used here. For this study the no-slip conditions are used for the streamwise and tangential cross plane velocity components, i.e.,

$$w_l = 0 \quad (16)$$

and

$$w_T = 0 \quad (17)$$

where again the subscript l refers to the streamwise direction and the subscript T refers to the cross plane tangential velocity direction. For the cross plane normal velocity component either the normal velocity or the normal mass flux are specified, i.e.,

$$w_n = w_w \quad (18)$$

or

$$(\rho w)_n = \rho_w w_w \quad (19)$$

where the subscript W refers to the wall value (specified). The fourth condition (the thermal condition) used is to either specify an adiabatic wall

or to specify the wall temperature (a cold or hot wall). The condition can be specified respectively as

$$\vec{n}_w \cdot \nabla T = 0 \quad (20)$$

or

$$T = T_w \quad (21)$$

where in this case \vec{n}_w represents the unit vector normal to the wall. In addition, a fifth condition, not required by the characteristic analysis, is used to close the set of equations. The need for this fifth condition could be removed by the use of one-sided differencing or by applying one of the governing equations at the wall. In this study for convenience the second method was used and the boundary layer approximation to the normal momentum equation was applied at the wall. This can be expressed as

$$\vec{n}_w \cdot \nabla P = 0 \quad (22)$$

Studies have indicated that there is little difference between using this equation and the nonapproximated normal momentum equation.

The symmetry conditions are meant to be applied on a plane or axis of symmetry. The velocity conditions used require that the cross plane velocity component normal to the axis or plane of symmetry equals zero, i.e.,

$$\vec{n}_s \cdot \vec{V} = 0 \quad (23)$$

where n_s is the unit vector normal to the axis or plane of symmetry and that the first derivatives of the remaining two velocity components equal zero. Two other conditions must be set on the axis or plane of symmetry. Usually the symmetry conditions on pressure and temperature are used, viz.

$$\vec{n}_s \cdot \nabla P = 0 \quad (24)$$

and

$$\vec{n}_s \cdot \nabla T = 0 \quad (25)$$

The final category of boundary conditions used in this investigation is the boundary conditions to be used on what can be considered to be external surfaces. Specifically these boundary conditions are meant to be used on the external boundary of the coflowing ambient stream. In this case a set of boundary conditions that will allow all disturbances which originate from within the computational domain to pass through the boundary without spurious reflection. The technique used in this investigation is based on the concept that in a simple wave region the flow properties remain constant along Mach lines. Thus the first derivatives of the flow variables in the direction of the Mach angle should be small and are here set equal to zero. The technique is termed Mach wave extrapolation and yields the boundary conditions

$$\vec{n}_m \cdot \nabla \vec{V} = 0 \quad (26)$$

$$\vec{n}_m \cdot \nabla P = 0 \quad (27)$$

and

$$\vec{n}_m \cdot \nabla T = 0 \quad (28)$$

where \vec{n}_m is the unit vector in the direction of the local Mach angle. This technique requires computation of the Mach angle and has been successfully applied to a number of test cases both by the present authors and the authors of Ref. 25 and 26.

SOLUTION OF THE GOVERNING EQUATIONS

Numerical Methods

The governing equations in both the supersonic and the embedded subsonic portion of the flow are simultaneously solved by the consistently split linearized block implicit (LBI) technique described in detail in Refs. 27 and 28. This technique can be logically divided into three parts: (1) linearization of the governing equations (2) discretization of the resulting set of linearized equation by finite difference approximation of derivative terms and (3) simultaneous solution of the resultant set of linear coupled algebraic equations. Application of the LBI technique to a set of governing equations (and boundary conditions) that is well posed for forward marching is straightforward. The system of governing equations can be written in the following form:

$$\frac{\partial H(\phi)}{\partial x} = D(\phi) + S(\phi) \quad (29)$$

where ϕ is the column vector of dependent variables (w_1, w_2, w_3, ρ, h_0), H and S are column vector algebraic functions of ϕ , and D is a column vector whose elements are the spatial differential operators.

When a solution at the $i + 1^{st}$ station, at some distance Δx downstream, is desired after a solution is obtained at an arbitrary i^{th} streamwise station, the solution procedure is based on the following implicit marching direction difference approximation of Eq. (29)

$$(H^{i+1} - H^i) / \Delta x = (D^{i+1} + S^{i+1}) \quad (30)$$

where, for example, H^{i+1} denotes $H(\phi^{i+1})$. A local spatial linearization (Taylor series expansion about ϕ^i) of requisite formal accuracy is introduced, and this serves to define a linear differential operator L such that

$$D^{i+1} = D^i + L^i (\phi^{i+1} - \phi^i) + O(\Delta x^2) \quad (31)$$

Similarly

$$H^{i+1} = H^i + \left(\frac{\partial H}{\partial \phi}\right)^i (\phi^{i+1} - \phi^i) + O(\Delta x^2) \quad (32)$$

$$S^{i+1} = S^i + \left(\frac{\partial S}{\partial \phi}\right)^i (\phi^{i+1} - \phi^i) + O(\Delta x^2) \quad (33)$$

Eqs. (31-33) are inserted into Eq. (30) to obtain the following system which is linear in ϕ^{i+1}

$$(A - \Delta x L^i)(\phi^{i+1} - \phi^i) = \Delta x (D^i + S^i) \quad (34)$$

and which is termed the linearized block implicit (LBI) scheme. Here A denotes a square matrix defined by

$$A \equiv \left(\frac{\partial H}{\partial \phi}\right)^i - \Delta x \left(\frac{\partial S}{\partial \phi}\right)^i \quad (35)$$

Eq. (35) is $O(\Delta X)$ accuracy.

To obtain an efficient algorithm, the linearized system, Eq. (34) is split using ADI techniques. To obtain the split scheme, the multidimensional operator, L, is rewritten as the sum of two 'one-dimensional' sub-operator L_1 ($i = 2, 3$) each of which contains all terms having derivatives with respect to the i^{th} -cross plane coordinate. The split form of Eq. (34) can be derived either as in Ref. 27 by following the procedure described by Douglas and Gunn (Ref. 29) in their generalization and unification of scalar ADI schemes, or using the approximate factorization as in Ref. 30. For the present system of equations, the split algorithm is given by

$$(A - \Delta x L_1^i)(\phi^* - \phi^i) = \Delta x (D^i + S^i) \quad (36)$$

$$(A - \Delta x L_2^i)(\phi^{i+1} - \phi^i) = A(\phi^* - \phi^i) \quad (37)$$

where ϕ^* is the consistent intermediate solution (Ref. 28). If spatial derivatives in L_1 and D are replaced by the difference formulae indicated previously, then each step in Eq. (36) and Eq. (37) can be solved by a block tridiagonal elimination.

Combining Eqs. (36) and (37) gives

$$(A - \Delta x L_1^i) A^{-1} (A - \Delta x L_2^i) (\phi^{i+1} - \phi^i) = \Delta x (D^i + S^i)$$

which approximates the unsplit scheme, Eq. (34) to $O(\Delta X^2)$. Since the intermediate step is also a consistent approximation to Eq. (34), physical boundary conditions can be used for ϕ^* (Refs. 28, 31).

TEST CASES

A primary objective of this study was to develop a computational procedure which is capable of analyzing a supersonic jet flow interacting with an external stream. Therefore, three three-dimensional and one axisymmetric test cases were considered to demonstrate the capability of the analysis and the associated computer program (PEPSIN). Three-dimensional cases deal with the underexpanded supersonic jet flow (i.e., $P_J > P_E$) exhausting from the rectangular nozzle of three different aspect ratios (1, 2 and 5 respectively). As discussed in the Introduction Section, a supersonic jet was assumed to interact with a supersonic external stream. However, since no data were available to validate the results obtained by PEPSIN analysis for these three-dimensional cases, it was decided to consider an axisymmetric case (Figure 3) first because of the existing computational data (Ref. 17) to validate the PEPSIN results. Compared to the three-dimensional case, the axisymmetric results are, in general, easy to interpret. Moreover, experience and insight obtained during the study of the axisymmetric case is useful for the study of three-dimensional cases. Most of the flow conditions utilized in the computation of the axisymmetric case were obtained from Ref. 17. Some of the unavailable conditions were either assumed or estimated. The analysis was performed in the same axisymmetric geometry as reported in Ref. 17. The Mach number of both jet and external stream was 2.0. The jet flow was hot ($T_J = 1500^\circ\text{K}$) and the static pressure ratio of jet with respect to the external stream was $P_J/P_E = 1.45$. The static temperature of the external stream was 240°K . The static pressure of the external flow was assumed as $2864 \text{ (Newton/m}^2\text{)}$. Thus, the computed Reynolds number per unit length based on the ambient flow conditions was 1.6685×10^6 . To analyze the interaction of the jet flow with the coflowing ambient supersonic flow, 98 mesh points were distributed in the radial direction. The grid points were tightly packed in the vicinity of estimated turbulent mixing layer region to achieve the maximum resolution. The continuity equation, two momenta equations and the energy equation were used as governing equations. For the present case, the subsonic regions associated with the nozzle boundary layer and the base of nozzle wall are embedded in the supersonic flow. However, these embedded subsonic regions appeared to be excluded from consideration in Ref. 17 because the technique

used in Ref. 17 was not capable of analyzing such regions. Therefore, since it was desired to exercise the PEPSIN code under the same conditions as in Ref. 17 for this test case, the solution was marched with the initial profiles devoid of subsonic flow in this study. However, it should be noted that proper treatment of the subsonic regions may be very important in simulating physical situations. Since Ref. 17 didn't specify explicitly how the initial profiles were generated, the shape of initial profiles in the present calculations was approximately represented by the profiles which would be expected downstream in the mixing layer. For instance, the resulting velocity profile at the initial station would consist of two different uniform streams connected by the smooth hyperbolic tangent curve which approximate the transverse distribution of streamwise velocity component in the mixing layer. The boundary conditions imposed on the axis of symmetry are symmetry conditions, while the conditions on the external boundary are Mach line extrapolations. The streamwise step size used for marching the solution was 0.005 of the transverse size of computational domain, i.e., 0.025 of jet radius (corresponding to a Courant number of 1.26).

The computed results by the PEPSIN code are compared with the calculation of Dash et al. (Ref. 17) in Figures 4(a) and 4(b). The figures show static pressure variation in the streamwise direction at two different radial locations (along the jet axis and $r/r_j = .5$ where r_j refers to the radius of axisymmetric jet). Considering the uncertainties of the initial flow conditions which were used in PEPSIN analysis, the agreement between two different calculations is reasonable. The PEPSIN analysis indicates a stronger streamwise damping of wave strengths compared to the computation (Ref. 17). This appears to be associated with the difference in turbulent dissipation which occurs as a result of using different turbulence models in the two separate computations. The PEPSIN analysis is based on an algebraic mixing-length turbulence model, whereas a two-equations model ($k\epsilon$ model) was utilized by Dash and co-workers. However, both calculations show the absence of any noticeable wave structure beyond the first shock cell, which indicates that the reflected wave resulting from the interaction at the end of the first shock cell becomes very weak. The favorable comparison with the results of Ref. 17 indicates that both PEPSIN approach and its computer program are fundamentally sound.

After the PEPSIN code was successfully validated for an axisymmetric case, three-dimensional cases were considered. As discussed above, the underexpanded supersonic jet was assumed to be exhausted from a rectangular nozzle of aspect ratio 1, 2 and 5 respectively (Figure 5). An aspect ratio of a cross-section is defined by the ratio of spanwise dimension divided by the transverse dimension. Unlike the previously considered axisymmetric case, estimation of initial profiles for three-dimensional cases was not straightforward. Based upon our experience with the previous supersonic flow calculations, an initial profile must be not only smooth but also consistent with the governing equations. If not, perturbations, inconsistencies, etc. can persist far downstream. The difficulty of being consistent with the governing equations has been found to be further pronounced for three-dimensional cases. Therefore, in this study the problem was slightly modified such that initial profiles could be generated more easily. Thus, the jet was assumed to be exhausted from a short straight duct with a square or rectangular cross-section. In the present study we are primarily concerned with developing a computer code capable of predicting the interaction of a supersonic jet with an ambient supersonic flow downstream of exit plane. Since no specific nozzle geometry was defined in the present investigation, the length of duct was kept short mainly to reduce the computation time. The PEPSIN code is, however, capable of analyzing the flow field within a longer nozzle of more complex geometry as shown by the applications of the PEPSIS code to inlet flow systems (Ref. 16).

In this study the streamwise marching solution procedure began at a location upstream of the duct entrance. As an initial profile for this problem, the flow was assumed to consist of two coflowing uniform streams at different velocities as shown in Figure 5. One stream at faster speed moves into the duct, whereas the external flow moving at a slower speed moves around the duct. The initial conditions such as velocity ratio of two streams and corresponding pressure ratio were assumed to be the same as the previously considered axisymmetric case. As a consequence of the modification, the flow at the duct exit was expected to contain some extra physical features due to the development of flow near the duct entrance. The flow both within and outside the duct was complicated because of the shock waves generated due to the initial shock wave-boundary layer development on



the walls of the duct. In particular, the pressure field within the cross-section became non-uniform as one would expect in a rectangular duct flow.

The Mach number of both the initial streams was 2.0, while the Reynolds number per unit length based on the free stream (external flow) properties was 1.6685×10^6 (a jet exit Reynolds number was 2.847×10^5). In order to analyze both the internal and external flow of the duct as well as the jet flow interacting with the external stream, 50×50 mesh points for aspect ratio 1 and 50×80 mesh points for both aspect ratio 2 and 5 were distributed in each cross-sectional plane. Mesh points were packed in the region of the interaction. Because of the geometrical shape of both duct and jet flow, two planes of symmetry can be associated with this problem, and hence the flow need only be solved in the quarter plane. On the planes of symmetry, symmetry boundary conditions were utilized. On the other hand, three no-slip conditions for the velocity components, normal momentum equation and adiabatic wall conditions were imposed on the solid walls. On the external boundary of flow symmetry boundary conditions were used again. For the three-dimensional cases, the continuity equation, three momenta equations and the energy equation were used as governing equations. The turbulence model utilized in this study was an algebraic mixing length model. This model was selected primarily because it is convenient to use at this point (demonstration of capability of new computer code was one of the primary goals in this study) and, furthermore, it can save some computer resources (time and storage). However, if a demonstrated need for advanced turbulence model exists, this can be easily accommodated within the existing code framework. The mixing length was assumed to be proportional to the half width of mixing region and, therefore, constant at each streamwise location. In the present study, for the purpose of the turbulence model the spreading angle of the mixing region was assumed to be 3° .

The computed results of three-dimensional cases are presented in Figs. 8 through 16. Since experimental data is not available for direct comparison, discussion will primarily focus on qualitative description of the essential physical features predicted by the computation. To assist the reader in interpreting the plots of various variables, both Figs. 6 and 7 are presented. Figure 6 illustrates a sideview of the computational domain

on a vertical plane when the computational domain is cut through the duct vertically. Figure 7 provides a cross-sectional view of the domain.

As discussed before, three-dimensional test cases were run for three different aspect ratios of rectangular cross-section. Therefore, discussion will first concentrate on the description of the results for an aspect ratio equal to 1. Then, the effects of larger aspect ratios on the flow field will be considered.

Calculated results in the form of stagnation pressure and cross-sectional secondary velocity vectors for square nozzle case (aspect ratio 1) are presented in Figs. 8-9. Stagnation pressure isobars in the cross-sections at seven streamwise locations are presented to define a streamwise development of plume boundary (Fig. 8). Initial upstream contours were obtained at a distance of $X/H = 0.33$ from the exit plane of the duct where H is a height of the duct. H is chosen to be 0.4. Meanwhile, final downstream contours were obtained at a distance of $X/H = 22$ from the exit plane of the duct. The plume boundary experiences a severely distorted square shape before evolving into a smooth shape far downstream. This is probably due to strong three-dimensional effects of the flow. Compared to the usual supersonic jet exhausted from a nozzle, these three-dimensional effects may have been more pronounced by the use of a short straight duct as a means of avoiding the difficulty associated with generating three-dimensional initial profiles. As discussed before, a uniform flow was assumed to move into the duct entrance. As a consequence, the flow within the duct becomes highly three-dimensional due to the generation of shock waves associated with the leading edge. Combined with the three-dimensional effects, a highly non-uniform pressure develops in the cross-section of duct. In particular the pressure in the corner region is large. Thus, the largest pressure difference across the duct wall occurs in the corner region. Because of this non-uniform pressure distribution, a distortion of the plume boundary occurs. As can be seen in Fig. 8, the distortion is slightly asymmetric about the bisecting line (45° line) from the corner. The asymmetry was caused by the approximations used in the subsonic layer of the corner region of a nozzle. As discussed in the analysis section, both the continuity and normal momentum equations are approximated. The nearest solid wall from a grid point is identified to implement the subsonic approximations. However, the grid points located on the bisecting line have

two such surfaces. In this case the upper surface was arbitrarily chosen and, hence, a slight asymmetry introduced. It should be noted that asymmetry can be reduced by providing more grid points in the corner region, and as the flow proceeds downstream this effect significantly diminishes. A streamwise development of secondary velocity vectors in the cross-section is presented in Fig. 9. A strong secondary flow is seen in the corner region. As a result of the non-uniform pressure distribution, the flow develops two streamwise vortices which will eventually be diffused by the turbulent mixing action. To show the effects of jet aspect ratio on the flow field, Figs. 10 and 11 are presented. Both figures illustrate a streamwise development of stagnation pressure contours. Initial upstream contours are obtained at a distance of $X/H = 0.675$ from the exit plane of the duct where H is a height of duct. H is taken to be 0.2. Final downstream contours are obtained at a distance of $X/H = 44$.

The outer edge of the mixing region may be defined qualitatively based on these two figures. Examination of the plots indicates that the mixing layer spreads out more quickly in the corner region as discussed previously in the case of aspect ratio 1. Streamwise development of cross-sectional plume boundary is very similar to that for aspect ratio 1, although distortion of plume boundary is localized in the corner region at an aspect ratio 5. It appears that the rapid mixing in the corner region is related to the three-dimensional effects. However, as both figures show, the plume boundary gradually approaches a smooth elliptic or circular shape in far field. In the near field downstream of the nozzle exit, the high pressure in the corner region associated with the shock waves may have played a significant role in enhancing the mixing. It should be noted that similar mixing behavior may not be observed when the calculation is performed for a realistic nozzle under the initial profiles based on the exit flow conditions.

DISCUSSION AND CONCLUSIONS

The primary objective of this investigation was to develop and validate a numerical procedure for the calculation of the interaction of three-dimensional supersonic jet with an external flow. The new computer code (named PEPSIN) was developed by extending the capability of existing code (PEPSIS) suitable for an analysis of jet flows. The major difference between these two codes lies in the new capability of calculating flow fields when the computational domain contains internally embedded solid bodies. To validate the code, one two-dimensional and three three-dimensional cases were computed. Comparison of the two-dimensional results with other computations was performed to validate the new code for this class of cases. Three-dimensional calculations were successfully performed, and essential physical features were predicted.

USERS' MANUAL

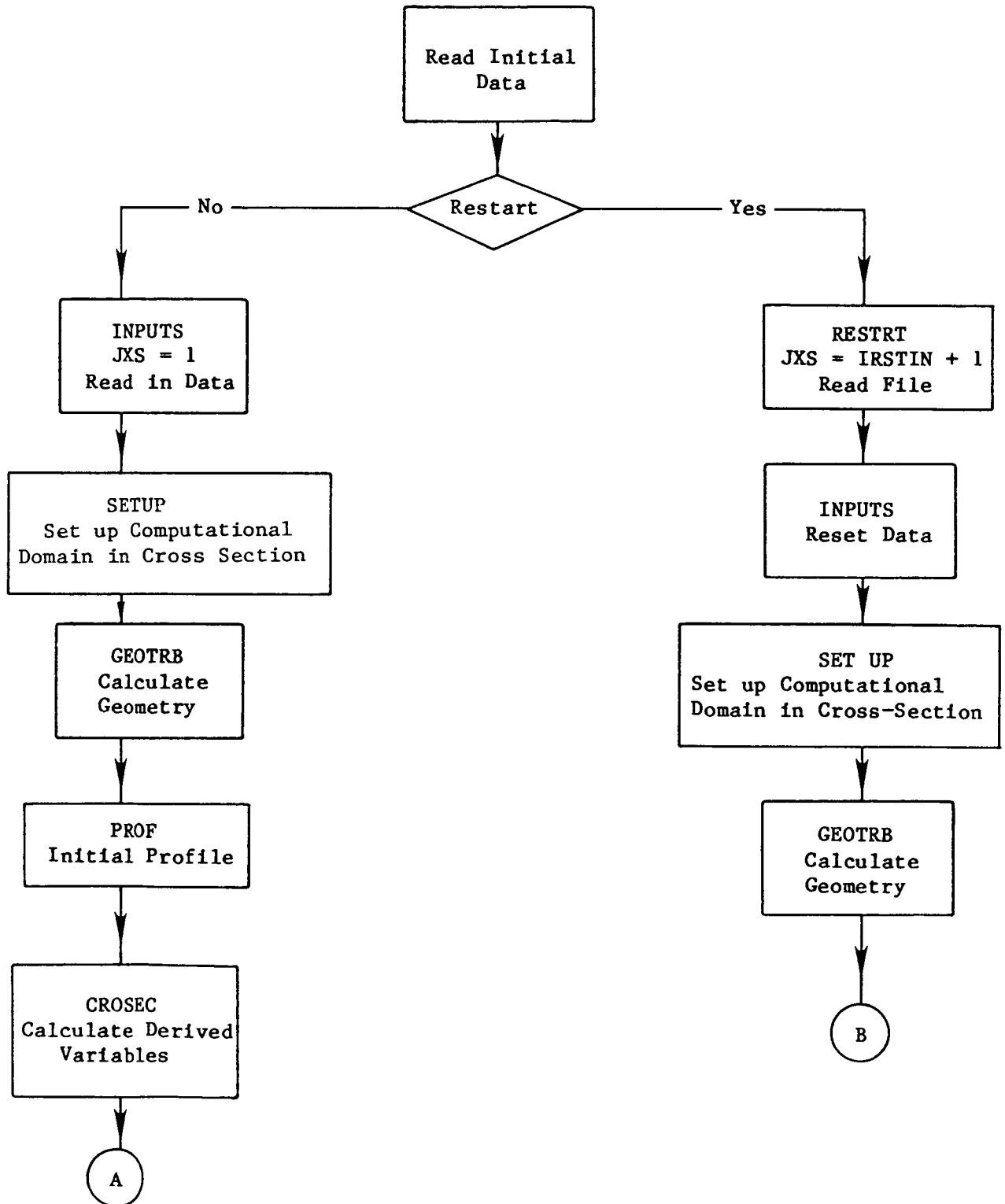
The PEPSIN Users' Manual is meant to serve as a guide in helping the user make successful runs with the PEPSIN computer program. The degree of success obtained by the user will depend on the skill of the user and his ability to correctly apply the code to his particular problem. The code will solve the governing equations, subject to the user supplied boundary conditions, however, meaningful results will only be obtained if the boundary conditions are appropriate to the problem. In addition, the user must specify viscosity models, initial conditions, a coordinate system and the location of grid points to adequately resolve the flow. The user with a good knowledge of the physics involved in his problem and how the code models the physics should with a moderate amount of experience be able to successfully apply the code to a wide variety of supersonic flow problems.

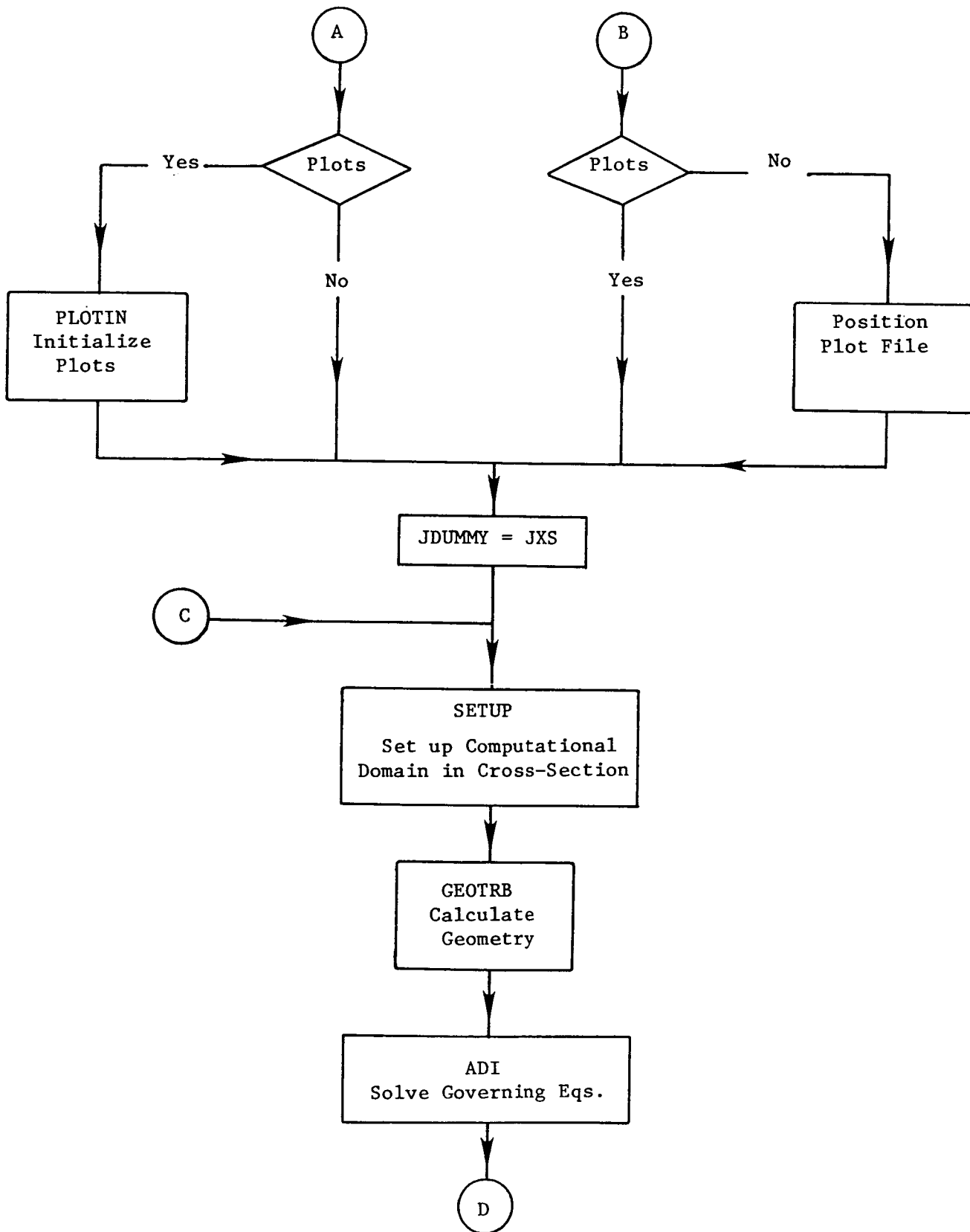
The Users' Manual is divided into eight parts consisting of: (1) a flow diagram, (2) a brief description of each subroutine and its use, (3) a list of the Fortran variables and a description of their meaning, (4) a description of the logical file units utilized by the PEPSIN computer code, (5) a detailed description of the input required by the PEPSIN computer code, (6) a description of the common error conditions that may be encountered during the execution of a PEPSIN run and the corrective action to be taken, (7) sample input for a three-dimensional case and (8) sample output for the corresponding case.

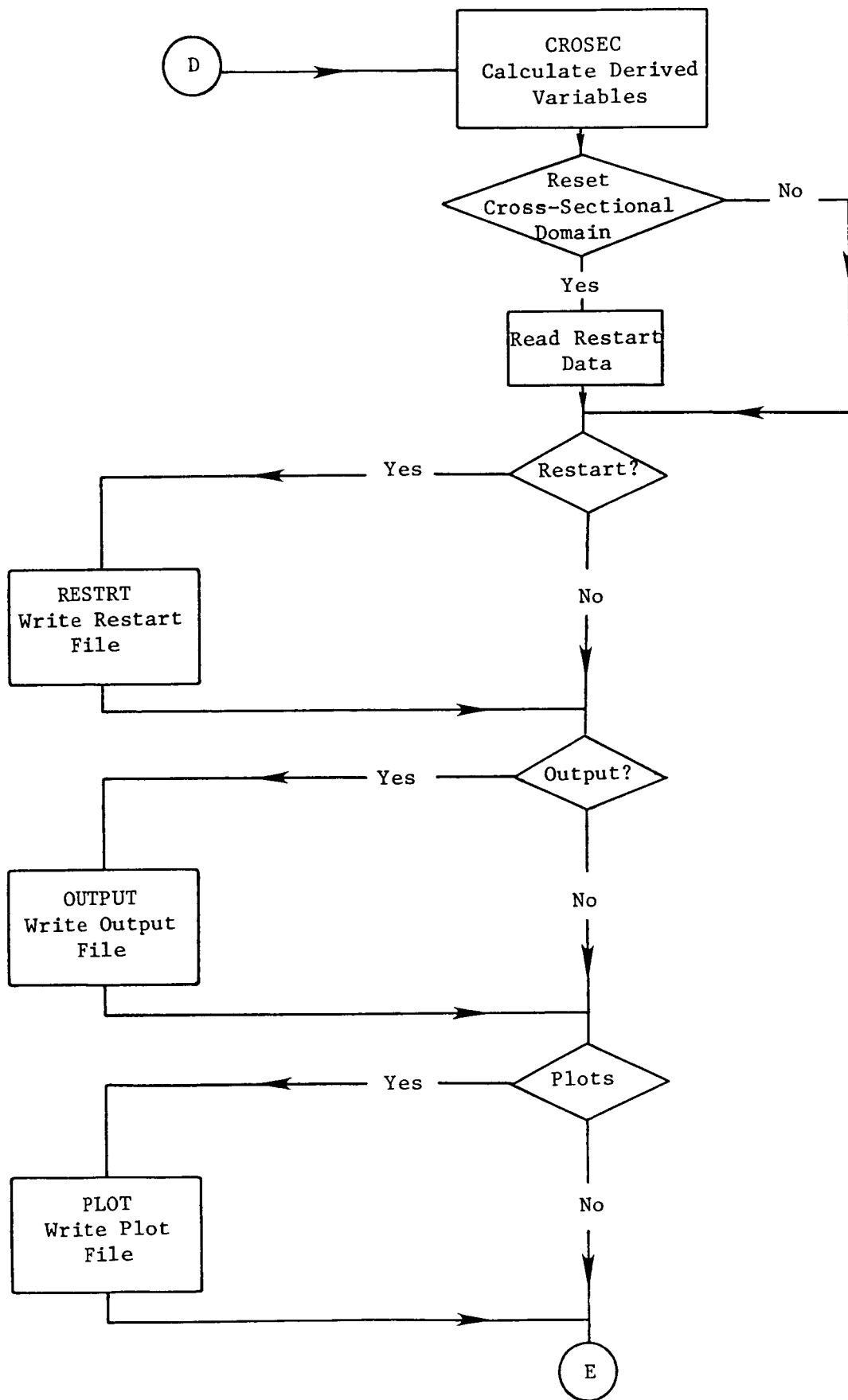
Flow Diagram

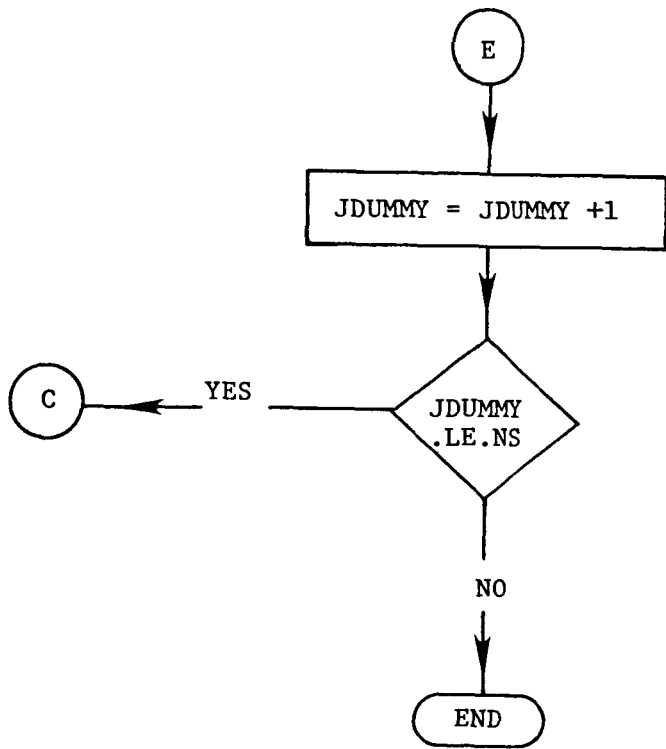
The purpose of the flow diagram is to help the user understand the basic flow of information within the PEPSIN computer code. Because of the size of the code (approximately 13,000 cards), a detailed flow diagram would be prohibitively large and probably be of little value to the user. Therefore, the flow diagram is intended only to give a general overview of the structure of the code. The interested user is urged to consult the program listing for details.

Flow Diagram for the PEPSIN Computer Code









PEPSIN Subroutines

<u>Subroutine</u>	<u>Purpose</u>
ADDRES	Calculate addresses for finite difference representation of metric and fluid dynamic variables.
ADI	Master control subroutine for ADI procedure.
ADICP	Control subroutine for coupled equations.
ADIUN	Control subroutine for uncoupled equations.
AMARCH	Linearizes streamwise convective terms.
AMATRX	Linearizes all streamwise terms.
ARTVIS	Artificial dissipator subroutine.
AVRG	Calculates averaged quantities in cross plane.
BC	Boundary condition subroutine.
BLKDATA	Stores default values of key variables.
BLT	Calculates boundary layer thickness.
BULEEV	Calculates Buleev mixing length.
CONVCT	Linearizes cross plane convective terms.
CORBND	Calculates geometry transformation information on boundaries.
CORTRN	Calculates geometry transformation information for interior points.
CROSEC	Control subroutine for calculation of derived variables.
CURVT	Linearizes curvature terms.
DATAS	Logical file control subroutine.
DELTX	Calculates transformation information for ICORD = 2 option.
DELTXZ	Calculates transformation information for ICORD = 3 option.
DIFF	Linearizes diffusion terms.

<u>Subroutine</u>	<u>Purpose</u>
DISFCN	Calculates dissipation function.
DIV	Calculates divergence of velocity.
DOP2	Control subroutine for linearization of Y-direction and source terms.
DOP3	Control subroutine for linearization of Z-direction terms.
ENDCAP	Control subroutine for endcap conditions.
EOS	Equation of state subroutine linearizes and updates pressure and temperature.
FGFUN	Calculates geometry groupings.
GAUSS	Solves uncoupled tridiagonal set of equations.
GENCBC	Control subroutine for coupled boundary conditions.
GENUBC	Control subroutine for uncoupled boundary conditions.
GEORD	Controls setup of computational domain and calculates geometry at each cross-section.
GEOTRB	Generates metric information.
INDIC	Determines if flow is subsonic or supersonic at grid points.
INPUTS	Input subroutine. Input data enters and is processed.
INTEBC	Performs a two-dimensional linear interpolation for wall transpiration rates.
LAMP	Calculates laminar profile.
LAW	Calculates nondimensional velocity, U^+ as a function of nondimensional distance Y^+ .
LENGTH	Calculates mixing length.
LOOP	Determines the loop index at a grid point in both Y and Z-direction.
MAIN	Main control program.
MATPRT	Prints elements of block tridiagonal matrix.

<u>Subroutine</u>	<u>Purpose</u>
MGAUSS	Control subroutine for solving block tridiagonal systems of equations.
MGERR	Calculates error associated with solving block tridiagonal system of equations.
NMLIST	Subroutine for printing namelist input information.
OUTPUT	Control subroutine for printing out results on a cross-sectional (Y-Z) plane.
PLOT	Writes plot information on logical file unit JPLOT.
PLOTIN	Writes first record of general information on logical file unit JPLOT.
PROF	Generates initial profiles.
QUICK	Matrix elimination subroutine.
READZ	Prepares variables for printing.
RESTRT	Reads and writes restart information.
ROTATE	Rotates data from columns to rows and vice versa.
SETBVL	Updates boundary information a line at a time.
SETBVP	Updates boundary information a point at a time.
SETUP	Determines the extent of computational domain, number of loops and subsections at each cross-section
SHEAR	Control subroutine for the calculation of wall shear velocity.
SONIC	Determines the extent of supersonic and subsonic region.
SPREAD	Spreads two-dimensional data to three dimensions.
STORG	Control subroutine of the storage of temperature and density on boundaries for viscosity calculation.
SUB	Contain special subsonic logic.
SWITCH	Calculates streamwise location for switch of boundary condition.
TANHYP	Grid stretch subroutine.

Subroutine

Purpose

TNDER	Calculates normal derivative of temperature at a wall.
TRANS	Transition model subroutine.
TURB	Turbulence model subroutine.
TURBP	Calculates turbulent profile based on theory of Maise-McDonald.
VISCOS	Constant and laminar viscosity subroutine.
WALLFN	Calculates wall shear velocity.
WHERE	Determines the surface number of four nearest boundaries for a given point.
WRMATR	Writes block tridiagonal dump information on logical file device NUNERR.
YCALC	Calculates Y and Z locations.
ZERO	Zeros out linearization arrays.

Logical File Units Utilized by PEPSIN Computer Code

The PEPSIN computer code utilizes up to eleven (11) logical file units during the execution of a run stream. In many cases not all eleven units are used, and hence in these cases there is no need to define all eleven units. All references to a logical file unit in the PEPSIN computer code is accomplished through the use of a FORTRAN name rather than through a specific unit number. Thus, if the user desires to change a logical file unit number, this can be done through the input file. A list of the logical file units utilized by the PEPSIN computer code, their FORTRAN name, default value unit number, and a brief description of the use of the unit is presented below. All units are sequential.

<u>FORTRAN Name</u>	<u>Default Unit Number</u>	<u>Description</u>
MIN	5	Input data unit.
MOUT	6	Printed output unit.
MASS1	8	First unit which stores dependent and derived variables either by rows or columns. Not needed for two-dimensional cases, i.e., when TWOD = .TRUE.
MASS2	9	Second unit which stores dependent and derived variables either by rows or by columns. Not needed for two-dimensional cases, i.e., when TWOD = .TRUE.
MSDD	15	Unit which stores dependent and derived variables by rows or columns. Not needed for two-dimensional cases, i.e., when TWOD = .TRUE.
JDRUM	11	Unit which contains output of ADD computer code. Only needed when IGEOM = 10 or 11.

<u>FORTRAN Name</u>	<u>Default Unit Number</u>	<u>Description</u>
KDRUM	12	Unit which stores final metric information. Needed in all cases.
NUNERR	14	Unit which stores information concerning the block tridiagonal matrix inversion. Needed when MGDMP \neq 0.
JPLOT	15	Unit which stores plotting information. Needed when IPLOT \neq 0.
JRSTIN	10	Input restart unit. This unit contains appropriate common block information and the values of the dependent and derived variables at each cross-sectional grid point at the restart streamwise station. Needed only when IRSTIN \neq 0.
JRSTOT	10	Output restart unit. This unit contains appropriate common block information, and the values of the dependent and derived variables at each cross-sectional grid point at the restart streamwise station. Needed only when IRSTOT \neq 0. Default is JRSTIN = IRSTOT; however, it is desired to have separate input restart and output restart files set JRSTOT = 17.

PEPSIN Input

Except for an initial title card and plot file input data, the entire PEPSIN input is entered by means of the NAMELIST format. There are two primary advantages to the use of the NAMELIST format: (1) that if the default values (defined in the block data subroutine) are acceptable, the user need not input that variable, and (2) the order (within a given NAMELIST) in which the variables are entered is irrelevant. There are seven NAMELIST input files in the PEPSIN code, \$REST, \$LIST1 through \$LIST5 and \$LISTR. The first file is read in the main program and enters restart information. The second through sixth NAMELIST files are read in subroutine INPUTS. Basically, the NAMELISTS \$LIST1 through \$LIST5 can be divided by function. \$LIST1 enters information about the governing equations and appropriate boundary conditions, \$LIST2 enters reference and free stream conditions, \$LIST3 enters geometric information, \$LIST4 enters viscosity model and initial profile information and \$LIST5 enters file output information. The last NAMELIST file is read in subroutine CROSEC. \$LISTR enters information needed to reset the grid array indicator, IFBW, for the computational domain in the cross-section. The PEPSIN computer code evolved from the PEPSES computer code (Ref. 16) which was developed primarily for flows in supersonic inlets and for external flow situations. The primary difference between the two codes is in the ability of PEPSIN to consider cross-sectional geometric configuration that contain re-entrant corners as for example, might occur in the geometry illustrated in Fig. 12. In concept, the extension of the PEPSES procedure to such geometric configurations is straightforward. However, to incorporate the re-entrant corner logic into the code in a general manner adds considerable complexity to the computer code. To minimize the effect of the complexities on the user while at the same time not detract from the generality that may be necessary at the present time or in the future, a very general procedure was incorporated into the PEPSIN code. This procedure utilizes the concept of a "grid array indicator" (FORTRAN variable IFBW) to type the grid points in the cross-sectional plane. Referring to Fig. 12, it can be seen that the idea is to type the grid points according to the function they serve. The convention is to type grid points as follows:

- IFBW=1 Indicates that a grid point is an interior fluid point.
- IFBW=2 Indicates that a grid point is an interior solid point, and thus does not effect the calculation.
- IFBW=3 Indicates that a grid point is a noncorner boundary point.
- IFBW=4 Indicates that a grid point is an inward corner point.
- IFBW=5 Indicates that a grid point is a re-entrant corner point.

The FORTRAN variable is dimensioned IFBW(NN,NN). Based upon the information supplied by the user, subroutine SETUP sets up the necessary parameters to control the ADI procedure. Initially, the grid array indicator is introduced through NAMELIST LIST3. As the solution is marched downstream, the values of IFBW will remain unchanged. However, when it is desired to change the cross-sectional grid structure this can be accomplished by requesting that NAMELIST LISTR be read. This is determined by the input FORTRAN variable NBRKX which is read in NAMELIST LIST 3.

In addition to the explanation of the grid array indicator, it is convenient at this point to explain the surface number (KSURF) convention and direction (IDIR) convention utilized throughout the PEPSIN computer code. Several input variables, e.g. IBOUND(KSURF, IDIR) require a knowledge of this convention to correctly input data. The boundary surfaces are numbered according to a surface number relative to a cross-sectional computational direction. The convention is to allow values of IDIR=1 and 2 to correspond to the y and z physical directions, respectively. Referring to Fig. 12, it can be seen that the surfaces (with respect to y-direction) are numbered 1Y to 10Y. This corresponds to values of KSURF ranging from 1 to 10 and a value of IDIR corresponding to the y-direction i.e. IDIR=1. The analogous convention is also applied to the z-direction surfaces. Thus, the value of KSURF represents the surface number relative to a given cross-sectional direction, IDIR.

A description of all the PEPSIN input information will be given below.

Card 1

<u>Columns</u>	<u>Format</u>	<u>Variable</u>	<u>Function</u>
1 - 24	6A4	TITLE(I)	Title Card

Card 2

<u>Columns</u>	<u>Format</u>	<u>Variable</u>	<u>Function</u>
1 - 2	1I2	ISYM	Reciprocal of Symmetry
3 - 12	1F10.0	SYSTEM	SYSTEM = 1 - Quasi-Cartesian Coordinates SYSTEM = 2 - Quasi-Cylindrical Coordinates

Namelist Input Description

Namelist or Variable Name <u>REST</u>	Description <u>Restart Options</u>
IRSTIN	Marching station number where data is to be read in for restart case. IRSTIN = 0: Dead start case. IRSTIN ≠ 0: Restart case started at station IRSTIN. Default: 0.
IRSTOT	Interval for saving restart information. IRSTOT = 0: No restart information is saved. IRSTOT ≠ 0: Information is saved at each IRSTOTth station. Default: 0
JRSTIN	Logical file name of input restart file. Default: 10.
JRSTOT	Logical file name of output restart file. JRSTOT and JRSTIN do not have to be same file. Default: 10:
NFILE	File number on unit .JRSTIN desired for restart. Default: 0.
NSAVED	Number of restart stations saved on JRSTOT. On a restart by setting JRSTOT = JRSTIN and NFILE = NSAVED, one file can be used for both reading and writing without destroying the information previously saved. Default: -1.

Namelist Input Description

Namelist or
Variable Name
REST

Description
Restart Options

ICOMP

Flag for computer options:

ICOMP = 1: Univac computer option.

ICOMP = 2: CDC computer option.

ICOMP = 3: IBM computer - virtual memory option.

ICOMP = 4: Disk writing computer option.

Default: 4.

LIST1

Equations and Boundary Conditions

IHSTAG

IHSTAG = 0: Energy equation formulated in terms of static enthalpy.

IHSTAG = 1: Energy equation formulated in terms of stagnation enthalpy.

IHSTAG = 2: Stagnation enthalpy is constant.

Default: 1.

IBOUND(KSURF, IDIR)

Boundary characteristics (wall or non-wall) on surface KSURF in a computational domain.

IBOUND (KSURF, IDIR) = 1: Solid wall boundary.

IBOUND (KSURF, IDIR) = 2: Non-wall boundary.

Default: 40*1.

IEQBC(KSURF, IDIR, IEQ)

Boundary condition of the governing equation IEQ on solid surface KSURF.

Default: 120*2, 40*16, 40*11, 80*2.

JEQBC(KSURF, IDIR, IEQ)

Boundary condition of the governing equation IEQ on non-wall surface KSURF.

Default: 40*11, 20*2, 40*11, 20*2, 160*1.

Boundary condition options used for either IEQBC or JEQBC are as follows:

ϕ : Any dependent variable.

P: Pressure.

T: Temperature.

n = Normal to boundary.

\vec{n} = Unit vector perpendicular to axis of symmetry.

subscript C = Cartesian component.

Namelist Input Description

LIST1

Equations and Boundary Conditions

<u>Index</u>	<u>Description</u>
1	$\Delta\phi = 0$ (No change of ϕ at boundary)
2	$\phi = 0$
3	V or W known
4	ρV or ρW known
5	$\Delta P = 0$
6	$P = \text{PRESS}(\text{KSURF}, \text{IDIR})$
7	$\Delta T = 0$
8	$T = \text{TWALL}(\text{KSURF}, \text{IDIR})$
11	$\frac{\partial\phi}{\partial n} = 0$ (gradient of ϕ normal to boundary specified at boundary)
12	Mach Line Extrapolation using one-sided difference weights
13	Slip boundary condition for velocity using wall function
14	$\frac{\partial P}{\partial n} = 0$ (gradient of pressure normal to boundary)
15	$\frac{\partial P}{\partial n} = \text{curvature}$ (pressure gradient normal to boundary with curvature effects)
16	Momentum equation in direction normal to boundary
17	$\frac{\partial T}{\partial n} = 0$ (adiabatic condition for wall or symmetry condition for non-wall)
18	$\frac{\partial T}{\partial n} = \text{DTDN}(\text{KSURF}, \text{IDIR})$
19	Wall function boundary condition for temperature
20	$\frac{\partial\phi}{\partial n} = 0$ (same as 11, but applied at one grid point off the

Namelist Input Description

<u>LIST1</u>	<u>Equations and Boundary Conditions</u>
<u>Index</u>	<u>Description</u>
21	Mach Line Extrapolation using central difference scheme at one point off the boundary
41	$\frac{\partial^2 \phi}{\partial n^2} = 0$
42	$\frac{\partial^2 P}{\partial n^2} = 0$
43	$\frac{\partial^2 T}{\partial n^2} = 0$
44	$\frac{\partial U_c}{\partial n} = 0$
45	$\frac{\partial V_c}{\partial n} = 0$
46	$\vec{n}_c \circ \nabla P = 0$
47	$\vec{n}_c \circ \nabla T = 0$
TWALL(KSURF, IDIR)	Specified temperature on surface KSURF. Default: 40*1.0.
PRESS(KSURF, IDIR)	Specified pressure on surface KSURF. Default: 40*0.0.
DTDN(KSURF, IDIR)	Specified temperature gradient on surface KSURF Default: 40*0.0.
ASW(KSURF, IDIR) BSW(KSURF, IDIR) CSW(KSURF, IDIR) DSW(KSURF, IDIR)	Coefficient of a cubic polynomial fit for KSURFth surface to determine the axial location where boundary characteristics on surface KSURF should be changed from wall to non-wall or vice versa, i.e., IBOUND(KSURF, IDIR) automatically changed.

Namelist Input Description

LIST1

Equations and Boundary Conditions

Description

Default:

ASW = 40*1.0E + 10

BSW = 40*0.0

CSW = 40*0.0

DSW = 40*0.0

LIST2

Freestream and Reference Conditions

IUNITS	Sentinel for units. IUNITS = 1: English units IUNITS = 2: Metric units Default: 2.
LREF	Reference length. (ft or meters) No default.
REPL	Reynolds number per unit length (ft^{-1} or m^{-1}) No default.
MINF	Freestream Mach number. No default.
PINF	Freestream static pressure (lb/ft^2 or nt/m^2). No default.
PR	Laminar Prandtl number. Default: 0.74.
PRT	Turbulent Prandtl number. Default: 1.0.
PZERO	Freestream stagnation pressure (lb/ft^2 or nt/m^2) No default.

Namelist Input Description

LIST3

Geometric Options

ICORD

Flag for coordinate transformation.

ICORD = 1: Conformal coordinates

ICORD = 2: Nonorthogonal coordinates

X → X
Y → Y
Z → $\zeta(X,Z)$

ICORD = 3: Nonorthogonal coordinates

X → X
Y → $\eta(X,Y,Z)$
Z → Z

Default: 1.

NE(IDIR)

Number of grid points in the Y(IDIR = 1) and Z(IDIR = 2) directions.

No default values.

NS

Last streamwise station in each run.
(Solution is marched from IRSTIN+1 to NS).

No default.

XENTR, DELX,
IAP(ICOUNT), AP(ICOUNT),
DXMIN(ICOUNT),
DXMAX(ICOUNT)

XENTR is the initial streamwise location. DELX is the initial stepsize in the streamwise (marching) direction, i.e., $X(2) = XENTR + DELX$. At streamwise station I the streamwise position is given by $X(I) = X(I-1) + AP(X(I-1) - X(I-2))$ where if AP is greater than 1.0, the streamwise step size will increase by $(AP-1.0)$ percent each step. If AP is less than 1.0, the streamwise step size will decrease by $(1.0-AP)$ percent each step. DXMIN and DXMAX are lower and upper overriding limits on the step size. AP, DXMIN and DXMAX are dimensional so that streamwise step size variation can be changed by the IAP parameter, IAP denoting the streamwise location where these variables change. Values of XENTR and DELX should normally only be set on the initial run as these variables are automatically calculated for restarts. Maximum ICOUNT is 10.

Namelist Input Description

LIST3

Geometric Options

Default:

XENTR, DELX, XENTR = 0.0
IAP(ICOUNT, AP(ICOUNT), IAP = 1,9*1000000
DXMIN(ICOUNT), AP = 10*1.0
DXMAX(ICOUNT), DXMIN = 10*0.0
(CONTINUED) DXMAX = 10*1.0E + 06

DELX = No default.

IGEOM

Flag for coordinate options

IGEOM = 1: Cartesian coordinates

IGEOM = 2: Cylindrical coordinates

IGEOM = 3: Polar coordinates

IGEOM = 10: General orthogonal coordinates
(Cartesian in cross plane)

IGEOM = 11: General orthogonal coordinates
(axisymmetric)

Default: 1.

TWOD

Sentinel for two-dimensional option.

If TWOD = .TRUE. TWO DIMENSIONAL

If TWOD = .FALSE. THREE DIMENSIONAL

Default: .FALSE.

TT1(IDIR)

Grid distribution factor (lower surface (IDIR=1) -
or, left surface (IDIR=2)). The closer the value is
to 1.0, the tighter the packing.

Default: 2*0.0.

TT2(IDIR)

Grid distribution factor (upper surface (IDIR=1) -
or, right surface (IDIR=2)). The closer the value
is to 1.0, the tighter the packing.

Default: 2*0.0.

Namelist Input Description

LIST3

Geometric Options

- T2(IDIR) Grid distribution factor (Y-direction (IDIR=1) - or Z-direction (IDIR=2)). The larger the value is, the tighter the packing. Use in conjunction with X0. The value should not exceed 5.0.
- Default: 2*0.0
- X0(IDIR) Clustering location of grid points within the computational domain (X0(1) is Y-location and X0(2) is Z-location). Use in conjunction with T2.
- Default: 2*0.0
- YS(ILIM,IDIR) Define computational domain in Y-Z cross plane. ILIM defines either lower or upper limit, ILIM=1(LOWER), ILIM=2(UPPER).
- YS(1,1) = 0.0 - lower limit Y-direction
YS(2,1) = 1.0 - upper limit Y-direction
YS(1,2) = 0.0 - lower limit Z-direction
YS(2,2) = 1.0 - upper limit Z-direction
Default: 0.0, 1.0, 0.0, 1.0.
- IFBW(JY,KZ) Grid array indicator needed to set up the computational domain in the cross plane at each streamwise station.
- IFBW(JY,KZ) Notation
- IFBW = 1 - Interior fluids point
IFBW = 2 - Interior solids point
IFBW = 3 - Conventional boundary point
 (fluids or solids)
IFBW = 4 - Boundary point outward corner
IFBW = 5 - Boundary point inward corner
- No default.
- XBRKX(ICOUNT) Streamwise (marching direction) physical locations where an embedded solid body starts or ends. Maximum ICOUNT is 5.
Default: 5*1.0E+06.

Namelist Input Description

Geometric Options

LIST3

NBRKX Total number of the streamwise locations where embedded solid bodies start or terminate.
Default: 0.

IBRKMN(KZ,ICOUNT) Minimum Y index of the grid points which change their characteristics at each spanwise (KZ) location of the cross-section. Maximum ICOUNT is NBRKX.
Default: 500*0.

IBRKMx(KZ,ICOUNT) Maximum Y index of the grid points which change their characteristics at each spanwise (KZ) location of the cross-section. Maximum ICOUNT is NBRKX.
Default: 500*0.

IEDGE Flag which tells whether grid point changes its characteristics from fluids to solids or vice versa.

IEDGE = 0: From fluids to solids.

IEDGE = 1: From solids to fluids.

No default.

LIST4

Initial Profile, Turbulence Information

IBCP(LP) Basic surface for initial profile generation for LPth loop.

Boundary Layer Profile in a loop

at lower surface 1	IBCP = 1
at upper surface 2	IBCP = 2
at left surface 3	IBCP = 3
at right surface 4	IBCP = 4

Default: 1.

DELTA P(IBCP, LP) Boundary layer thickness on surface IBCP of LPth loop needed to generate the initial profile referenced to each surface.
No default.

CFP(IBCP, LP) Skin friction coefficient on surface IBCP of LPth loop needed to generate the initial turbulent boundary layer profile.
No default.

I PROF

Flag for initial profile options.

I PROF = 1: Freestream profiles

I PROF = 2: Initial profiles supplied by user

I PROF = 3: Boundary layer profiles based on
necessary input

I PROF = 4: Same as I PROF=3, but angular components
are obtained for general orthogonal
coordinates.

Default value is 1.

Namelist Input Description

LIST4

Initial Profile, Turbulence Information

IMIXL Flag for mixing length options.

IMIXL = 1: McDonald-Camarrata mixing length model based on prescribed boundary layer thickness (DELTAB). With wall shear value used to calculate nondimensional distance

IMIXL = 2: Buleev mixing length model

IMIXL = 3: McDonald-Camarrata mixing length model based on dynamically obtained boundary layer thickness with fixed wall shear

IMIXL = 4: Same as IMIXL = 1, but local shear is used to calculate nondimensional distance

IMIXL = 5: Same as IMIXL = 3, but local shear is used

IMIXL = 6: Mixing length model for jet flow
Default: 1.

BETA Angle of attack in degrees.
Default: 0.0.

YAW Yaw angle in degrees.
Default: 0.0.

IVISC Flag for viscosity options.

IVISC = 1: Constant viscosity

IVISC = 2: Laminar viscosity obtained from Sutherland's relation

IVISC = 3: Turbulent viscosity is obtained from mixing length model

IVISC = 4: Turbulent viscosity obtained from TKE - mixing length model
Default: 1.

DELTAB(KSURF, IDIR) Specified boundary layer thickness on surface KSURF for mixing length model of turbulence.
No default values.

Namelist Input Description

LIST4

Initial Profile, Turbulence Information

ITRANS

Flag which tells whether transition turbulence model logic is used.

ITRANS = 0: No transitional model is used

ITRANS ≠ 0: Transitional model is used
Default: 0.

IBLT

Flag which tells whether boundary layer thickness is input or calculated dynamically.

IBLT = 0: Boundary layer thickness is input

IBLT ≠ 0: Boundary layer thickness is dynamically calculated.
Default: 0.

TKEINF

Freestream turbulent kinetic energy.
Default: 0.0.

NPROF(LP)

Number of initial profiles generated for each loop in Y or Z-direction.
Default: 10*0.

IDIRP

Basic direction for initial profile generation.

IDIRP = 1: Y-direction

IDIRP = 2: Z-direction
Default: 2.

LIST5

File Output Information

IVARPR(I)

Index of variables to be printed. Needed only for three-dimensional flow.

IVARPR(I) = 0: No print

IVARPR(I) = 1: Print every IPRINT steps

IVARPR(I) = 2: Print every JPRINT steps

I = 1: UVEL

I = 2: VVEL

I = 3: WVEL

I = 4: Density

I = 5: Enthalpy

I = 6: Turbulent kinetic energy

I = 7: Turbulent dissipation

Default: 5*1, 2*0, 3*1, 7*0, 1, 3*0, 1, 3*0.

Namelist Input Description

LIST5

Initial Profile, Turbulence Information

I = 8: Pressure
I = 9: Temperature
I = 10: Mach No.
I = 11: Mach No. indicator
I = 12: Stagnation temperature
I = 13: Stagnation pressure
I = 14: Pressure coefficient
I = 15: Laminar viscosity
I = 16: Mixing length
I = 17: Turbulent viscosity
I = 18: Effective viscosity
I = 19: Dissipation function
I = 20: Cell Reynolds number in Y-direction
I = 21: Cell Reynolds number in Z-direction
I = 22: ISS and JBOUND
I = 23: Heat transfer coefficient, skin friction
 coefficient and heat transfer rate
I = 24: Boundary layer thickness
I = 25: Cross-sectional average of flow properties

IPLLOT

Marching station interval for storage of plotting information.

IPLLOT = 0: No plotting

IPLLOT ≠ 0: Store plotting information every
 IPLLOT station

Default: 0.

IPRINT

Primary marching station interval for printing.

Default: 1.

JPRINT

Secondary marching station interval for printing.

Default: 1.

Namelist Input Description

Reset Information for Cross-Section

LISTR

IFBW	See LIST3
IBOUND	See LIST1
IEQBC	See LIST1
JEQBC	See LIST1
DTDN	See LIST1
TWALL	See LIST1
PRESS	See LIST1

Error Conditions in the PEPSIN Computer Code

Failure of the PEPSIN computer code to successfully execute a runstream can occur because of either inconsistent or incorrect input data or because of an attempt to apply the PEPSIN code to a case where the physics violate the assumptions inherent in the code. This section will address only the former mode of failure. Avoidance of the latter failure mode is dependent primarily on the users understanding of the basic physics of the case he is going to run, and the degree to which the PEPSIN code can be expected to model the physics.

One method of discussing the inconsistent or incorrect input data mode of failure is by examining the possible failures in the various subroutines. Since the individual subroutines are responsible for separate tasks during the execution of a run, (e.g. overall control of the program geometry generation, etc.), this technique will in essence outline the possible failure modes as the tasks are performed. Discussion will occur in the same order as the run is executed.

SUBROUTINE RESTRT

There are two modes by which SUBROUTINE RESTRT can fail. Both involve improper use of the restart file. A message, RESTART INFORMATION REQUESTED AT (IRSTIN marching number) BUT STORED INFORMATION AT SEQUENCE (NFILE) IS AT STATION (Station number). This message occurs because the marching station number read off the NFILEth restart file does not match the input value of IRSTIN. The corrective action is to make NFILE and IRSTIN consistent with each other. Another possible mode of failure occurs when NFILE exceeds the number of files on the restart device, JRSTIN, in which case an END OF INFORMATION (or analogous statement) will appear in the day file. The corrective action is to recheck the input value of NFILE. If JRSTIN \neq JRSTOT, the value of NFILE is the number of the restart on device JRSTIN.

SUBROUTINE INPUTS

There are two failure modes in SUBROUTINE INPUTS. On the first case, the message NS = (input value of NS) GREATER THAN NSMAX = (dimension of X vector) will be printed if the number of marching stations exceeds the dimensional value of X, the streamwise locations. The corrective action is

to lower the value of NS. The second failure mode occurs when the Buleev turbulence model is specified for a two-dimensional case. Since this model is not applicable to two-dimensional cases, the message CANNOT USE BULEEV TURBULENCE MODEL IN TWO-DIMENSIONAL FLOW is printed. The corrective action is to specify an alternate turbulence model.

SUBROUTINE SETUP

If grid point characteristics indicator, IFBW, is not correctly specified, SUBROUTINE SETUP can fail. When the message FAILURE IN SETUP DUE TO INCORRECT IFBW is printed, the corrective action is to recheck IFBW specified in INPUT DATA. IFBW should contain an information on the computational domain boundary which is specified by boundary indicator.

SUBROUTINE GEOTRB

At present SUBROUTINE GEOTRB is coded to calculate metric information for values of IGEOM = 1, 2, 3, 10 and 11. Values of IGEOM 4-9 are left for various coordinates that may be coded in the future. Input value of IGEOM = 4-9 will result in the message INVALID OPTION IN GEOTRB. The corrective action is to either change the value of IGEOM or to code in a new option. For IGEOM options 10 and 11 (conformal-Cartesian cross-section and conformal-axisymmetric cross-section) the metric information is externally generated by the ADD computer code. In this case, logical file units JDRUM and KDRUM must be defined. JDRUM contains the ADD code data which is then interpolated onto the PEPSIN mesh system. If the PEPSIN values of the streamwise coordinate is less than the first value of the ADD code streamwise coordinate no streamwise interpolation is possible and the message FAILURE IN GEOTRB - SQ12 = (PEPSIN position) SQ1 = (first ADD code position) SQ2 = (second ADD code position). The corrective action is to increase the value of XENTR (the first PEPSIN position) to a value greater than SQ1. On the other hand, if the value of a PEPSIN streamwise coordinate exceeds the last streamwise position generated by the ADD code and END OF INFORMATION message will appear in the day file. The corrective action is to either rerun the ADD code such that the maximum PEPSIN streamwise coordinate does not exceed the maximum ADD code streamwise coordinate or to reduce the maximum PEPSIN streamwise coordinate to an acceptable value.

SUBROUTINE INTEBC

SUBROUTINE INTEBC performs a two-dimensional linear interpolation of the transpiration schedules on both X-Y planes at X-Z planes. If the number of streamwise stations on a surface at which data is input exceeds 15 (the dimensional size of the data arrays) a message FAILURE IN INTEBC VALUE OF NPTSX (surface number IBC) = (value of NPTSX(IBC) EXCEEDS DIMENSION LIMITS OF 15 is printed. The corrective action is either to updimension NPTSX and associated variables or to decrease the value of NPTSX. Likewise, in the Y or Z direction data can be input at up to 15 locations. If the value of NPTSYZ exceeds 15, the message FAILURE IN INTEBC VALUE OF NPTSYZ (streamwise location, surface number) = (value of NPTSYZ) EXCEEDS DIMENSION LIMITS OF 15 is printed. The corrective action is either to updimension NPTSYZ and associated variables or to decrease the value of NPTSYZ.

SUBROUTINE QUICK

If the choice of boundary conditions is incorrectly made, it is possible that a singular matrix will result. This will manifest itself in SUBROUTINE QUICK in an attempt to divide by zero. The corrective action is to re-evaluate the choice of input boundary conditions to determine the source of the singularity. An example of an improper choice of a boundary condition set would be to choose as boundary conditions the three no-slip conditions for the three momenta equations, the normal pressure condition for the continuity equation and the normal momentum equation for the enthalpy equation. In this case, the enthalpy does not appear in any of the boundary conditions, and hence a singular matrix would result.

SUBROUTINE CROSEC

Often, if a case is not going to successfully run, the code will cease operation in SUBROUTINE CROSEC. This will occur because of the existence of a negative temperature in which case the Mach number calculation will fail in SQRT. There can be many reasons for this failure mode. Usually, however, it can be related to inadequate numerical resolution of the physical processes that are occurring. For instance, a lack of transverse grid points might lead to large oscillations in the pressure or too large a streamwise step in the region where a wall inclination is rapidly changing might result in a temperature becoming negative. Sometimes it is difficult to know a priori

what grid resolution is necessary for a given problem. Usually, experimentation with two-dimensional cases can ironically provide some guide lines for three-dimensional cases. This in addition with the users' overall experience with the code and his understanding of the physical processes will usually provide the means of resolving the above problem.

SUBROUTINE WHERE

There are two modes by which SUBROUTINE WHERE can fail. For the first case, the message PROBLEM IN SUBROUTINE WHERE MSECY = m JX= n_1 JY= n_2 KZ= n_3 will be printed where n_1 , n_2 and n_3 refers to x, y and z location respectively if MSECY is not correctly specified, i.e., not consistent with the number of Y-perspective subsections. The corrective action is to increase the value of MSECY corresponding to the number of Y-perspective subsections. The second failure mode occurs when MSECZ is not consistent with the number of Z-perspective subsections. In this case, the message PROBLEM IN SUBROUTINE WHERE MSECZ = m JX= n_1 JY= n_2 KZ= n_3 is printed with n_1 , n_2 and n_3 referring to x,y and z location respectively. The corrective action is to increase the value of MSECZ corresponding to the number of Z-perspective subsections.

PEPSIN FORTRAN Variables

FORTRAN SYMBOL	COMMON BLOCK	DESCRIPTION
ACON	LAWW	CONSTANT IN ARGUMENT OF EXPONENTIAL FUNCTION FOR TRANSITIONAL MODEL
AG(NN,9,2)	OPER	DIFFERENCE WEIGHTS IN PHYSICAL COORDINATES
AGEO	GEOM	COEFFICIENTS OF POLYNOMIAL FIT FOR BOUNDARY SHAPE
AG1D(9)	FGCOM	TEMPORARY STORAGE ARRAY OF METRIC INFORMATION
AG1P	FGCOM	TEMPORARY STORAGE ARRAY OF METRIC INFORMATION
AG2D(9)	FGCOM	TEMPORARY STORAGE ARRAY OF METRIC INFORMATION
AHP(5)	FGCOM	TEMPORARY STORAGE ARRAY OF METRIC INFORMATION
AH1D(5,9)	FGCOM	TEMPORARY STORAGE ARRAY OF METRIC INFORMATION
AIE(NN,7)	PREILE	INITIAL PROFILE ARRAY
AM(NCPLD,3*NCPLD+1)CCOM		UTILITY MATRIX USED IN BLOCK MATRIX INVERSION
AMACRT	SUPER	MACH NUMBER CRITERION USED IN LOCATING SONIC LINE
AN(NEQS,NN)	LIN	STORAGE FOR LINEARIZATION COEFFICIENTS OF X - DERIVATIVES
AP(10)	GEOM	AMPLIFICATION RATE OF MARCHING STEP SIZE
APLUS	LAWW	CONSTANT IN ARGUMENT OF EXPONENTIAL FUNCTION FOR VAN DRIEST DAMPING FORMULA
ASW(20,2)	BOUND	COEFFICIENTS OF POLYNOMIAL FIT FOR SWITCHING THE BOUNDARY SURFACE TYPE
AVISC(2,NEQS)	VISC	COEFFICIENT USED IN ARTIFICIAL DAMPING
BETA	REF	ANGLE OF ATTACK
BGEO	GEOM	COEFFICIENTS OF POLYNOMIAL FIT FOR BOUNDARY SHAPE
BLOCK1(IADD3)		STORAGE FOR ADD CODE METRIC INFORMATION EQUIVALENCED TO C(1,1,1)
BLOCK2(IADD3)		STORAGE FOR ADD CODE METRIC INFORMATION EQUIVALENCED TO C(1,1,NN/2+1)

FORTRAN SYMBOL	COMMON BLOCK	DESCRIPTION
BLTH(NN,5,4)	LAWW	DYNAMICALLY DETERMINED BOUNDARY LAYER THICKNESS
BSW(20,2)	BOUND	COEFFICIENTS OF POLYNOMIAL FIT FOR SWITCHING THE BOUNDARY SURFACE TYPE
BWD	LIN	CRANK-NICHOLSON FACTOR
BWDI	LIN	INVERSE OF BWD
C(NN,NCPLD,NN)	CCOM	BLOCK DIAGONAL MATRIX ELEMENTS
CDUM(NDIM)		TEMPORARY STORAGE ARRAY TO ROTATE DATA FROM COLUMNS TO ROWS AND VICE VERSA - EQUIVALENCED TO C(1,1,1) NDIM = MZVAR * MLEVEL * NN
CFP(4,10)	PROFILE	SKIN FRICTION COEFFICIENT
CGEO	GEOM	COEFFICIENTS OF POLYNOMIAL FIT FOR BOUNDARY SHAPE
CMUINF	VISC	CONSTANT IN TURBULENT VISCOSITY MODEL
CONGEO(11*NN)	GEOM	COORDINATE TRANSFORMATION INFORMATION
CONVDR	UNITS	CONVERSION FACTOR IN GOING FROM DEGREES TO RADIANS
CONVRD	UNITS	CONVERSION FACTOR IN GOING FROM RADIANS TO DEGREES
COOR(NN,4)	GEOM	PHYSICAL COORDINATE INFORMATION WITH RESPECT TO ABSOLUTE ORIGIN AT N+1ST STREAMWISE LOCATION
COORN(NN,4)	GEOM	PHYSICAL COORDINATE INFORMATION WITH RESPECT TO ABSOLUTE ORIGIN AT NTH STREAMWISE STATION
CPINF	FREE	FREE STREAM SPECIFIC HEAT
CPREF	REF	REFERENCE PRESSURE COEFFICIENT
CPREFI	REF	INVERSE OF REFERENCE PRESSURE COEFFICIENT
CRITU	OPER	CRITICAL VELOCITY USED FOR FLARE APPROXIMATION
CSOLN(NCPLD,NN)	CCOM	SOLUTION TO BLOCK TRI-DIAGONAL MATRIX INVERSION
CSW(20,2)	BOUND	COEFFICIENTS OF POLYNOMIAL FIT FOR SWITCHING THE BOUNDARY SURFACE TYPE

FORTRAN SYMBOL	COMMON BLOCK	DESCRIPTION
CTWO	REF	NUMERICAL CONSTANT IN GOVERNING EQUATION
CXI(NDIFM)	ADDR	STORAGE FOR FIRST DERIVATIVE DIFFERENCE WEIGHTS
CXXI(NDIFM)	ADDR	STORAGE FOR SECOND DERIVATIVE DIFFERENCE WEIGHTS
C1(NN)	CCOM	SUBDIAGONAL MATRIX ELEMENTS
C1SUTH	VISC	COEFFICIENT IN SUTHERLAND'S LAW OF LAMINAR VISCOSITY
C2(NN)	CCOM	DIAGONAL MATRIX ELEMENTS
C2SUTH	VISC	COEFFICIENT IN SUTHERLAND'S LAW OF LAMINAR VISCOSITY
C3(NN)	CCOM	SUPERDIAGONAL MATRIX ELEMENTS
C4(NN)	CCOM	VECTOR ELEMENTS
D	VAR	INDEX FOR DIVERGENCE
DELMAX(NEQS)	EQN	MAXIMUM VALUES OF THE DELTAS
DELTAB(20,2)	LAWW	SPECIFIED BOUNDARY LAYER THICKNESS FOR MIXING LENGTH MODEL OF TURBULENCE
DELTAP(4,10)	PRFILE	BOUNDARY LAYER THICKNESS
DELX	GEOM	STEP SIZE IN MARCHING DIRECTION
DGEO	GEOM	COEFFICIENTS OF POLYNOMIAL FIT FOR BOUNDARY SHAPE
DIFOP(6)	OPER	DIFFERENCE WEIGHTS IN COMPUTATIONAL COORDINATES
DL	VAR	STORAGE LEVEL OF DIVERGENCE IN GENERAL PURPOSE STORAGE
DM1(NCPLD,NCPLD)	CCOM	GENERAL PURPOSE STORAGE ARRAYS FOR BLOCK TRI-DIAGONAL MATRIX INVERSION
DM2(NCPLD)	CCOM	GENERAL PURPOSE STORAGE ARRAYS FOR BLOCK TRI-DIAGONAL MATRIX INVERSION
DM3(NCPLD,NCPLD)	CCOM	GENERAL PURPOSE STORAGE ARRAYS FOR BLOCK

FORTRAN SYMBOL	COMMON BLOCK	DESCRIPTION
		TRI-DIAGONAL MATRIX INVERSION
DS	VAR	INDEX FOR DISSIPATION FUNCTION
DSL	VAR	STORAGE LEVEL OF DISSIPATION FUNCTION IN GENERAL PURPOSE STORAGE
DSW(20,2)	BOUND	COEFFICIENTS OF POLYNOMIAL FIT FOR SWITCHING THE BOUNDARY SURFACE TYPE
DTDN(20,2)	BOUND	SPECIFIED TEMPERATURE GRADIENT NORMAL TO BOUNDARY
DTDNW(NN,5,4)	BOUND	STORAGE ARRAY FOR TEMPERATURE GRADIENT NORMAL TO BOUNDARY
DX	OPER	STEP SIZE IN X-DIRECTION
DXI	OPER	INVERSE OF DX
DXMAX(10)	GEOM	MAXIMUM MARCHING STEP SIZE
DXMIN(10)	GEOM	MINIMUM MARCHING STEP SIZE
D1(NEQS,NDIFM,NN)	LIN	STORAGE FOR LINEARIZATION COEFFICIENTS OF Y - DERIVATIVES
D1L(NEQS,NDIFM)	LIN	STORAGE OF LINEARIZATION COEFFICIENT FOR TEMPERATURE AND PRESSURE COMPUTATION
D2(NEQS,NDIFM,NN)	LIN	STORAGE FOR LINEARIZATION COEFFICIENTS OF Z - DERIVATIVES
E(NN,NCPLD,NN)		ARRAY USED IN MGAUSS ERROR CHECK - EQUIVALENCED TO C(1,1,1)
EPS	VAR	INDEX FOR DISSIPATION OF TURBULENCE KINETIC ENERGY
EPSMWF	LAWW	CONVERGENCE CRITERION FOR WALL FUNCTION FORMULATION
F(14,NN)	ZPLOT	TEMPORARY STORAGE FOR PLOT INFORMATION

FORTRAN SYMBOL	COMMON BLOCK	DESCRIPTION
FACLM(20,2)	LAWW	MULTIPLICATION FACTOR TO BOUNDARY LAYER THICKNESS
EG(8,3,NN)	METRIC	STORAGE FOR METRIC COEFFICIENTS AND DERIVATIVES
GAM(3)	GEOM	COORDINATE TRANSFORMATION COEFFICIENT FOR BOUNDARY CONDITIONS
GAMMA	REF	RATIO OF SPECIFIC HEATS
GC	UNITS	GRAVITY CONSTANT
H	VAR	INDEX FOR ENTHALPY
HEFORM	REF	HEAT OF FORMATION
HINF	FREE	FREE STREAM ENTHALPY
HREF	REF	REFERENCE ENTHALPY
HREFI	REF	INVERSE OF REFERENCE ENTHALPY
IA	CCOM	INDEX REFERRING TO SUBDIAGONAL MATRIX ELEMENTS
IADDO(NDIFM)	ADDR	ADDRESSES IN THE OPPOSITE DIRECTION
IADDP(NDIFM)	ADDR	ADDRESSES IN THE PRIMARY DIRECTION
IADDS1(NN)	ADDRE	ADDRESS FOR POINT LOGIC OF FLUID VARIABLES
IADDS2(NDIFM,NN)	ADDRE	ADDRESS FOR Y DERIVATIVE OF FLUID VARIABLES
IADDS3(NDIFM,NN)	ADDRE	ADDRESS FOR Z DERIVATIVE OF FLUID VARIABLES
IADDS4(NDIFM**2,NN)	ADDRE	ADDRESS FOR MIXED DERIVATIVE OF FLUID VARIABLES
IADDS5(NDIFM**2,NN)	ADDRE	ADDRESS FOR MIXED DERIVATIVE OF FLUID VARIABLES
IADD1	ADD	NO. OF GEOMETRIC VARIABLES USED IN ADD CODE
IADD2	ADD	NO. OF TRANSVERSE GRIDPOINT USED IN ADD CODE
IADD3	ADD	RECORD SIZE USED IN ADD CODE
IADI	SWEEP	ADI SWEEP DIRECTION
IADIM1	SWEEP	IADI - 1
IAP(10)	GEOM	MARCHING STEP INDEX AT WHICH AP,DXMIN,DXMAX

FORTRAN SYMBOL	COMMON BLOCK	DESCRIPTION
		ARE REINITIALIZED
IB	CCOM	INDEX REFERRING TO DIAGONAL MATRIX ELEMENTS
IBC	BOUND	INDEX FOR BOUNDARY SURFACE IDENTIFICATION
IBCP(10)	PROFILE	BASIC SURFACE FOR INITIAL PROFILE GENERATION
IBCPLP	PROFILE	BOUNDARY SURFACE NUMBER IN EACH LOOP WHERE INITIAL BOUNDARY LAYER PROFILE IS REQUIRED. IBCPLP = 1 OR 2 IF IDIRP = 2 IBCPLP = 3 OR 4 IF IDIRP = 3
IBLT	LAWW	FLAG WHICH TELLS WHETHER BOUNDARY LAYER THICKNESS IS INPUT OR CALCULATED DYNAMICALLY
IBOUND(20,2)	BOUND	BOUNDARY SURFACE TYPE INDICATOR
IBRKMx(NN,5)	BOUND	UPPER BOUNDARY OF AN EMBEDDED SOLID BODY EXPRESSED IN TERMS OF GRID POINT INDEX ON EACH Y-COORDINATE LINE AT UP TO 5 STREAMWISE LOCATIONS.
IEDGE	BOUND	SENTINEL WHICH SPECIFIES EITHER LEADING EDGE WHERE SOLID BODY STARTS OR TRAILING EDGE WHERE SOLID BODY TERMINATES.
IBRKMn(NN,5)	BOUND	LOWER BOUNDARY OF AN EMBEDDED SOLID BODY EXPRESSED IN TERMS OF GRID POINT INDEX ON EACH Y-COORDINATE LINE AT UP TO 5 STREAMWISE LOCATIONS.
IC	CCOM	INDEX REFERRING TO SUPERDIAGONAL MATRIX ELEMENTS
ICDC(NN+1,2)	CDC	RECORD INDEX FOR READMS AND WRITEMS MASS STORAGE DEVICES-CDC COMPUTER ONLY
ICOMP	REST	FLAG FOR COMPUTER OPTIONS
ICONS(3,NEQS)	OPER	FLAG FOR CONVECTIVE FORMULATION BASED ON MACH NUMBER AND EQUATION

FORTRAN SYMBOL	COMMON BLOCK	DESCRIPTION
ICORD	GEOM	FLAG FOR COORDINATE TRANSFORMATION OPTIONS
ICPLD(NEQS,2)	EQN	COUPLED EQUATION SENTINEL
ID	CCOM	INDEX REFERRING TO VECTOR MATRIX ELEMENTS
IDIE(40)	OPER	INDEX FOR TYPE OF DIFFERENCING OF BOUNDARY CONDITIONS
IDMPY	DMP	DUMP LINE NO. IN Y DIRECTION
IDMPZ	DMP	DUMP LINE NO. IN Z DIRECTION
IDUM2(NN)	ADDRG	INDICATOR OF THE POINT IN DIFFERENCE MOLECULE WHERE Y DERIVATIVE IS TAKEN
IDUM3(NN)	ADDRG	INDICATOR OF THE POINT IN DIFFERENCE MOLECULE WHERE Z DERIVATIVE IS TAKEN
IEQ	EQN	EQUATION NUMBER INDEX
IEQBC(20,2,NEQS)	BOUND	SPECIFIED BOUNDARY CONDITION FOR WALL
IEQNUM(NEQS)	EQN	IDENTIFICATION NUMBER OF EQUATIONS TO BE SOLVED
IEBW(NN,NN)	GRID	INDICATOR WHICH TYPES GRID POINTS IN THE COMPUTATIONAL CROSS-SECTION PLANE.
IFLARE	OPER	SENTINEL WHICH TELLS IF FLARE OPTION IS USED
IGDMP	DMP	FLAG FOR DUMP OPTIONS
IGEOM	GEOM	FLAG FOR COORDINATE SYSTEM OPTIONS
IH	GRID	UPPER BOUNDARY POINT ON THE LINE WHERE IMPLICIT SOLUTION IS OBTAINED
IHSTAG	EQN	FLAG FOR ENERGY EQUATION OPTIONS
IJ	DIFCOM	COLUMN OR ROW NUMBER ON WHICH CALCULATION IS BEING MADE
IL	GRID	LOWER BOUNDARY POINT ON THE LINE WHERE IMPLICIT SOLUTION IS OBTAINED

FORTRAN SYMBOL	COMMON BLOCK	DESCRIPTION
IMIXL	LAWW	FLAG FOR MIXING LENGTH OPTIONS
IND	VAR	FLAG WHICH TELLS IF MESH POINT BELONGS TO SUPERSONIC OR SUBSONIC REGION
INDC(NN)	DIFCOM	MACH NUMBER INDICATOR
INDL	VAR	STORAGE OF MACH NUMBER INDICATOR IN GENERAL PURPOSE STORAGE
INH12	ADD	SENTINEL USED TO DETERMINE FORMULATION USED IN CALCULATION OF TRANSVERSE DERIVATIVE OF H1
INH21	ADD	SENTINEL USED TO DETERMINE FORMULATION USED IN CALCULATION OF STREAMWISE DERIVATIVE OF H2
INH31	ADD	SENTINEL USED TO DETERMINE FORMULATION USED IN CALCULATION OF STREAMWISE DERIVATIVE OF H3
INH32	ADD	SENTINEL USED TO DETERMINE FORMULATION USED IN CALCULATION OF TRANSVERSE DERIVATIVE OF H3
IOPTWF	LAWW	SENTINEL WHICH DETERMINES WALL FUNCTION FORMULATION
IOPTYZ(3,NEQS,2)	OPER	FLAG FOR DIFFERENCING FORMULATION BASED ON MACH NUMBER, EQUATION, AND ADI DIRECTION
IPLOT	CIO	MARCHING STATION INTERVAL FOR STORAGE OF PLOTTING INFORMATION
IPRINT	CIO	PRIMARY MARCHING STATION INTERVAL FOR PRINTING
IPROF	PREFILE	FLAG FOR INITIAL PROFILE OPTIONS
IPRTE	GASL	FLAG WHICH DETERMINES EQ. OF STATE FORMULATION
IRSTIN	REST	STREAMWISE STATION NUMBER FOR RESTART
IRSTOT	REST	STREAMWISE INTERVAL FOR SAVING RESTART INFORMATION
ISONIC	SUPER	FLAG FOR SONIC LINE INTERPOLATION LOGIC

FORTRAN SYMBOL	COMMON BLOCK	DESCRIPTION
ISS(NN,5,4)	SUPER	GRID POINT LOCATION OF SONIC LINE
ISSHFT	SUPER	INDEX USED TO DETERMINE IF SONIC LINE IS LAST SUBSONIC POINT OR FIRST SUPERSONIC POINT
ISTART	METRIC	INITIAL CONDITION INDEX
ISURF(4)	BOUND	LOCATION OF FOUR BOUNDARIES AS IDENTIFIED BY NSURE IN TERMS OF GRID POINT INDEX. ISURE(1) AND ISURE(2) ARE Y-INDICES OF NSURE(1) AND NSURE(2) RESPECTIVELY, WHEREAS ISURE(3) AND ISURF(4) ARE Z-INDICES OF NSURE(3) AND NSURE(4) RESPECTIVELY.
ISW	UNIVAC	SENTINEL FOR WORD ADDRESSABLE OR SECTOR- ORIENTED MASS STORAGE DEVICE - UNIVAC ONLY
ISYM	ZPLOT	SYMMETRY OPTION FOR PLOTS
ITRANS	LAWW	FLAG WHICH TELLS WHETHER TRANSITION TURBULENCE MODEL LOGIC IS USED
IUNITS	UNITS	FLAG USED TO DETERMINE SET OF DIMENSION UNITS USED
IVARNO(NEQS)	EQN	IDENTIFICATION NUMBER OF DEPENDENT VARIABLES
IVARPR(25)	PRNT	INDEX OF VARIABLES TO BE PRINTED
IVISC	VISC	FLAG FOR VISCOSITY OPTIONS
IWALE	VISC	SENTINEL WHICH DETERMINES IF WALL FUNCTION LOGIC IS NEEDED IN THE CALCULATION OF WALL VISCOSITY
IWR	CIO	SENTINEL FOR NAMELIST REST PRINT
IYGD(NDIFM)	ADDR	GEOMETRY ADDRESSES
IZCT(3)	ZEX1	RELATIVE UNIT NO. FOR VIRTUAL MEMORY STORAGE
IIIG(8,3)	EGCOM	INDEX NEEDED IN THE CALCULATION OF METRIC

FORTRAN SYMBOL	COMMON BLOCK	DESCRIPTION
		INFORMATION
I2IG(8,3)	FGCOM	INDEX NEEDED IN THE CALCULATION OF METRIC INFORMATION
JA(5)	ADDRE	SHIFT LOGIC INDEX
JADDO(NDIFM)	ADDR	ADDRESSES IN THE OPPOSITE DIRECTION
JADDP(NDIFM)	ADDR	ADDRESSES IN THE PRIMARY DIRECTION
JBOUND(NN,5,4)	BOUND	BOUNDARY TYPE INDICATOR AT EACH POINT ON BOUNDARY
JDMAX	EQN	Y GRID POINT LOCATION OF MAXIMUM DELTA
JDRUM	CIO	ADD CODE DEVICE
JDUM	DIFCOM	INDEX DENOTING RELATIVE POINT ABOUT WHICH DERIVATIVE IS LOCATED
JEQBC(20,2,NEQS)	BOUND	SPECIFIED BOUNDARY CONDITION FOR NON-WALL
JEQN(NEQS,2)	EQN	EXTERNAL EQUATION NUMBER
JGSTOR	LIN	VALUE OF JG NEEDED BY SUBROUTINE EOS
JMIN(LP,NN)	BOUND	LOWER GRID POINT INDEX LIMIT OF EACH COMPUTATIONAL LOOP(LP) ON EACH OF NN Y-COORDINATE LINES
JPLOT	CIO	DEVICE FOR PLOTTING
JPRINT	CIO	SECONDARY MARCHING STATION INTERVAL FOR PRINTING
JPROF(4)	PROFILE	SENTINEL FOR BOUNDARY VALUES DURING INITIAL PROFILE GENERATION
JRSTIN	REST	LOGICAL FILE FROM WHICH RESTART INFORMATION IS READ
JRSTOT	REST	LOGICAL FILE ON WHICH RESTART INFORMATION IS WRITTEN
JVAR(NEQS,2)	EQN	VARIABLE NUMBER ASSOCIATED WITH EACH EQUATION DURING AN ADI SWEEP

FORTRAN SYMBOL	COMMON BLOCK	DESCRIPTION
JWR(5)	CIO	SENTINEL FOR NAMELIST PRINT OPTION
JX	OPER	RELATIVE MARCHING STATION COUNTER
JXDUM	OPER	ABSOLUTE MARCHING STATION COUNTER
JXDUMP	DMP	MARCHING STATION WHEN DUMP OUTPUT IS REQUESTED
KA(5)	ADDRG	INDICIES NECESSARY TO CALCULATE GEOMETRIC GROUPINGS
KDMAX	EQN	Z GRID POINT LOCATION OF MAXIMUM DELTA
KDRUM	CIO	DEVICE FOR TEMPORARY STORAGE - USED IN GEOMETRY GENERATION
KMAX(LP,NN)	BOUND	UPPER GRID POINT INDEX LIMIT OF EACH COMPUTATIONAL LOOP(LP) ON EACH OF NN Z-COORDINATE LINES
KMIN(LP,NN)	BOUND	LOWER GRID POINT INDEX LIMIT OF EACH COMPUTATIONAL LOOP(LP) ON EACH OF NN Z-COORDINATE LINES
JMAX(LP,NN)	BOUND	UPPER GRID POINT INDEX LIMIT OF EACH COMPUTATIONAL LOOP(LP) ON EACH OF NN Y-COORDINATE LINES
LADD(3)	BOUND	ADDRESSES FOR BOUNDARY CONDITIONS
LBRKY(10)	BOUND	BREAK-OFF POINTS ON THE SPANWISE(Z-DIRECTION) COMPUTATIONAL BOUNDARY TO BE USED TO DETERMINE THE SURFACE NUMBER OF Y-PERSPECTIVE SEGMENTED BOUNDARY IN SUBROUTINE WHERE.
LBRKZ(10)	BOUND	BREAK-OFF POINTS ON THE TRANSVERSE(Y-DIRECTION) COMPUTATIONAL BOUNDARY TO BE USED TO DETERMINE THE SURFACE NUMBER OF Z-PERSPECTIVE SEGMENTED BOUNDARY IN SUBROUTINE WHERE.
LDRUM	CIO	DEVICE FOR FINAL METRIC INFORMATION
LEQ1	EQN	LOWEST INDEX OF EQUATIONS SOLVED EITHER BY COUPLED OR UNCOUPLED ADI SWEEP

FORTRAN SYMBOL	COMMON BLOCK	DESCRIPTION
LEQ2	EQN	HIGHEST INDEX OF EQUATIONS SOLVED EITHER BY COUPLED OR UNCOUPLED ADI SWEEP
LEV(3)	ADDR	GEOMETRY LEVEL
LEVEL	ADDRG	GEOMETRY LEVEL
LEXTY(2,NN)	BOUND	EXTENTS OF COMPUTATIONAL DOMAIN OF EACH Y-COORDINATE LINE LEXTY(1,NN) = LOWER LIMIT; LEXTY(2,NN) = UPPER LIMIT
LEXTZ(2,NN)	BOUND	EXTENTS OF COMPUTATIONAL DOMAIN OF EACH Z-COORDINATE LINE LEXTZ(1,NN) = LOWER LIMIT; LEXTZ(2,NN) = UPPER LIMIT
LGA1(NN)	ADDRG	ADDRESS FOR POINT LOGIC OF GEOMETRIC VARIABLES
LGA2(NDIFM,NN)	ADDRG	ADDRESS FOR Y - DERIVATIVE OF GEOMETRIC VARIABLES
LGA3(NDIFM,NN)	ADDRG	ADDRESS FOR Z - DERIVATIVE LOGIC OF GEOMETRIC VARIABLES
LGA4(NDIFM**2,NN)	ADDRG	ADDRESS FOR CROSS DERIVATIVE(Y-Z) LOGIC OF GEOMETRIC VARIABLES
LGA5(NDIFM**2,NN)	ADDRG	ADDRESS FOR CROSS DERIVATIVE(Z-Y) LOGIC OF GEOMETRIC VARIABLES
LP	SECT	INDEX OF COMPUTATIONAL LOOP IN EITHER Y OR Z DIRECTION.
LREF	REF	REFERENCE LENGTH
LREFI	REF	INVERSE OF REFERENCE LENGTH
LSHFT	GEOM	SHIFT INDEX FOR COORDINATE TRANSFORMATION

FORTRAN SYMBOL	COMMON BLOCK	DESCRIPTION
LVG(8)	BOUND	BOUNDARY POINT INDICATOR FOR BOUNDARY CONDITION
MASS1	CIO	GENERAL PURPOSE MASS STORAGE DEVICE
MASS2	CIO	GENERAL PURPOSE MASS STORAGE DEVICE
MCPLD	EQN	NUMBER OF COUPLED EQUATIONS TO BE SOLVED
MEFF	VAR	INDEX FOR EFFECTIVE VISCOSITY
MEFFL	VAR	STORAGE LEVEL OF EFFECTIVE VISCOSITY IN GENERAL PURPOSE STORAGE
MEQK	EQN	LEQ1 - 1
MEQS	EQN	TOTAL NUMBER OF EQUATIONS TO BE SOLVED
MEQS1	EQN	INDEX OF FIRST EQUATION TO BE SOLVED
MEQS2	EQN	INDEX OF LAST EQUATION TO BE SOLVED
MGDMP	DMP	FLAG FOR DUMP OPTIONS
MGD1	GRID	IL + 1
MGD2	GRID	IH - 1
MIN	CIO	INPUT DEVICE
MINE	FREE	FREE STREAM MACH NUMBER
ML	VAR	INDEX FOR MIXING LENGTH
MLEVEL	PARAM	MAXIMUM NO. OF STORAGE LEVELS
MLL	VAR	STORAGE LEVEL OF MIXING LENGTH IN GENERAL PURPOSE STORAGE
MN	VAR	INDEX FOR MACH NUMBER
MNL	VAR	STORAGE LEVEL OF MACH NO IN GENERAL PURPOSE STORAGE
MOUT	CIO	OUTPUT DEVICE
MREF	REF	REFERENCE MACH NUMBER
MREF I	REF	INVERSE OF REFERENCE MACH NUMBER

FORTRAN SYMBOL	COMMON BLOCK	DESCRIPTION
MSDD	CIO	TEMPORARY MASS STORAGE DEVICE
MSD1	CIOD	GENERAL PURPOSE MASS STORAGE DEVICE
MSD2	CIOD	GENERAL PURPOSE MASS STORAGE DEVICE
MSECY	SECT	MAXIMUM NO. OF Y-PERSPECTIVE SUBSECTIONS (USED TO SET UP THE SUBSECTIONS FOR CROSEC)
MSECZ	SECT	MAXIMUM NUMBER OF Z-PERSPECTIVE SUBSECTIONS (USED TO SET UP THE SUBSECTIONS FOR CROSEC)
MSGVAR(25)	PRNT	TITLE OF VARIABLES TO BE PRINTED
MU	VAR	INDEX FOR LAMINAR VISCOSITY
MUINF	FREE	FREE STREAM LAMINAR VISCOSITY
MUL	VAR	STORAGE LEVEL OF LAMINAR VISCOSITY IN GENERAL PURPOSE STORAGE
MUREF	REF	REFERENCE VISCOSITY
MUREFI	REF	INVERSE OF REFERENCE VISCOSITY
MUT	VAR	INDEX FOR TURBULENT VISCOSITY
MUTL	VAR	STORAGE LEVEL OF TURBULENT VISCOSITY IN GENERAL PURPOSE STORAGE
MWINE	FREE	FREE STREAM MOLECULAR WEIGHT
MWREF	REF	REFERENCE MOLECULAR WEIGHT
MWREFI	REF	INVERSE OF REFERENCE MOLECULAR WEIGHT
MZVAR	PARAM	MAXIMUM NUMBER OF STORAGE VARIABLES
NABC	CCOM	NABC = ID
NANG	METRIC	ANGLE OF COORDINATE LINES RELATIVE TO HORIZONTAL
NBRKX	BOUND	NUMBER OF STREAMWISE LOCATIONS WHERE SOLID BODIES EMBEDDED IN THE COMPUTATIONAL DOMAIN START OR TERMINATE.

FORTRAN SYMBOL	COMMON BLOCK	DESCRIPTION
NCMAX(5)	SECT	UPPER LIMIT OF BOUNDARY LINE WHERE ENDCAP SOLUTION IS OBTAINED.
NCMIN(5)	SECT	LOWER LIMIT OF BOUNDARY LINE WHERE ENDCAP SOLUTION IS OBTAINED.
NCPLD	PARAM	MAXIMIUM NUMBER OF COUPLED EQUATIONS
NCPLD2	CCOM	NCPLD**2
NCRF	SECT	EQUAL TO EITHER NYCRF(ISEC) OR NZCRF(ISEC) WHERE ISEC INDICATES A SUBSECTION IN THE CROSS-SECTION.
NCRL	SECT	EQUAL TO EITHER NYCRL(ISEC) OR NZCRL(ISEC) WHERE ISEC INDICATES A SUBSECTION IN THE CROSS-SECTION.
NCTR	DIFCOM	CENTER OF DIFFERENCE MOLECULE
NCUP	EQN	NUMBER OF COUPLED EQUATIONS
NDIFM	PARAM	MAXIMIUM NUMBER OF GRID POINTS IN A DIFFERENCE MOLECULE
NDIFM2	DIFCOM	2*NDIFM
NDIFM1	DIFCOM	NDIFM - 1
NDIFP1	DIFCOM	NDIFM + 1
NE(2)	GEOM	NUMBER OF GRID POINTS IN Y AND Z DIRECTIONS
NEQN(NEQS,2)	EQN	NUMBER OF COUPLED EQUATIONS TO BE SOLVED IN EACH ADI SWEEP
NEQS	PARAM	MAXIMIUM NUMBER OF EQUATIONS IN CODE
NEY	GRID	NUMBER OF GRID POINTS IN Y DIRECTION
NEYM1	GRID	NEY - 1
NEZ	GRID	NUMBER OF GRID POINTS IN Z DIRECTION
NEZM1	GRID	NEZ - 1

FORTRAN SYMBOL	COMMON BLOCK	DESCRIPTION
NE2S	CIO	SENTINEL FOR SPREADING OF 2-D PROFILE TO 3-D
NFILE	REST	SEQUENCE NUMBER OF RESTART INFORMATION
NGEOMV	METRIC	NUMBER OF METRIC COEFFICIENTS AND DERIVATIVES
NH1	METRIC	INDEX FOR METRIC COEFFICIENT IN X-DIRECTION
NH12	METRIC	INDEX FOR DERIVATIVE OF X METRIC IN Y DIRECTION
NH2	METRIC	INDEX FOR METRIC COEFFICIENT IN Y-DIRECTION
NH21	METRIC	INDEX FOR DERIVATIVE OF Y METRIC IN X DIRECTION
NH3	METRIC	INDEX FOR METRIC COEFFICIENT IN Z-DIRECTION
NH31	METRIC	INDEX FOR DERIVATIVE OF Z METRIC IN X DIRECTION
NH32	METRIC	INDEX FOR DERIVATIVE OF Z METRIC IN Y DIRECTION
NIIT	CIO	NO. OF FALSE MARCHING STEPS USED TO GENERATE THE INITIAL PROFILE
NIN	DIFCOM	MAXIMUM LINES OF STORAGE IN CORE AT ONE TIME.
NINC	DIFCOM	$NIN/2 + 1$
NJD	DIFCOM	GRID POINT LOCATION FOR START OF SECOND SWEEP
NJF(10)	SECT	LEFT BOUNDARY INDEX OF EACH Y-PERSPECTIVE SUBSECTION USED FOR Y-SWEEP OF ADI.
NJL(10)	SECT	RIGHT BOUNDARY INDEX OF EACH Y-PERSPECTIVE SUBSECTION USED FOR Y-SWEEP OF ADI.
NJSEG	SECT	NUMBER OF SUBSECTIONS IN EACH CROSS SECTION USED FOR Y-SWEEP OF ADI
NKE(10)	SECT	LOWER BOUNDARY INDEX OF EACH Z-PERSPECTIVE SUBSECTION USED FOR Z-SWEEP OF ADI.
NKL(10)	SECT	UPPER BOUNDARY INDEX OF EACH Z-PERSPECTIVE SUBSECTION USED FOR Z-SWEEP OF ADI.
NKSEG	SECT	NUMBER OF SUBSECTIONS IN EACH CROSS SECTION

FORTRAN SYMBOL	COMMON BLOCK	DESCRIPTION
		USED FOR Z-SWEEP OF ADI.
NLOOPY(NN)	SECT	NUMBER OF LOOPS ON Y-COORDINATE LINE
NLOOPZ(NN)	SECT	NUMBER OF LOOPS ON Z-COORDINATE LINE.
NMAXWF	LAWW	MAXIMUM NUMBER OF ITERATIONS ALLOWABLE IN CALCULATION OF WALL SHEAR VELOCITY
NN	PARAM	MAXIMUM NUMBER OF GRID POINTS IN Y OR Z DIRECTION
NPADI	EQN	NUMBER OF COUPLED AND UNCOUPLED EQUATIONS TO BE SOLVED DURING EACH ADI SWEEP
NPROF(10)	PROFILE	NUMBER OF SURFACES WHERE INITIAL BOUNDARY LAYER PROFILES ARE GENERATED IN EACH LOOP EITHER IN Y OR Z DIRECTION. NPROF IS EITHER 1 OR 2.
NPISX(4)	INTBC	NUMBER OF STREAMWISE LOCATIONS WHERE TRANSPIRATION DATA IS INPUT
NPISYZ(15,4)	INTBC	NUMBER OF CROSS-PLANE LOCATIONS WHERE TRANSPIRATION IS INPUT
NPUNCH	CIO	PUNCH DEVICE
NRGT(2)	DIFCOM	NCTR POINTS FROM RIGHT OR TOP BOUNDARY
NS	GEOM	LAST MARCHING STATION
NSAVED	REST	SEQUENCE NUMBER OF RESTART STATIONS SAVED
NSECRY	SECT	NUMBER OF Y-PERSPECTIVE SUBSECTIONS IN THE CROSS-SECTION FOR SUBROUTINE CROSEC.
NSECRZ	SECT	NUMBER OF Z-PERSPECTIVE SUBSECTIONS IN THE CROSS-SECTION FOR SUBROUTINE CROSEC.
NSMAX	PARAM	2 GREATER THAN NS
NSURE(4)	BOUND	SURFACE NUMBER OF FOUR BOUNDARIES WITH MINIMUM DISTANCE AWAY FROM A GRID POINT CONSIDERED.

FORTRAN SYMBOL	COMMON BLOCK	DESCRIPTION
		NSURF(1) AND NSURF(2) INDICATE Y-PERSPECTIVE SURFACE NUMBER, WHEREAS NSURF(3) AND NSURF(4) INDICATE Z-PERSPECTIVE SURFACE NUMBER
NUNERR	CIO	DEVICE FOR MGAUSS ERROR CHECK
NVSOLV	EQN	NUMBER OF DEPENDENT VARIABLES
NWORD2(50)	STRAGE	SIZE OF EACH COMMON BLOCK
NYCRF(10)	SECT	LOWER BOUNDARY INDEX OF EACH Z-PERSPECTIVE SUBSECTION FOR USE IN CROSEC.
NYCRL(10)	SECT	UPPER BOUNDARY INDEX OF EACH Z-PERSPECTIVE SUBSECTION FOR USE IN CROSEC.
NZCRF(10)	SECT	LEFT BOUNDARY INDEX OF EACH Y-PERSPECTIVE SUBSECTION FOR USE IN CROSEC.
NZCRL(10)	SECT	RIGHT BOUNDARY INDEX OF EACH Y-PERSPECTIVE SUBSECTION FOR USE IN CROSEC.
OMBWD	LIN	1.0 - BWD
OMEGWF	LAWW	UNDER-RELAXATION FACTOR FOR WALL FUNCTION FORMULATION
P	VAR	INDEX FOR STATIC PRESSURE
PCON1	REF	(GAMMA-1.0)/GAMMA
PCON2	REF	0.5 * PCON1
PINF	FREE	FREE STREAM STATIC PRESSURE
PL	VAR	STORAGE LEVEL OF STATIC PRESSURE IN GENERAL PURPOSE STORAGE
PLTFLD(NN, NN, 8)	ZPLOT	GENERAL PURPOSE STORAGE FOR PLOT INFORMATION
PR	REF	PRANDTL NUMBER
PREF	REF	REFERENCE PRESSURE

FORTRAN SYMBOL	COMMON BLOCK	DESCRIPTION
PREFI	REF	INVERSE OF REFERENCE PRESSURE
PREPS	VISC	PRANDTL NO. IN TURBULENT ENERGY DISSIPATION EQUATION
PRESS(20,2)	BOUND	SPECIFIED PRESSURE AT BOUNDARY
PRT	REF	TURBULENT PRANDTL NO.
PRIKE	VISC	PRANDTL NO. IN TURBOLENT KINECTIC ENERGY EQUATION
PZERO	FREE	STAGNATION PRESSURE
Q1D(8,NN)	METRIC	INTERMEDIATE STORAGE ARRAY FOR METRIC INFORMATION
Q2D(8,NN)	METRIC	INTERMEDIATE STORAGE ARRAY FOR METRIC INFORMATION
R	VAR	INDEX FOR DENSITY
RATLD	LAWW	EMPIRICAL NUMERICAL CONSTANT IN MIXING LENGTH COMPUTATION
RE	REF	REYNOLDS NUMBER
REI	REF	INVERSE OF REYNOLDS NUMBER
REI2	REF	2.0 * REI
REPL	FREE	REYNOLDS NUMBER PER UNIT LENGTH
RGAS	REF	GAS CONSTANT
RHO(NDIFM)	ADDR	STORAGE OF DENSITY FOR FIRST DERIVATIVES
RHOINF	FREE	FREE STREAM DENSITY
RHOREF	REF	REFERENCE DENSITY
RHOWL(NN,5,4)	BOUND	STORAGE FOR DENSITY ON THE BOUNDARY
RHREFI	REF	INVERSE OF REFERENCE DENSITY
RUNIV	UNITS	UNIVERSAL GAS CONSTANT
SAVE(NEQS,NN)	EQN	STORAGE FOR CHANGES DURING FIRST ADI SWEEP

FORTRAN SYMBOL	COMMON BLOCK	DESCRIPTION
SN(NN)	LIN	STORAGE FOR N TH LEVEL TERMS
SQ1	ADD	ADD CODE STREAMWISE LOCATION
SQ2	ADD	ADD CODE STREAMWISE LOCATION
SYSTEM	ZPLOT	SENTINEL FOR COORDINATE SYSTEM - PLOTS ONLY
T	VAR	INDEX FOR STATIC TEMPERATURE
TEMPS(NN,5,4)	BOUND	STORAGE ARRAY FOR TEMPERATURE ON BOUNDARY
TEMPSN(NN,5,4)	BOUND	STORAGE ARRAY FOR TEMPERATURE AT NTH STREAMWISE STATION - BOUNDARIES ONLY
TINE	FREE	FREE STREAM STATIC TEMPERATURE
TITLE(6)	ZPLOT	TITLE FOR PLOT FILE
TKE	VAR	INDEX FOR TURBULENT KINETIC ENERGY
TKEINF	LAWW	FREE STREAM TURBULENT KINETIC ENERGY
TL	VAR	STORAGE LEVEL OF STATIC TEMPERATURE IN GENERAL PURPOSE STORAGE
TREF	REF	REFERENCE TEMPERATURE
TREFI	REF	INVERSE OF REFERENCE TEMPERATURE
TT1(2)	GEOM	MESH DISTRIBUTION FACTOR
TT2(2)	GEOM	MESH DISTRIBUTION FACTOR
TWALL(20,2)	BOUND	SPECIFIED TEMPERATURE AT BOUNDARY
TWOD	GEOM	FLAG FOR TWO DIMENSIONAL LOGIC
TZERO	FREE	STAGNATION TEMPERATURE
T2(2)	GEOM	MESH DISTRIBUTION FACTOR
U	VAR	INDEX FOR VELOCITY IN X-DIRECTION
UDUE(20,2)	LAWW	BOUNDARY LAYER THICKNESS SAMPLING CRITERIA
UDUM(NDIFM)	ADDR	STORAGE OF VELOCITY FOR FIRST DERIVATIVES
UINF	FREE	FREE STREAM VELOCITY

FORTRAN SYMBOL	COMMON BLOCK	DESCRIPTION
UREF	REF	REFERENCE VELOCITY
UREFI	REF	INVERSE OF REFERENCE VELOCITY
USCALE	ADD	METRIC SCALE FACTOR
USTAR(NN,5,4)	LAWW	FRICITION VELOCITY ON SOLID WALL BOUNDARY
UTIL(NDIFM)	ADDR	STORAGE OF DEPENDENT VARIABLE FOR FIRST DERIVATIVES
V	VAR	INDEX FOR VELOCITY IN Y-DIRECTION
VELSQ(NN,NN)		STORAGE FOR $U^2 + V^2 + W^2$ - EQUIVALENCED TO PLIFLD(1,1,4)
VKB	LAWW	SECOND CONSTANT IN LOGARITHMIC LAW OF THE WALL
VKC	LAWW	VON KARMAN CONSTANT
VNO(15,15,4)	INTBC	INPUT TRANSPIRATION RATES
W	VAR	INDEX FOR VELOCITY IN Z-DIRECTION
X(502)	GEOM	STREAMWISE LOCATION
XBRKX(5)	BOUND	STREAMWISE LOCATION WHERE AN EMBEDDED SOLID BODY STARTS OR TERMINATES
XENTR	GEOM	STARTING STREAMWISE LOCATION
XG1(NN,2)	OPER	FIRST DERIVATIVES OF COMPUTATIONAL COORDINATES WITH RESPECT TO PHYSICAL COORDINATES
XG2(NN,2)	OPER	SECOND DERIVATIVES OF COMPUTATIONAL COORDINATES WITH RESPECT TO PHYSICAL COORDINATES
XOB(4)	BOUND	INITIAL LOCATION OF SOLID OBSTACLE IN X DIRECTION
XVNO(15,15,4)	INTBC	STREAMWISE LOCATIONS WHERE TRANSPIRATION DATA IS INPUT
XO(2)	GEOM	MESH DISTRIBUTION FACTOR
Y(NN,NN,2)		PHYSICAL DISTANCES FROM BOUNDARIES - EQUIVALENCED TO PLIFLD(1,1,2)

FORTRAN SYMBOL	COMMON BLOCK	DESCRIPTION
YAW	REF	YAW ANGLE
YPLUSL(NN,NN)		STORAGE FOR RHO * UTAU / VISLAM - EQUIVALENCED TO PLTELD(1,1,1)
YS(2,2)	GEOM	NONDIMENSIONAL EXTENTS OF COMPUTATIONAL DOMAIN
YSAVE(NN,2)	GEOM	COMPUTATIONAL COORDINATES
YZPROF(NN)	PROFILE	TEMPORARY STORAGE ARRAY FOR PHYSICAL COORDINATES
YZUND(15,15,4)	INTBC	CROSS-PLANE LOCATIONS WHERE TRANSPIRATION DATA IS INPUT
ZNIRN(NDIM,3)	ZEX1	ARRAY FOR VIRTUAL MEMORY STORAGE NDIM = NN * NN * MZVAR * MLEVEL
ZZ(M,L,K)	VARZZ	GENERAL PURPOSE STORAGE FOR DEPENDENT AND DERIVED VARIABLES - M = MZVAR, L = MLEVEL, K = NDIEM * NN

Sample Input and Sample Output

Tables I and II present sample input and output for one of the test cases previously discussed. The sample input was used to calculate the flow field of rectangular supersonic jet (aspect ratio = 1) interacting with the ambient stream. The input data is for an initial run (IRSTIN = 0) with a restart to be written every 10 marching steps (IRSTOT=10). The case is to be run on CRAY-1 computer. The streamwise and two transverse momentum as well as continuity and stagnation enthalpy (IHSTAG = 1) version of the energy equation are to be solved. The reference length is 2.0m (IUNITS = 2), the Reynold's number per m is 1.6685×10^6 , the free stream Mach number 2.0 and the free stream pressure is 2864.0 Nt/m². 50 x 50 grid points are utilized in both directions of the computational cross-section (NE = 50,50) and a Cartesian coordinate system is to be utilized (IGEOM = 1). The initial run is to be marched 10 steps (NS = 10) starting at a streamwise location of 0.0 (XENTR = 0.0). The streamwise marching step size is 0.01 (DELX = 0.01). Then grid point characteristics is specified (IFBW(1,1) =) to define a computational domain in the cross-section. For a detailed explanation of the indicators, computer program list should be consulted. During this initial run grid point characteristics will change at one streamwise location (NBRKX = 1). At the streamwise location 0.015 (XBRKX(1) = 0.015) an embedded solid body will begin (IEDGE = 0). The solid body is a splitter bounded by two surface-fitted coordinate lines (18 and 19 in Y-direction and 18 and 19 in Z-direction). In the Namelist LISTR, IFBW is respecified as shown in Table I. An information on IBOUND and JEQBC corresponding to the new IFBW is also provided. Grid points are clustered in the vicinity of the embedded solid body, i.e., about 0.2 in Y-direction and 0.2 in Z-direction (XO(1) = 0.2,0.2). The packing is to be moderately tight (T2(1) = 3.0, 3.0). An initial profile is generated within the program to supply a uniform stream needed for this case (IPROF = 1) and modified to give two different magnitudes of velocity. Printout is given every 5 steps (IPRINT = 5) and plot information is written every 5 steps (IPLOT = 5).

The output for the three-dimensional case consists of NAMELIST information and difference weight information and flow field information at each 5th streamwise station. The NAMELIST information is provided as a means

for the user to check the input data. Three-dimensional flow field output is controlled by the variable IVARPR. For three dimensions, however, the output is in the form of a cross-sectional plane of output. All variables (except the pressure) are in a non-dimensional form with respect to the reference conditions which are displayed in NAMELIST LIST 2. The pressure terms are nondimensionalized with respect to the freestream pressure. The integer variables IY and IZ represent the transverse and spanwise grid point locations respectively while Z and Y are the corresponding computational positions. Table II is a portion of the output for the three-dimensional rectangular jet case i.e., the cross plane distribution of the streamwise velocity (UVEL) and pressure (PRES). Other variables can (and were) printed out, but for reasons of economy of space are not presented here. Following the flow field information is the subsonic-supersonic grid point position indicator (ISS) with respect to the lower and upper surface (right and left surface for IADI = 3), and the boundary indicator (JBOUND). The ISS values tell the grid point where the flow transitions from subsonic to supersonic flow while the variable JBOUND tells the type of surface (JBOUND = 1 corresponding to a wall and JBOUND = 2 corresponding to a nonwall). Finally, plot file information is displayed.

REFERENCES

1. Grossman, B. and Melnick, R.: The Numerical Computation of the Transonic Flow over Afterbodies Including the Effect of Jet Plume and Viscous Interactions, AIAA Paper 75-62, January 1975.
2. Cosner, R.R. and Bower, W.W.: A Patched Solution of the Transonic Flow Fields About an Axisymmetric Boattail, AIAA Paper 77-227, January 1977.
3. Forester, C.K.: Numerical Simulation of the Interaction of Jet and Freestream Flows in Engine Exhaust Systems, AIAA Paper 78-144, January 1978.
4. Hasen, G.A.: Navier-Stokes Solutions for an Axisymmetric Nozzle, AIAA Journal, Vol. 20, September 1982, pp. 1219-1227.
5. Mikhail, A.G., Hankey, W.L. and Shang, J.S.: Computation of a Supersonic Flow Past an Axisymmetric Nozzle Boattail with Jet Exhaust, AIAA Paper 78-993, July 1978.
6. McDonald, H. and Briley, W.R.: Three-Dimensional Supersonic Flow of a Viscous or Inviscid Gas, J. Comp. Physics, Vol. 19, October 1975, pp. 150-178.
7. Garvine, R.W.: Upstream Influence in Viscous Interaction Problems, The Physics of Fluids, Vol. 11, July 1968, pp. 1413-1423.
8. Rudman, S. and Rubin, S.G.: Hypersonic Viscous Flow over Slender Bodies having Sharp Leading Edges, AIAA Journal, Vol. 6, October 1968, pp. 1883-1889.
9. Lubard, S.C. and Helliwell, W.S.: Calculation of the Flow on a Cone at High Angle of Attack, AIAA Journal, Vol. 7, July 1974, pp. 965-976.
10. Vigneron, Y.C., Rakich, J.V. and Tannehill, J.C.: Calculation of Supersonic Viscous Flow Over Delta Wings with Sharp Subsonic Leading Edges, NASA TM 78500, June 1978.
11. Schiff, L.B. and Steger, J.L.: Numerical Simulation of Steady Supersonic Viscous Flow, AIAA Journal, Vol. 18, December 1980, pp. 1421-1430.
12. Helliwell, W.S. and Lubard, S.C.: An Implicit Method for Three-Dimensional Viscous Flow with Application to Cones at Angle of Attack, Computer and Fluids, Vol. 3, 1975, pp. 83-101.
13. Lubard, S.C. and Rakich, J.V.: Calculation of the Flow on a Blunted Cone at a High Angle of Attack, AIAA Paper 75-147, 1975.
14. Helliwell, W.S., Dickinson, R.P. and Lubard, S.C.: Viscous Flows Over Arbitrary Geometries at High Angle of Attack, AIAA Journal, Vol. 19, No. 2, February 1981.

REFERENCES (Continued)

15. Rubin, S.G. and Lin, A.: Marching with the PNS Equations, Israel Journal of Technology, Vol. 18, 1980.
16. Buggeln, R.C., Kim, Y.-N. and McDonald, H.: Computation of Multi-Dimensional Viscous Supersonic Flow, NASA Contractor Report CR-4021, 1986.
17. Dash, S.M. and Wolf, D.E.: Shock-Capturing Parabolized Navier-Stokes Model (SCIPVIS) for the Analysis of Turbulent Underexpanded Jets, AIAA Paper 83-704, April 1983.
18. Dash, S.M. and Wolf, D.E.: Interactive Phenomena in Supersonic Jet Mixing Problems, Part I: Phenomenology and Numerical Modeling Techniques, AIAA Journal, Vol. 22, No. 7, July 1984.
19. Dash, S.M., Wolf, D.E. and Sinha, N.: Parabolized Navier-Stokes Analysis of Three-Dimensional Supersonic and Subsonic Jet Mixing Problems, AIAA Paper No. 84-1525, June 1984.
20. Vatsa, V.N., Werle, M.J., Anderson, D.L. and Hankins, G.B.: Solutions for Three-Dimensional Over-or Underexpanded Exhaust Plumes, AIAA Journal, Vol. 20, September 1982, pp. 1188-1194.
21. Favre, A.: Statistical Equations of Turbulent Gases, Problems of Hydrodynamics and Continuum Mechanics, Soc. Indust. and Appl. Math., 1969, pp. 231-266.
22. Beer, J.M. and Chiger, N.A.: Combustion Aerodynamics, John Wiley and Sons, Inc., New York, 1972.
23. McDonald, H. and Camarata, F.J.: An Extended Mixing Length Approach for Computing the Turbulent Boundary-Layer Development, In Proceedings, Stanford Conference on Computation of Turbulent Boundary Layers, Vol. I, Stanford University, 1969, pp. 83-98.
24. Van Driest, E.R.: On Turbulent Flow near a Wall, Journal of Aeronautical Sciences, November 1956.
25. Anderson, B.H. and Benson, T.J.: Numerical Solution to the Glancing Sidewall Oblique Shock Wave/Turbulent Boundary Layer in Three-Dimension, AIAA Paper 83-0136, 1983.
26. Benson, T.J. and Anderson, B.H.: Validation of a Three-Dimensional Viscous Analysis of Axisymmetric Supersonic Inlet Flow Fields, AIAA Paper 83-0135, 1983.
27. McDonald, H. and Briley, W.R.: Three-Dimensional Supersonic Flow of a Viscous or Inviscid Gas, J. Comp. Physics, 1975.
28. Briley, W.R. and McDonald, H.: Solution of the Multidimensional Compressible Navier-Stokes Equations by a Generalized Implicit Method, J. of Comp. Physics, Vol. 24, No. 4, August 1977, p. 372.

REFERENCES (Continued)

29. Douglas, J. and Gunn, J.E.: A General Formulation of Alternating Direction Methods, Numerische Math., Vol. 6, 1964, p. 2128.
30. Beam, R.M. and Warming, R.F.: An Implicit Factored Scheme for the Compressible Navier-Stokes Equations, AIAA Journal, Vol. 16, April 1978, p. 393.
31. Briley, W.R. and McDonald, H.: On the Structure and Use of Linearized Block ADI and Related Schemes. J. of Comp. Physics, Vol. 34, 1980, p. 54.

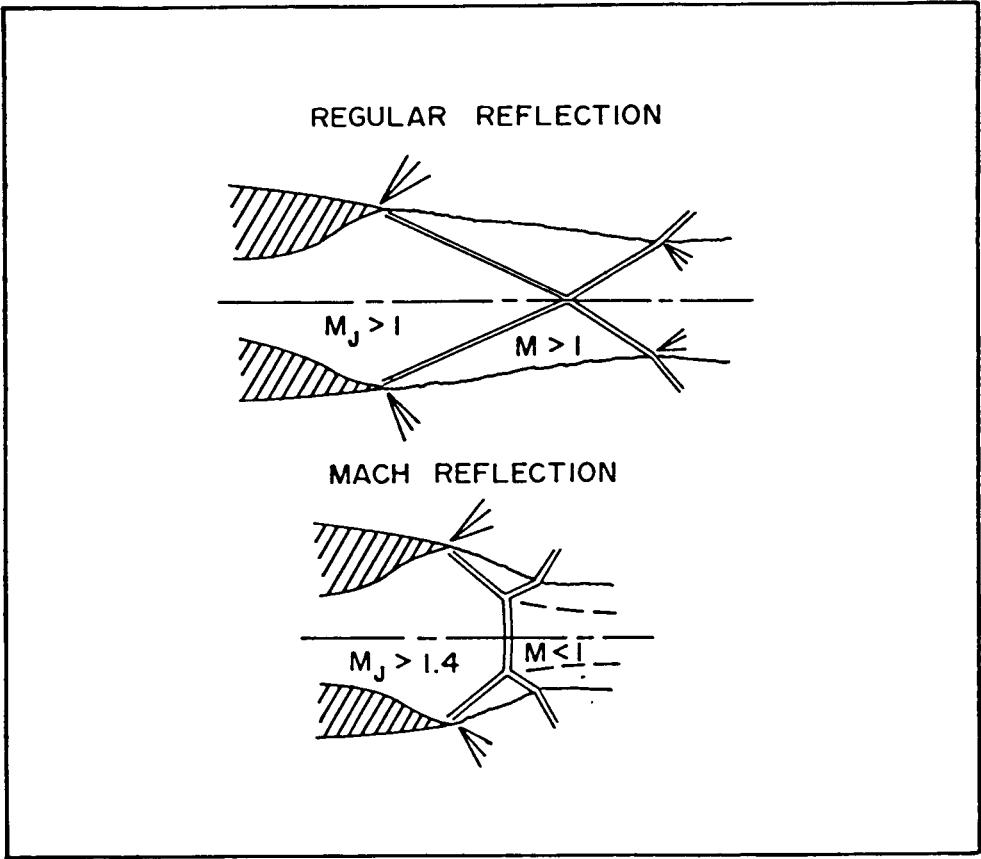


FIGURE 1. - SHOCK STRUCTURE FOR A TYPICAL
OVEREXPANDED AXISYMMETRIC NOZZLE

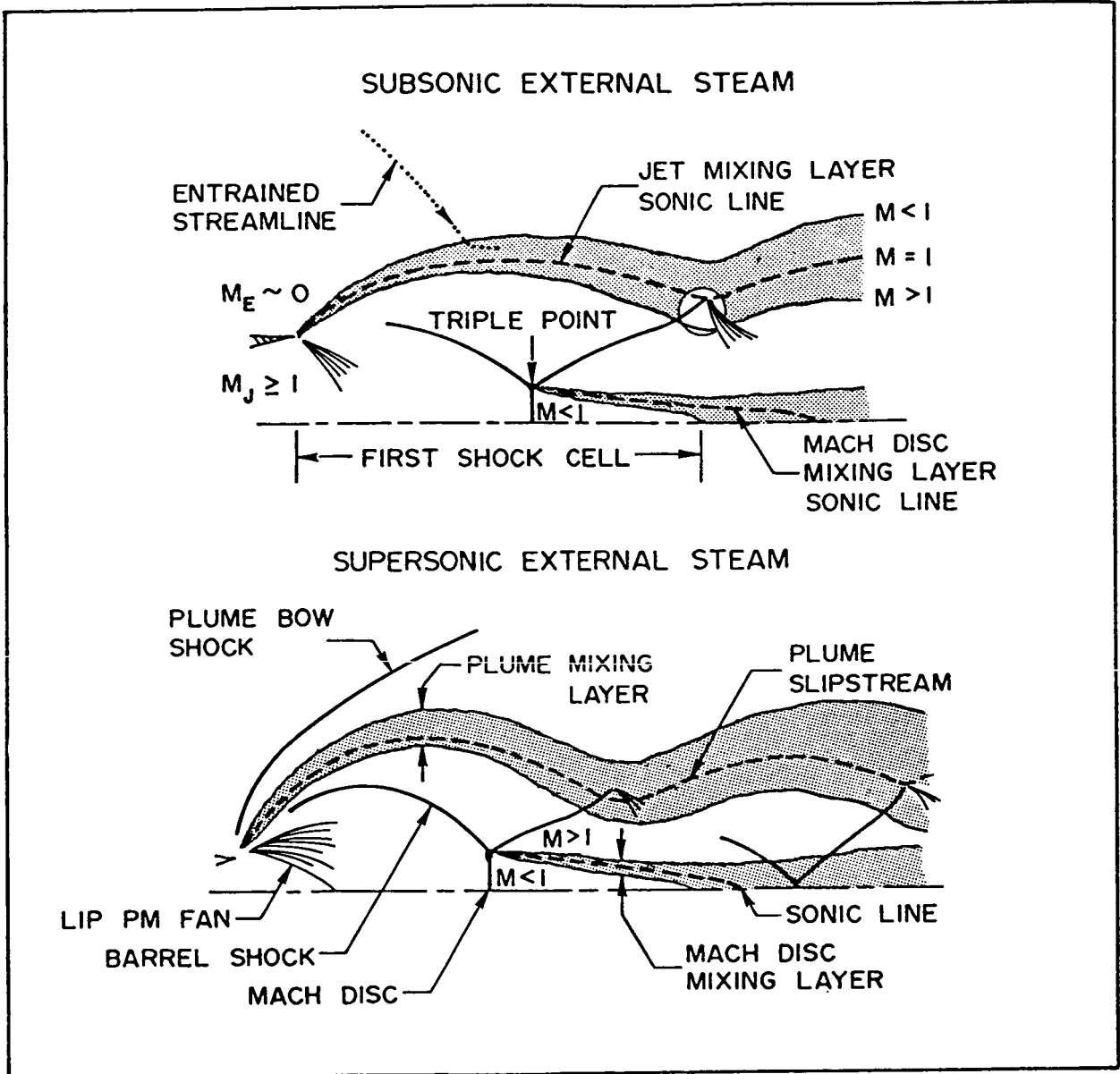


FIGURE 2 - SCHEMATIC OF JET NEAR FIELD STRUCTURE FOR SUPERSONIC AND SUBSONIC EXTERNAL FLOWS (REF. 18)

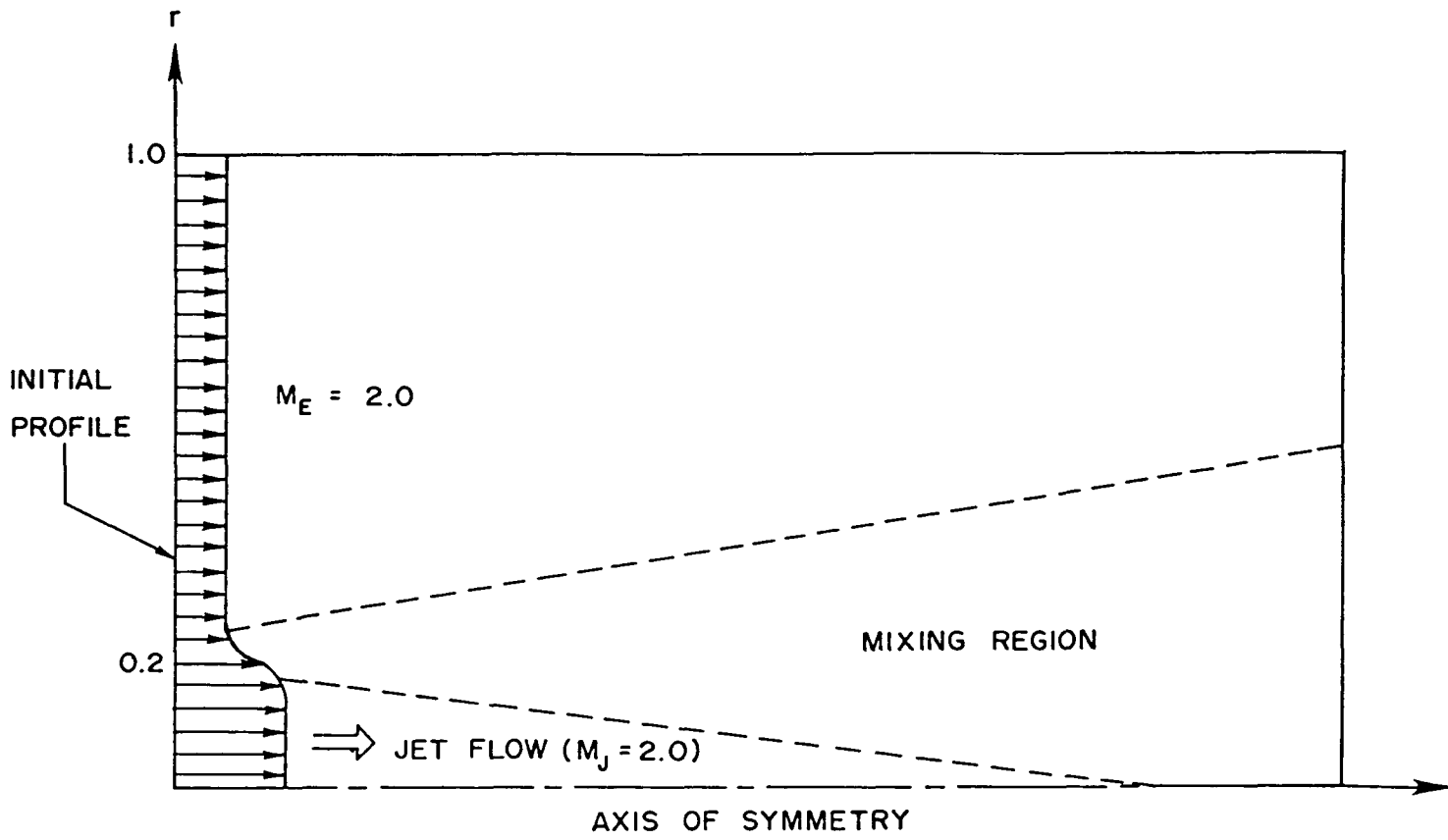


FIGURE 3 - SCHEMATIC OF AXISYMMETRIC JET FLOW

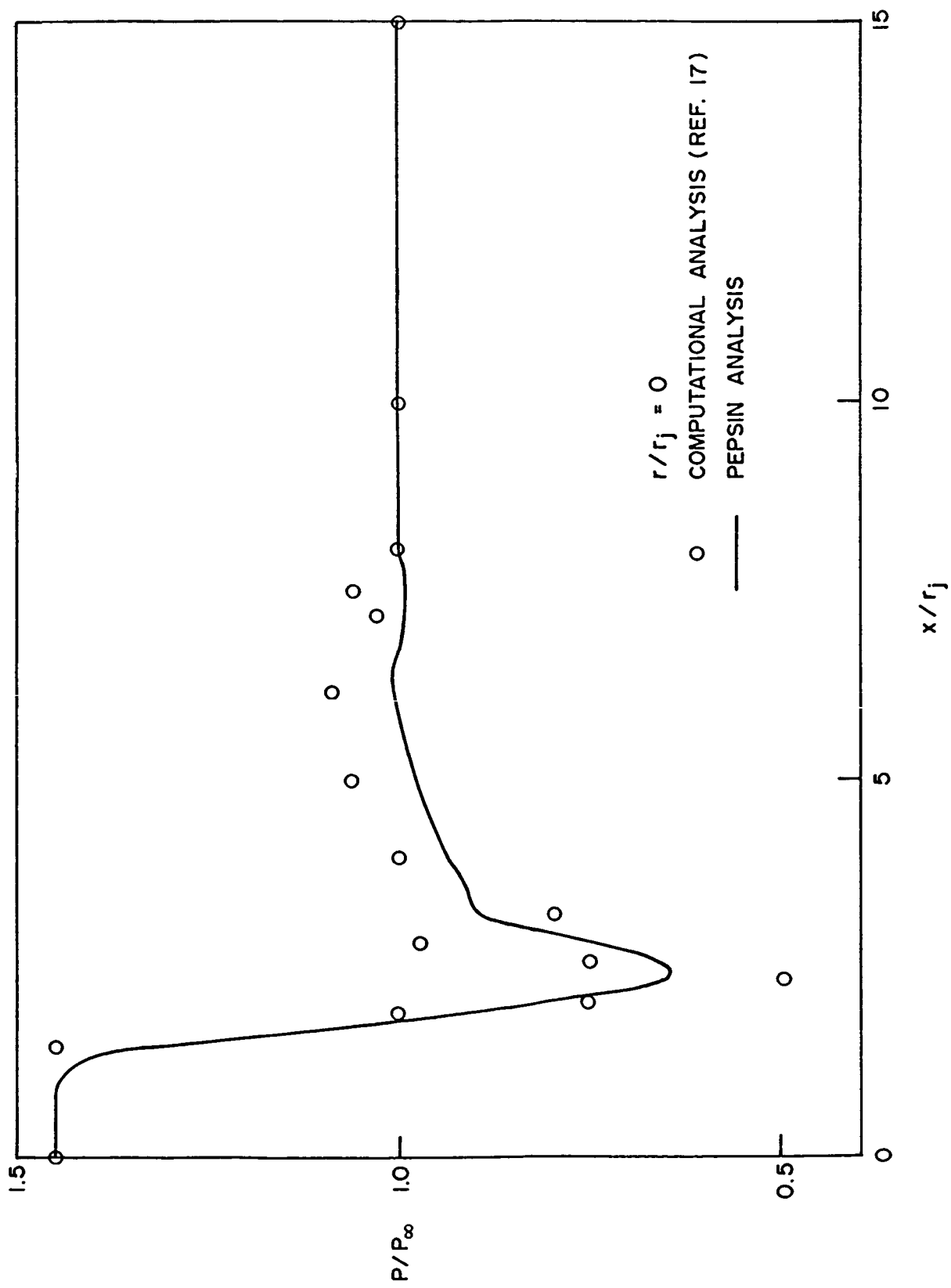


FIGURE 4(a) - STREAMWISE STATIC PRESSURE DISTRIBUTION

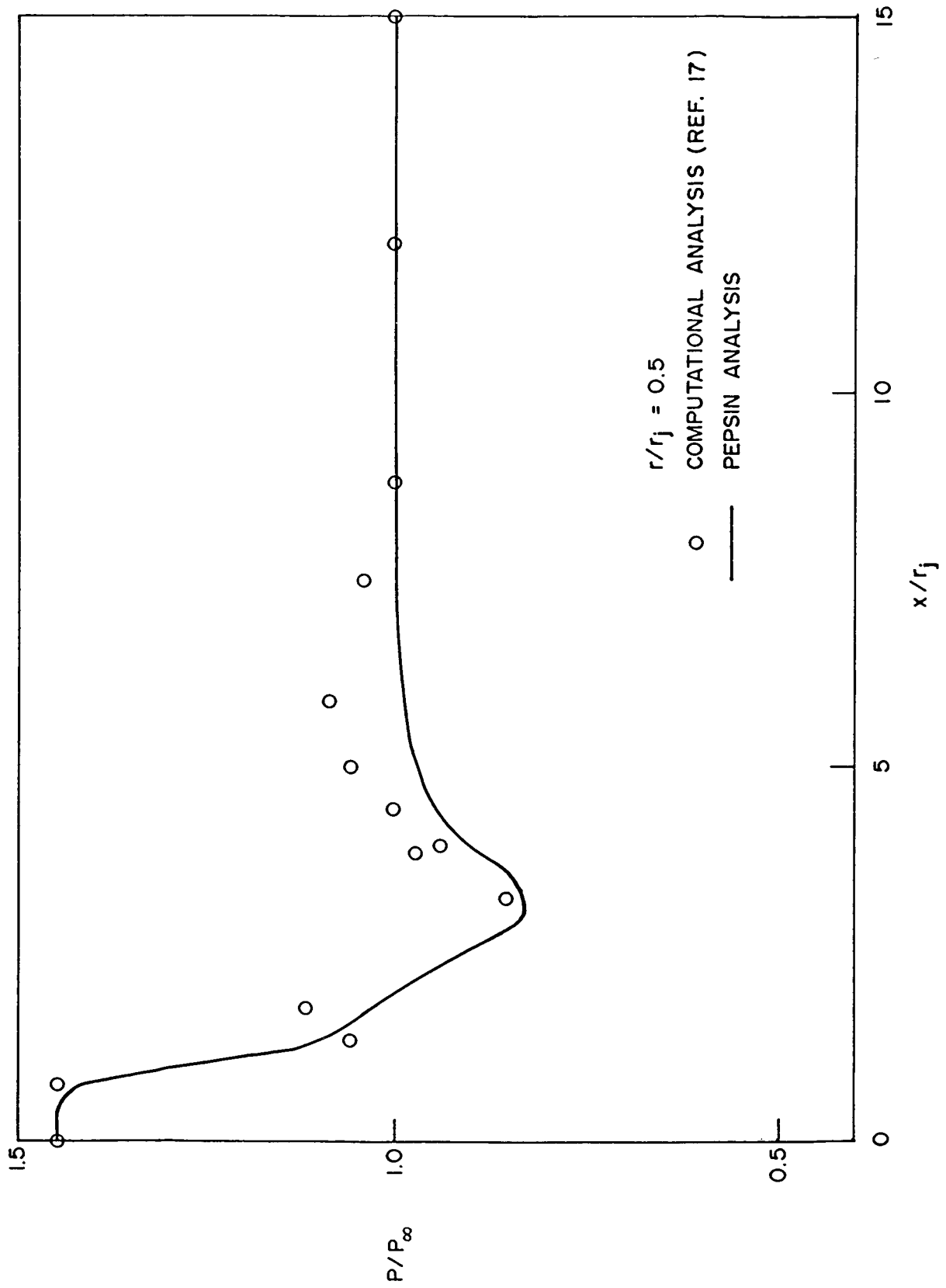
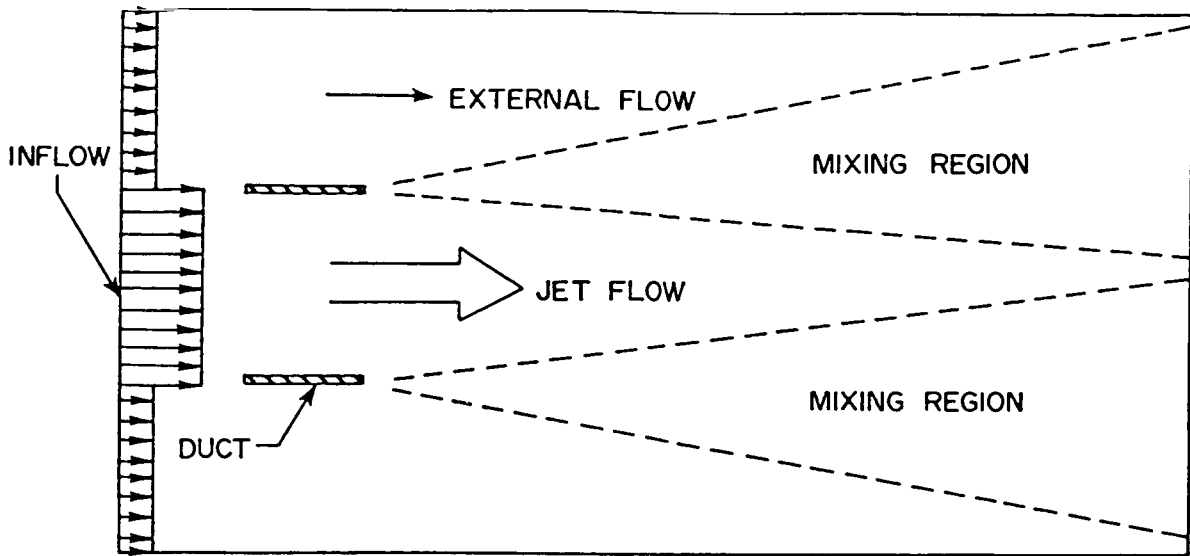
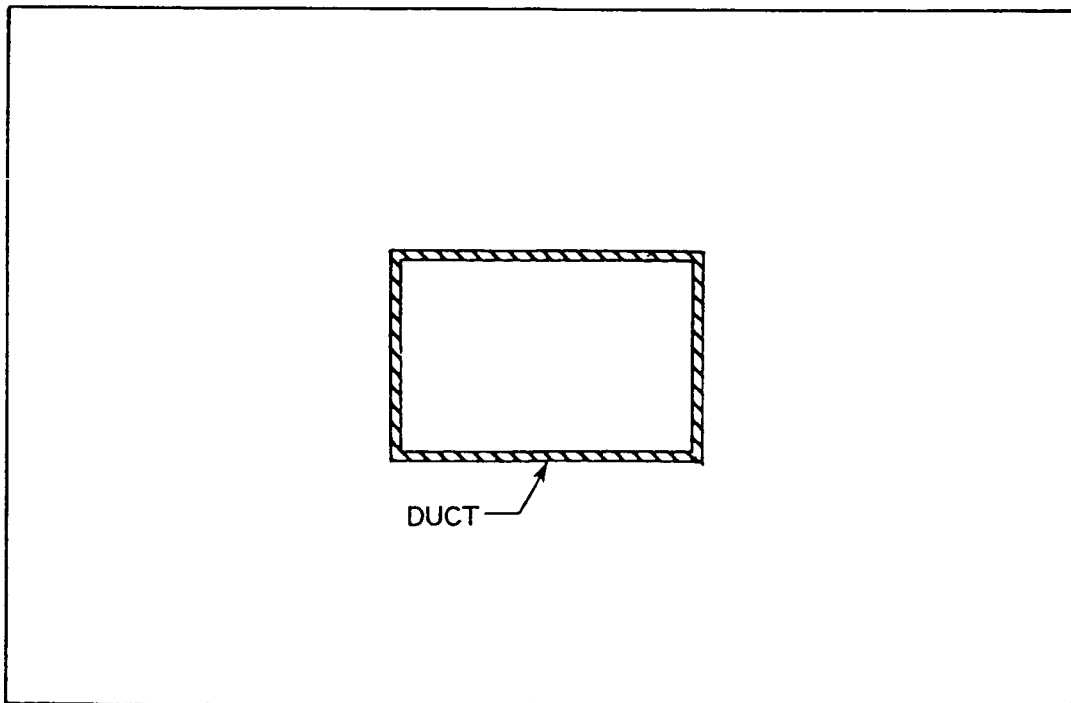


FIGURE 4(b) - STREAMWISE STATIC PRESSURE DISTRIBUTION



SIDE VIEW



FRONT VIEW

FIGURE 5 - SCHEMATIC OF 3-DIMENSIONAL JET FLOW

C-2

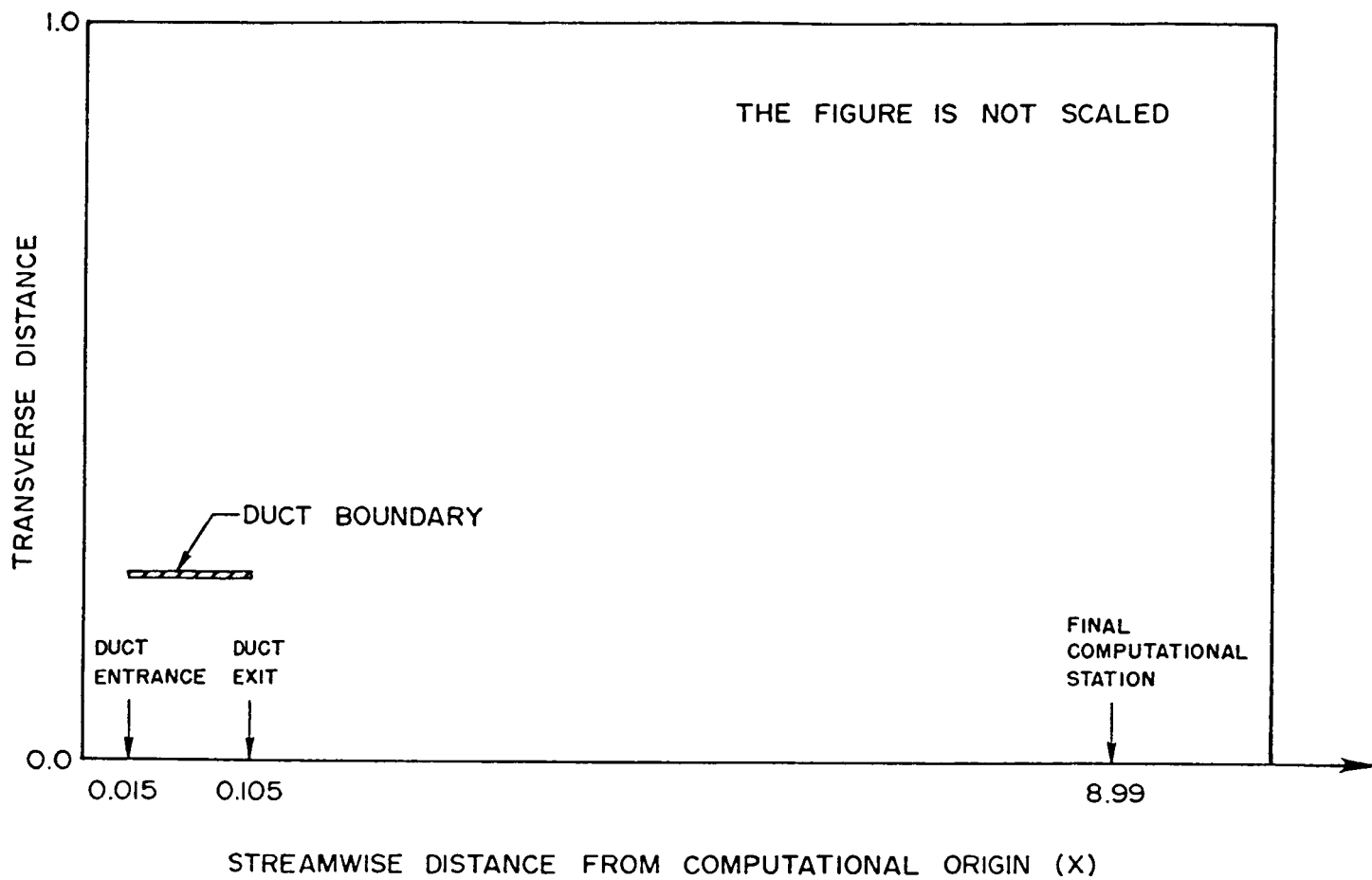


FIGURE 6 - SCHEMATIC OF COMPUTATIONAL DOMAIN (SIDE VIEW)



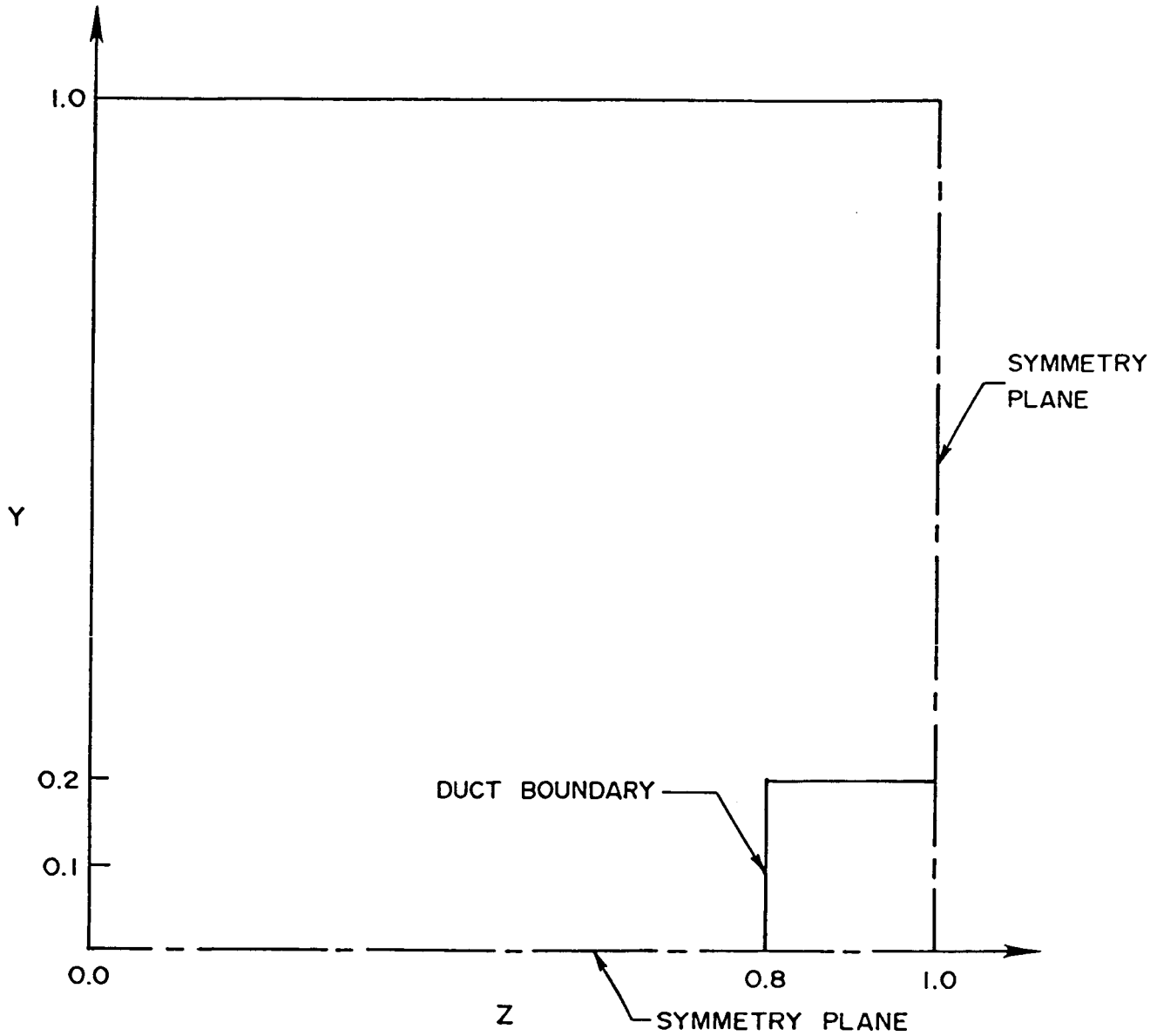


FIGURE 7 - CROSS-SECTION OF COMPUTATIONAL DOMAIN
(ASPECT RATIO = 1)

CSA

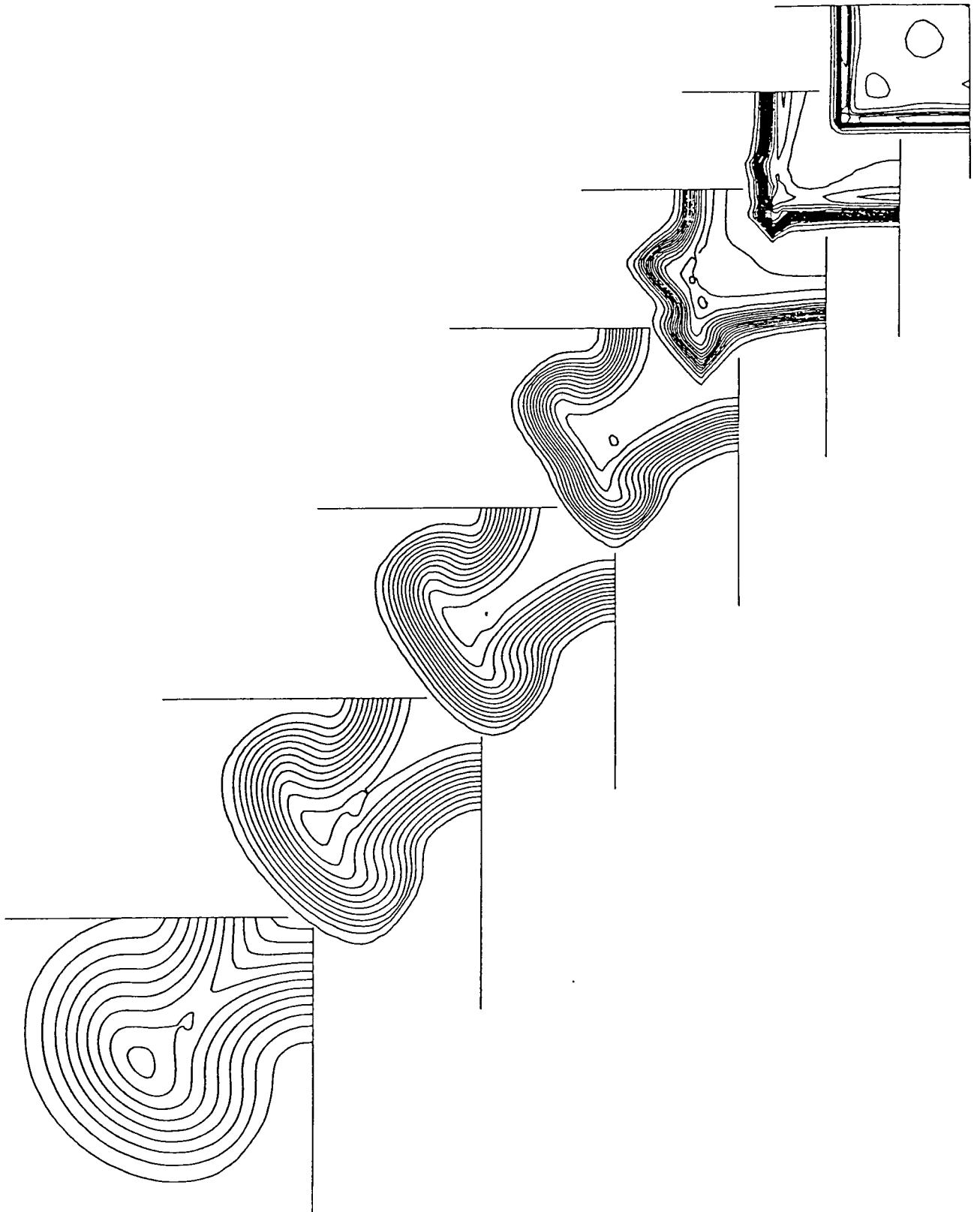


FIGURE 8 - ASPECT RATIO = 1 - STREAMWISE DEVELOPMENT OF STAGNATION PRESSURE ISOBARs

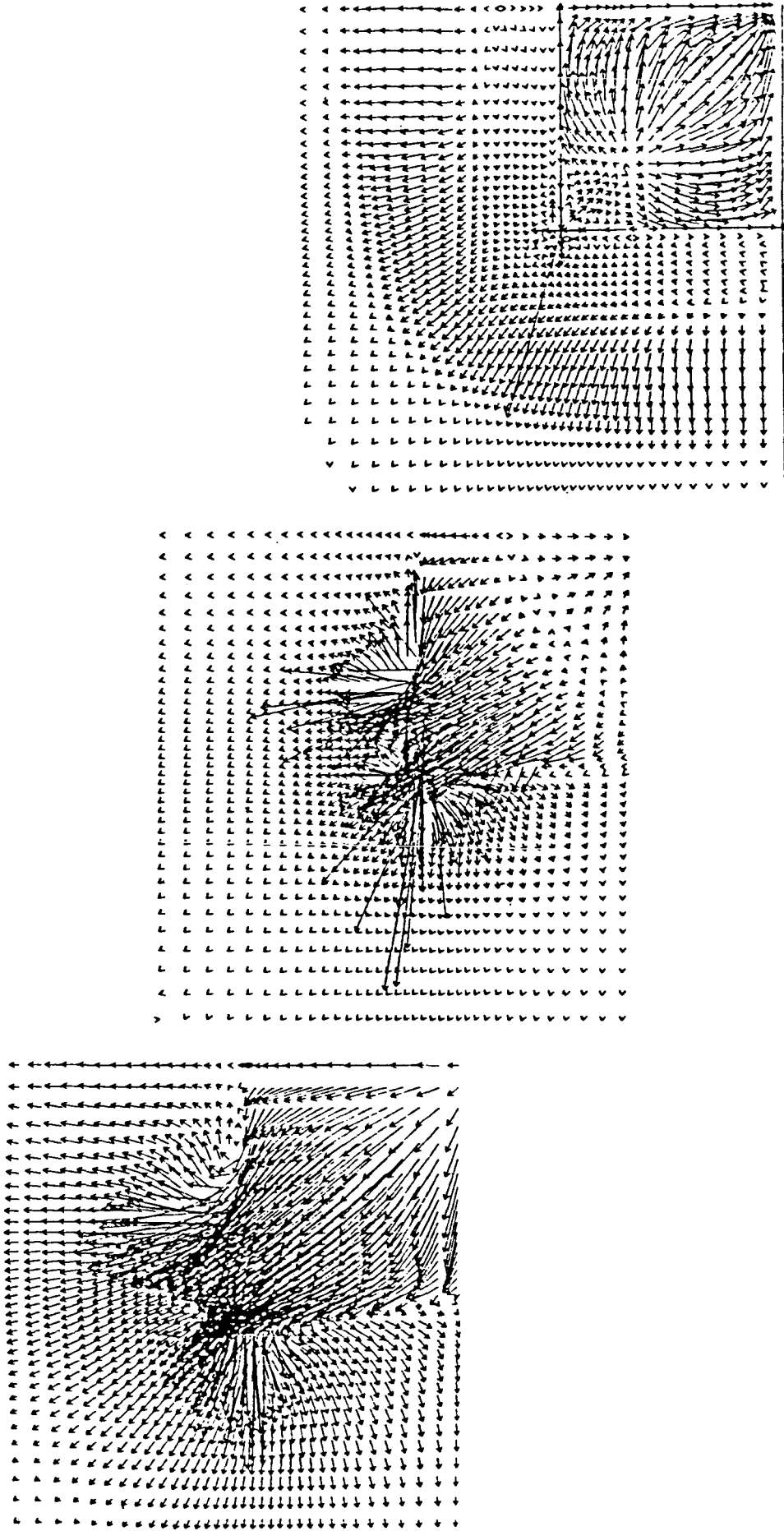


FIGURE 9(a) - SUPERSONIC JET FLOW (ASPECT RATIO = 1) - STREAMWISE DEVELOPMENT OF THE SECONDARY VELOCITY IN THE CROSS-SECTION

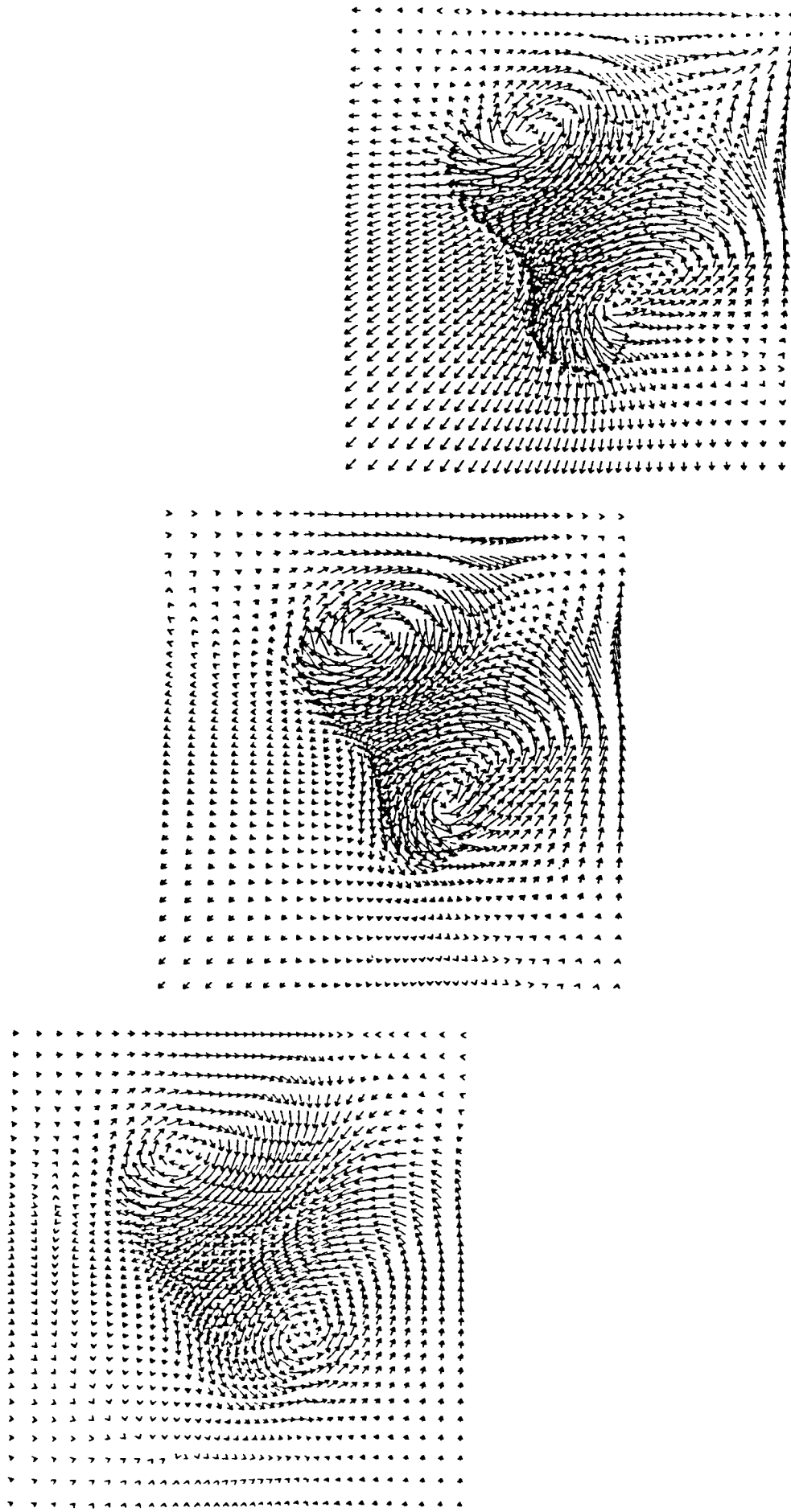


FIGURE 9(b) - SUPERSONIC JET FLOW (ASPECT RATIO = 1) - STREAMWISE DEVELOPMENT OF THE SECONDARY VELOCITY IN THE CROSS-SECTION

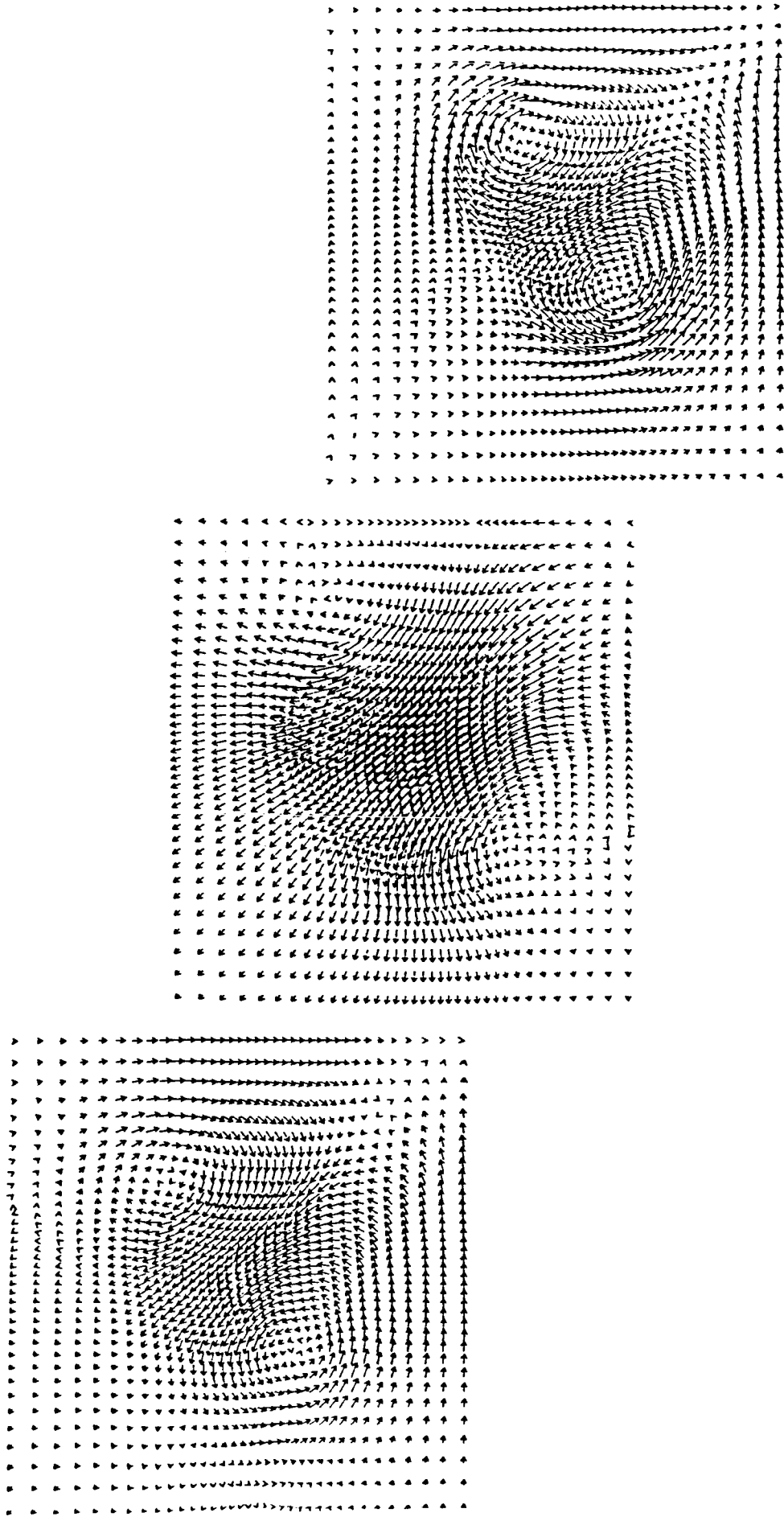


FIGURE 9(c) - SUPERSONIC JET FLOW (ASPECT RATIO = 1) - STREAMWISE DEVELOPMENT OF THE SECONDARY VELOCITY IN THE CROSS-SECTION

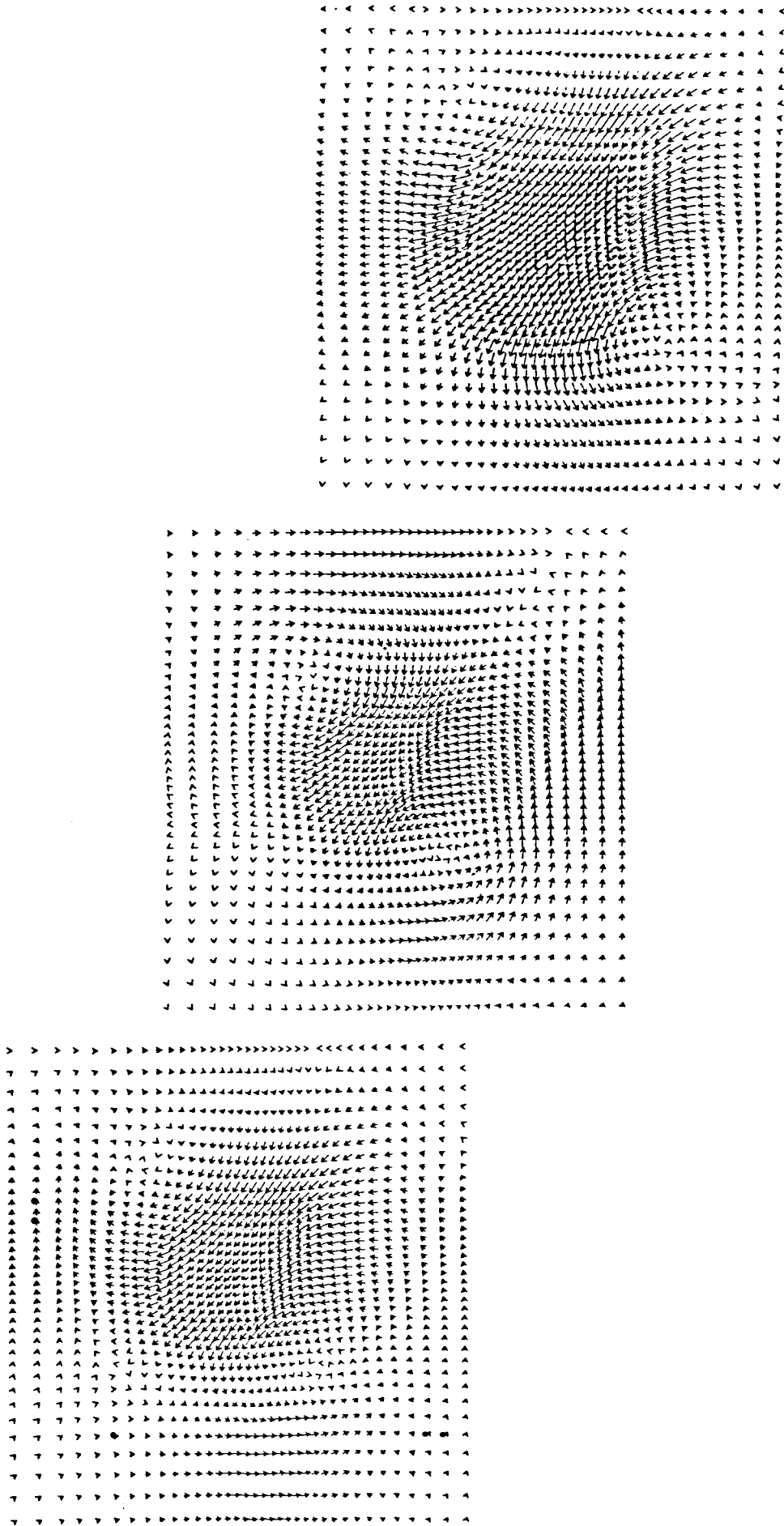


FIGURE 9(d) - SUPERSONIC JET FLOW (ASPECT RATIO = 1) - STREAMWISE DEVELOPMENT OF THE SECONDARY VELOCITY IN THE CROSS-SECTION

ORIGINAL PAGE 88
OF POOR QUALITY

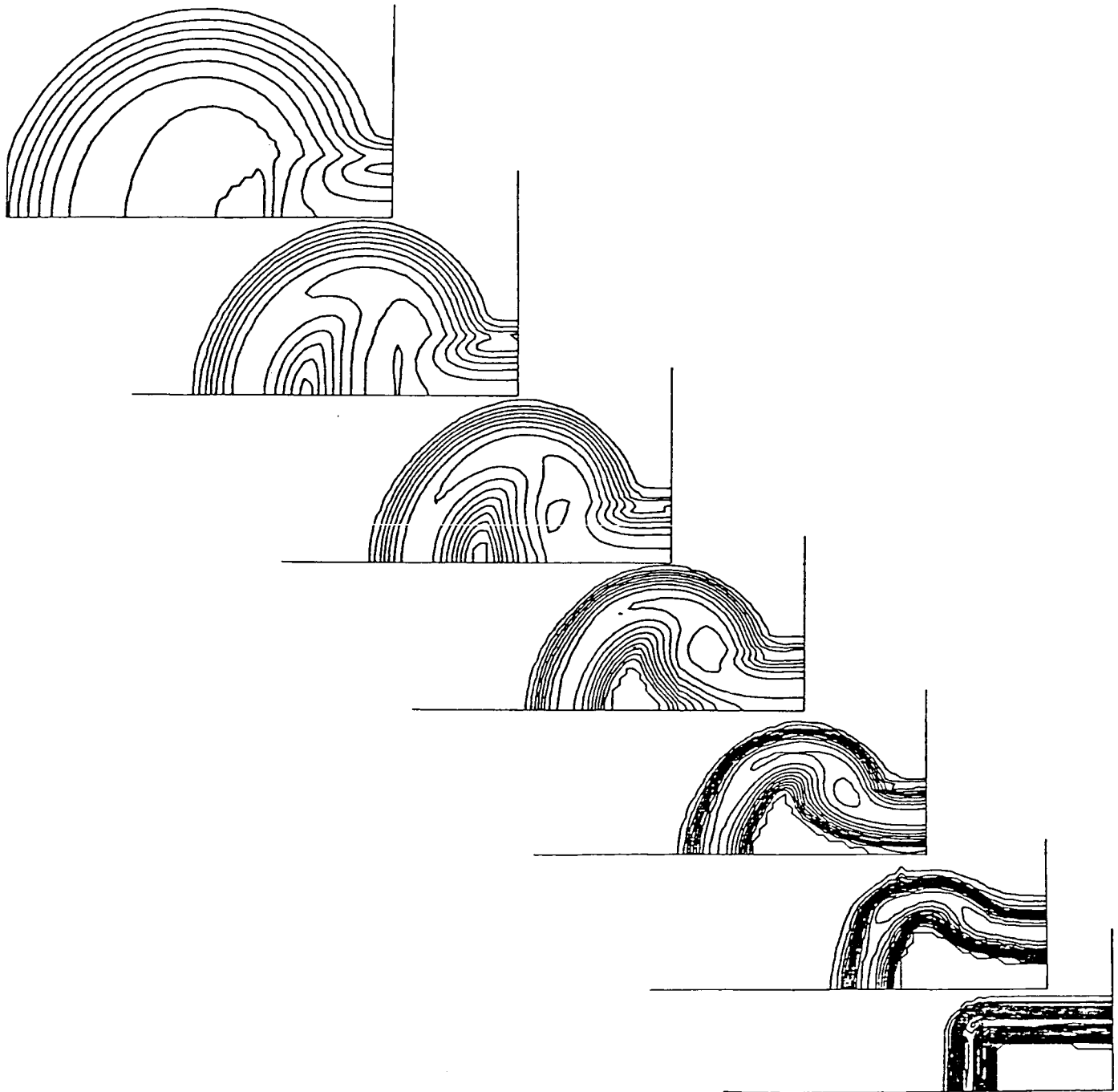


FIGURE 10 - ASPECT RATIO = 2 - STREAMWISE DEVELOPMENT
OF STAGNATION PRESSURE ISOBARs

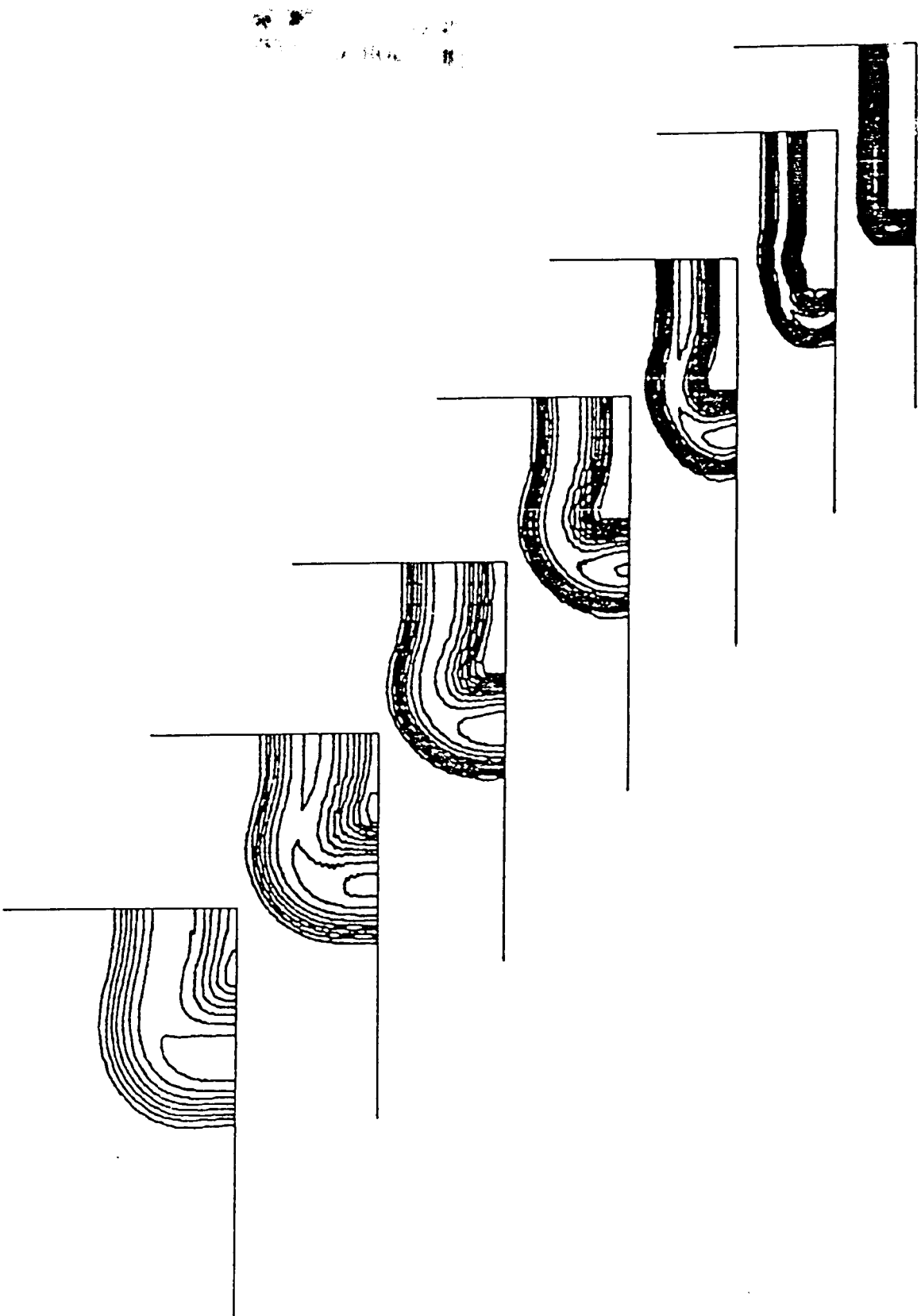


FIGURE 11 - ASPECT RATIO = 5 - STREAMWISE DEVELOPMENT OF STAGNATION PRESSURE ISOBARS

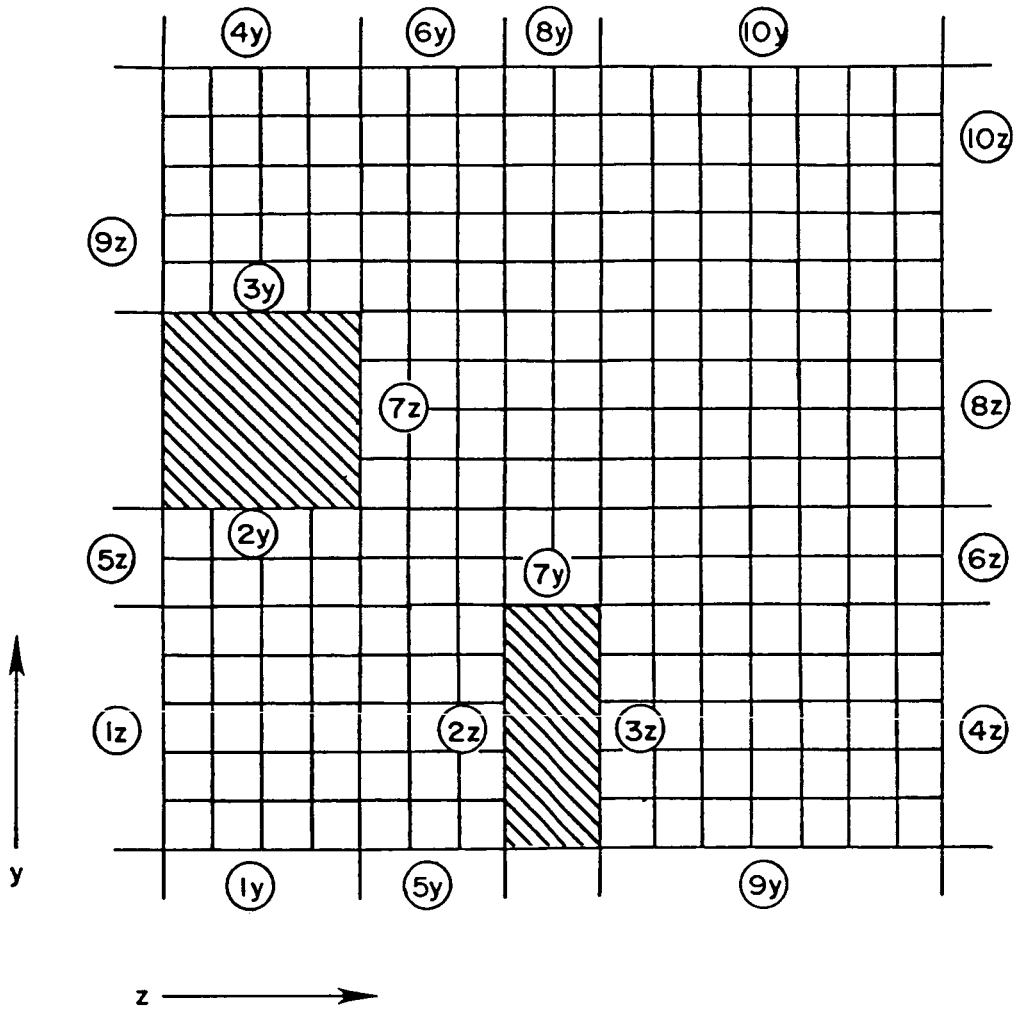


FIGURE 12 - A SAMPLE CROSS-SECTION WITH EMBEDDED SOLID BODIES.

TABLE I - Sample Three-Dimensional Input

```

TOP RECORD
  NOZZLE(AR=1)
  1      1.0
  &REST
  ICOMP = 3,
  IRSTIN = 0, NFILE = 0, NSAVED = 0,
  IRSTOT = 10,
  JRSTOT = 10,
  &END
  &LIST1
  IHSTAG = 1,
  IBOUND = 40*2,
  IEQBC(1,1,1) = 40*2,
  IEQBC(1,1,2) = 40*2,
  IEQBC(1,1,3) = 40*2,
  IEQBC(1,1,4) = 40*16,
  IEQBC(1,1,5) = 40*8,
  JEQBC(1,1,1) = 11,12,38*11,
  JEQBC(1,1,2) = 2,12,18*2,20*11,
  JEQBC(1,1,3) = 11,12,18*11,20*2,
  JEQBC(1,1,4) = 14,12,38*14,
  JEQBC(1,1,5) = 17,12,38*17,
  &END
  &LIST2
  LREF = 1.0,
  REPL = 1.6685E+06,
  MINE = 2.0,
  PINE = 2864.0,
  PR = 0.71,
  IUNITS = 2,
  &END
  &LIST3
  TWOD = .FALSE.,
  XO(1) = 0.2,0.2,
  T2(1) = 3.0,3.0,
  NE = 50,50,
  IGEOM = 1,
  DELX = 0.01,
  IAP = 1,
  DXMIN = 0.01,
  DXMAX = 0.01,
  AP = 1.0,
  NS = 10,
  XENTR = 0.0,
  IFBW(1,1) = 5,48*3,5,50*2,
               3,48*1,3,50*2,
               3,48*1,3,50*2,
               3,48*1,3,50*2,

```



```

NBRKX = 1,
XBRKX(1) = 0.015,
IBRKMN = 17*18,2*1,481*0,
IBRKMX = 19*19,481*0,
IEDGE = 0,
&END
&LIST4
IVISC = 3,
IPROF = 1,
IMIXL = 1,
&END
&LIST5
IPRINT = 5,
IPLOT = 5,
&END
&LISTR
IFBW(1,1) = 5,16*3,2*5,30*3,5,50*2,
            3,16*1,2*3,30*1,3,50*2,
            3,16*1,2*3,30*1,3,50*2,
            3,16*1,2*3,30*1,3,50*2,
            3,16*1,2*3,30*1,3,50*2,
            3,16*1,2*3,30*1,3,50*2,
            3,16*1,2*3,30*1,3,50*2,
            3,16*1,2*3,30*1,3,50*2,
            3,16*1,2*3,30*1,3,50*2,
            3,16*1,2*3,30*1,3,50*2,
            3,16*1,2*3,30*1,3,50*2,
            3,16*1,2*3,30*1,3,50*2,
            3,16*1,2*3,30*1,3,50*2,
            3,16*1,2*3,30*1,3,50*2,
            3,16*1,2*3,30*1,3,50*2,
            3,16*1,2*3,30*1,3,50*2,
            3,16*1,2*3,30*1,3,50*2,
            3,16*1,2*3,30*1,3,50*2,
            3,16*1,2*3,30*1,3,50*2,
            3,16*1,2*3,30*1,3,50*2,
            3,16*1,2*3,30*1,3,50*2,
            3,16*1,2*3,30*1,3,50*2,
            5,16*3,5,3,30*1,3,50*2,
            5,17*3,4,30*1,3,50*2,
IBOUND = 2,2*1,2,3*1,3*2,10*2,2,2*1,2,3*1,3*2,10*2,
JEQBC(1,1,1) = 3*11,12,3*11,12,11,12,30*11,
JEQBC(1,1,2) = 3*2,12,3*2,12,2,12,10*2,20*11,
JEQBC(1,1,3) = 3*11,12,3*11,12,11,12,10*11,20*2,
JEQBC(1,1,4) = 3*14,12,3*14,12,14,12,30*14,
JEQBC(1,1,5) = 3*17,12,3*17,12,17,12,30*17,

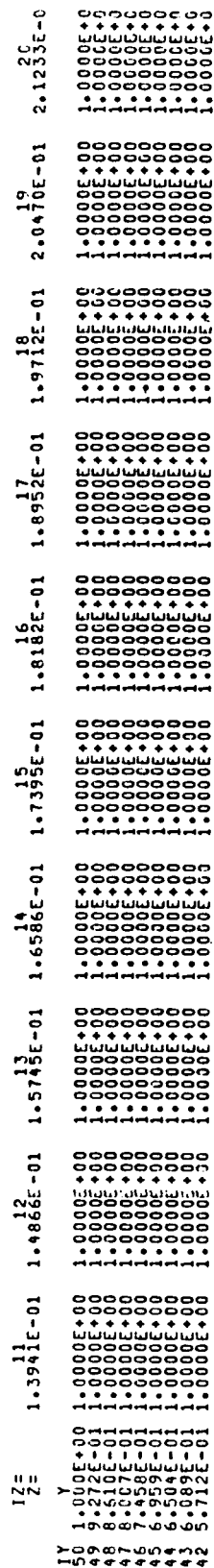
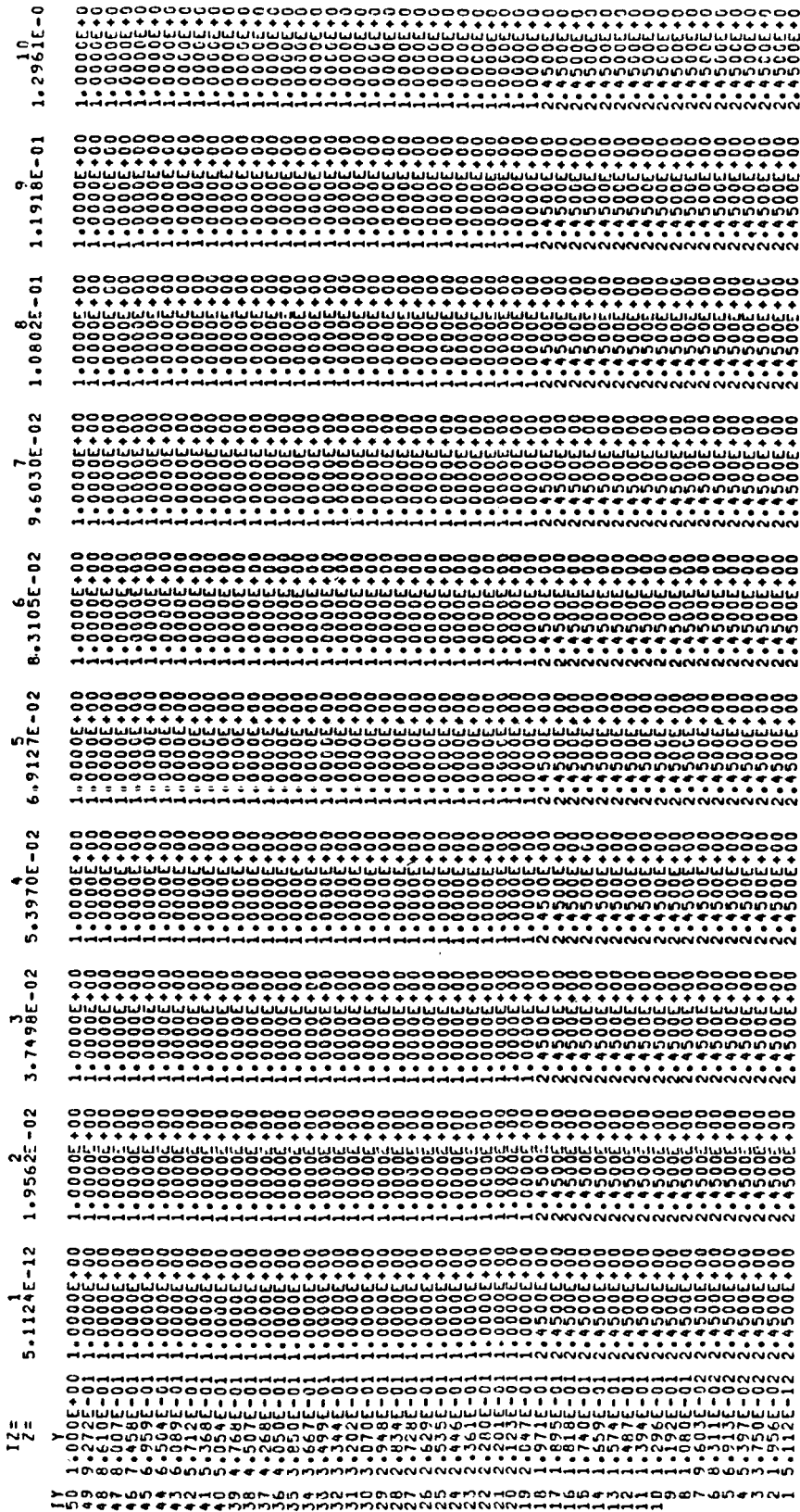
&END
EOF

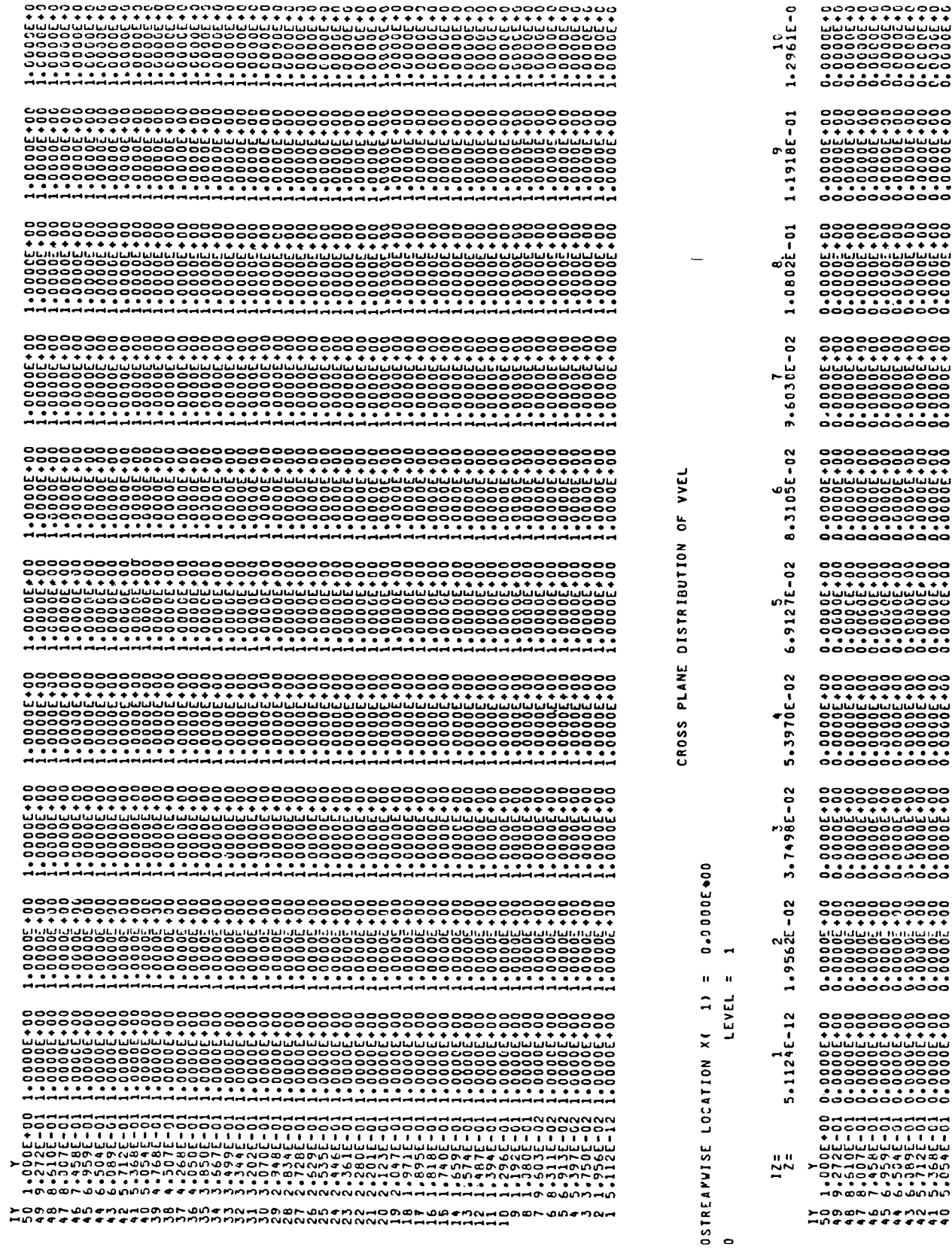
```


CROSS PLANE DISTRIBUTION OF UVEL

OSTREAMWISE LOCATION X(1) = 0.0000E+00

LEVEL = 1





1. Report No. NASA CR-4020		2. Government Accession No.		3. Recipient's Catalog No.	
4. Title and Subtitle Computation of Multi-Dimensional Viscous Supersonic Jet Flow				5. Report Date October 1986	
				6. Performing Organization Code	
7. Author(s) Y. N. Kim, R. C. Buggeln, and H. McDonald				8. Performing Organization Report No. None (E-3210)	
				10. Work Unit No. 505-62-21	
9. Performing Organization Name and Address Scientific Research Associates, Inc. P.O. Box 498 Glastonbury, Connecticut 06033				11. Contract or Grant No. NAS3-22759	
				13. Type of Report and Period Covered Contractor Report Final	
12. Sponsoring Agency Name and Address National Aeronautics and Space Administration Lewis Research Center Cleveland, Ohio 44135				14. Sponsoring Agency Code	
15. Supplementary Notes Project Manager, Allan R. Bishop, Internal Fluid Mechanics Division, NASA Lewis Research Center.					
16. Abstract A new method has been developed for two and three-dimensional computations of viscous supersonic flows with embedded subsonic regions adjacent to solid boundaries. The approach employs a reduced form of the Navier-Stokes equations which allows solution as an initial-boundary value problem in space, using an efficient noniterative forward marching algorithm. Numerical instability associated with forward marching algorithms for flows with embedded subsonic regions is avoided by approximation of the reduced form of the Navier-Stokes equations in the subsonic regions of the boundary layers. Supersonic and subsonic portions of the flow field are simultaneously calculated by a consistently split linearized block implicit computational algorithm. The results of computations for a series of test cases relevant to internal supersonic flow is presented and compared with data. Comparison between data and computation are in general excellent thus indicating that the computational technique has great promise as a tool for calculating supersonic flow with embedded subsonic regions. Finally, a User's Manual is presented for the computer code used to perform the calculations.					
17. Key Words (Suggested by Author(s)) Analysis; Inlets; Supersonic; Navier-Stokes			18. Distribution Statement Unclassified - unlimited STAR Category 02		
19. Security Classif. (of this report) Unclassified		20. Security Classif. (of this page) Unclassified		21. No. of pages 125	22. Price* A06